Evidence from Late Cretaceous-Paleogene volcanic rocks of the Kyrenia Range, northern Cyprus for the northern, active continental margin of the Southern Neotethys

Citation for published version:
Chen, G & Robertson, AHF 2021, 'Evidence from Late Cretaceous-Paleogene volcanic rocks of the Kyrenia Range, northern Cyprus for the northern, active continental margin of the Southern Neotethys', *Lithos*, vol. 380-381, pp. 105835. https://doi.org/10.1016/j.lithos.2020.105835

Digital Object Identifier (DOI):
10.1016/j.lithos.2020.105835

LITHOS

Evidence from Late Cretaceous-Paleogene volcanic rocks of the Kyrenia Range, northern Cyprus for the northern, active continental margin of the Southern Neotethys

--Manuscript Draft--

Manuscript Number:	LITHOS9043R2
Article Type:	Regular Article
Keywords:	Late Cretaceous-Paleogene; Volcanic rocks; Kyrenia Range; Arc magmatism; Marginal basin formation; Southern Neotethys
Corresponding Author:	Guohui Chen Institute of Geology and Geophys, Chinese Academy of Sciences Beijing, CHINA
First Author:	Guohui Chen
Order of Authors:	Guohui Chen
	Alastair Robertson
Abstract:	Late Cretaceous felsic and latest Cretaceous-Paleogene basaltic volcanic rocks are exposed throughout the Kyrenia Range, N Cyprus. Field mapping of the key, well-exposed western range indicates that the felsic volcanics are mainly crop out in the southerly, frontal part of the range, separated from the latest Cretaceous-Paleogene basaltic volcanics farther north by a thrust. New U-Pb zircon dating of the felsic volcanics indicates a primary age of c. 74.0 Ma (Late Campanian). The felsic volcanics are characterised by evolved compositions that were probably generated in an extensional subduction-related setting. Their relatively low Nb and Y but high Rb concentrations, together with characteristic Th/Ta ratios (6-20), suggest a mature continental arc setting. The latest Cretaceous-Paleogene basaltic volcanics have mainly within-plate chemical characteristics (in the east), although some have a subordinate subduction influence; e.g. negative Nb (in the west). Sr-Nd-Hf isotopic signatures (i.e. high positive εNd(t) and εHf(t) values) suggest derivation of the basalts from several OIB-like mantle sources, with probable involvement of a crustal (recycled) component (i.e. elevated Nb/Y ratios). Comparisons with SE Turkey, where Late Cretaceous arc-related granitic rocks are widely developed, suggest that the Kyrenia Range igneous rocks may have originated to the south of the Alanya metamorphic massif (N of Cyprus) and correlative continental units in SE Turkey. The latest Cretaceous-Paleogene basaltic volcanics in N Cyprus and SE Turkey (Maden Complex) are interpreted to represent incipient marginal basin formation, possibly in an oblique-convergent setting, prior to Miocene suturing with Arabia. In the light of alternatives, we infer genesis of the N Cyprus Late Cretaceous and Paleogene volcanic rocks related to stages in the development of the northerly active continental margin of the Southern Neotethys.
Suggested Reviewers:	Fatih Karaoğlan fkaraoglan@cu.edu.tr expert on arc magmatism in SE Turkey
	Osman Parlak parlak@cu.edu.tr expert on magmatism and tectonics especially in Turkey
	Pamela Kempton pkempton@ksu.edu
Opposed Reviewers:	

Title page

Evidence from Late Cretaceous-Paleogene volcanic rocks of the Kyrenia Range, northern Cyprus for the northern, active continental margin of the Southern Neotethys

Guohui Chen[1]*, Alastair H. F. Robertson[1]

[1]School of GeoSciences, University of Edinburgh, West Mains Road, Edinburgh EH9 3JW, UK

*Current Address: State Key Laboratory of Lithospheric Evolution, Institute of Geology and Geophysics, Chinese Academy of Sciences, P.O. Box 9825, Beijing 100029, China

Corresponding author: Guohui Chen (Guohui.Chen@live.cn)

Revision notes:

Dear Professor Shellnutt,

Thank you for considering the further revision of our paper. We have acted on the comments made. We have marked the main edits using track changes. Please note that we not made any significant changes to the results or discussion, only refinements in the light of the review comments.

The main further changes of the paper are:

1) *The field descriptions are reorganized somewhat, with local description first, and then a summary;*
2) *The section on the Late Cretaceous magmatic rocks in SE Turkey are revised beginning with units in the south, then the units in the north. More consideration is given to possible equivalents in the Kyrenia Range volcanics (see new section 5.4);*
3) *More information is given on the HP-LT metamorphism and shoshonites related to Late Cretaceous subduction and possible collision in SE Turkey (lines 492-497) as this is relevant to the regional setting;*
4) *The Eocene volcanics are discussed in slightly more detail, as suggested (lines 585-593, 653-664).*

In summary, we hope that you will decide that our paper is now suitable for publication in Lithos.

Yours sincerely,
Guohui Chen and Alastair Robertson

COMMENTS FROM EDITORS AND REVIEWERS

<u>Editor:</u> I requested the previous reviewers of your manuscript to evaluate the revised version however, only Reviewer #2 accepted the invitation. As you will see, Reviewer #2 is mostly satisfied with the improvements but, points out a few minor issues in the discussion that should be addressed. Furthermore, I think it is appropriate to move section 2 after section 3. It is common to have the methods after the 'geological background'. Please update the manuscript accordingly.

All the best.
Greg Shellnutt
Co-Editor-in-Chief

Comments
Line 73. The methods should come after the geological background… or in this case the "Volcanism in the Kyrenia Range.

OK. It is reordered now.

Line 75. Delete 'initially'
OK. It is deleted now.

Line 100. Should it be "Whole rock procedural blanks"?
No. It refers the total procedural blanks. So it is correct;

Line 208. Should be either "… and a felsic debris-flow deposit are exposed." Or "… and felsic debris-flow deposits are exposed.".
OK. It is revised to be "a felsic debris-flow deposit are exposed" now.

Lines 534-535. Should be, "… arc was explained by northward…"
Yes. Revised as suggested.

Line 565. Should be, "… work is needed…".
Line 670. Should be, "... alternatives are suggested; …".
OK. They are revised now.

<u>Reviewer #2: Dear Editor and authors,</u>
I review the revised MS entitled "Evidence from Late Cretaceous-Paleogene volcanic rocks of the Kyrenia Range, Northern Cyprus for northern, active continental margin of the Southern Neotethys" submitted by Chen and Robertson.

First of all, I want to respond one of the authors' comments in "General Response (7)": "Also, it is normal for this research community to widely cite relevant literature (it is not uncommon in Turkey for aggrieved authors to take cases to university ethics committees if they feel their work has not been adequately cited)."

As a Turkish scientist, this sentence is directly addressing myself and looks trying to provoking and manipulating me to make political review rather than a scientific review. So, I strongly suggest the authors relying on scientific comments. Here all my comments rely on nothing but my scientific vision. The rest is not the authors' business.

I suggest using the subtitle "Results and Discussion" instead "Discussion". The authors present mostly their field and analytical data in sections 5.1 and 5.2.
The Discussion section, especially sections 5.1 Genetic type/source characteristics and 5.2 Tectonic discrimination, provides further interpretation of the field and analytical data. So we think the subtitle "Discussion" here is OK and in line with use in similar papers.

The introduction, Methodology and the presentation of the results of the work seem to be alright. However, the discussion is still debatable.

Discussion

The authors still insisting on linking Kyrenia range to SE Anatolia. It is obvious that these units are continuation of each other in terms of paleogeography, however, their tectonic setting is quite different. The author should explain in detail, possibility of roll-back in a southerly located oceanic crust (Kızıldağ-Troodos oceanic crust) with an Eocene arc.

More details of the paleogeographic continuation (agreed) are now given, to help clarify the setting of the various tectonic units in SE Tukey. In addition, more detailed comparisons (paleogeographically and geochemically) between the possible equivalents of the Kyrenia Range volcanics are included, together with literature interpretations. Several additional relevant recent references are included (section 5.4). However, we have kept the additions to a necessary minimum to contain the length of this section.

If the Bitlis-Pütürge (BP) and Tauride platforms collided during late Cretaceous. The HP metamorphism of the BP and the shoshonitic magmatism during late Cretaceous located in Pertek (Elazığ) are addressing a late Cretaceous collision (see results of Öberhansli et al, 2010, 2014; Sar et al., 2019). After this there should be no Berit Ocean in SE Anatolia and BP attached to Tauride platform acting the active margin of southerly located subduction, which produces the Kızıldağ and Troodos ophiolites.

The genesis of oceanic crust, including Kızıldağ and Troodos ophiolites, by SSZ spreading is c. 90 Ma (e.g. Mukasa and Ludden, 1987). In contrast, the geochronology indicates a tectono-metamorphic age of Santonian-Campanian for the HP-LT metamorphism of the BP microcontinents (82-80 Ma; Oberhänsli et al., 2010, 2013; Çetinkaplan et al., 2016). Therefore, the younger magmatism is likely to result from an advanced stage of northward subduction of the oceanic plate, although a more southerly origin is possible for the Kyrenia volcanics, see Line 570-577. However, we agree that the Berit ocean probably sutured during the latest Cretaceous, while S Neotethys remained open to the south until the Miocene. We make this clearer.

The Eocene arc magmatism should be a result of the southerly located subduction and the authors proposal of roll-back during Paleogene rejects the arc magmatism during Eocene.

The Eocene arc magmatism could be caused by a southerly located subduction given the fact that the Berit meta-ophiolite is unconformably overlain by the Eocene Maden Complex N of the Malatya Metamorphic (Robertson et al., 2006). If the Meydan ophiolite and cross cutting granite are is the same unit (likely), then the Kyrenia Late Cretaceous volcanics should have a different origin, *maybe an arc further south. We indicated this before but now we are more explicit (lines 583-593).*

The proposed model does not reject the arc magmatism during Eocene. The proposed model suggests the Eocene volcanics formed in an oblique-convergent setting, in other words, arc magmatism could possibly take place especially in local regions where remnant oceanic crust still exists. In addition, the Eocene Kyrenia rocks are mainly within-plate in affinity, rather than arc-related.

If the authors proposal explains the existing of HP metamorphism and shoshonitic magmatism during late Cretaceous and arc magmatism during Eocene, I will be happy to read.
More information about the HP-LT metamorphism is given in Line 487-497, as requested. The Late Cretaceous shoshonitic magmatism is now mentioned. However, literature review indicates that shoshonitic magmatism does not have a unique tectonic origin but may occur in a range of extensional to post-collisional subduction-related settings (see lines 551-561). Concerning the Eocene arc magmatism, there is geochemical evidence for this in places in SE Turkey but little supporting evidence for a regional-scale arc although as we note this could have subducted (see lines 583-593). However, in agreement with the reviewer, we infer an active margin rather than post-collisional setting for these volcanics in contrast to some other authors.

Figures&tables look adequate and good in drawing.

My suggestion is accepting the MS with considering the comments above. The text should be spell checked.

Regards,
Dr. Fatih KARAOĞLAN

Oberhänsli R, Koralay E, Candan O, Pourteau A, Bousquet R (2014) Late Cretaceous eclogitic high-pressure relics in the Bitlis Massif Geodin Acta 26:175-190 doi:10.1080/09853111.2013.858951

Oberhänsli R, Candan O, Bousquet R, Rimmele G, Okay A, Goff J (2010) Alpine high pressure evolution of the eastern Bitlis complex, SE Turkey. In: Sosson M, Kaymakci N, Stephenson RA, Bergerat F, Starostenko V (eds) Sedimentary Basin Tectonics from the Black Sea and Caucasus to the Arabian Platform, vol 340. vol 1. Geological Society, London, Special Publications, London, pp 461-483. doi:10.1144/sp340.20

Sar A, Ertürk MA, Rizeli ME (2019) Genesis of Late Cretaceous intra-oceanic arc intrusions in the Pertek area of Tunceli Province, eastern Turkey, and implications for the geodynamic evolution of the southern Neo-Tethys: Results of zircon U-Pb geochronology and geochemical and Sr-Nd isotopic analyses Lithos 350-351:105263 doi:10.1016/j.lithos.2019.105263

These references were included.

Abstract

Late Cretaceous felsic and latest Cretaceous-Paleogene basaltic volcanic rocks are exposed throughout the Kyrenia Range, N Cyprus. Field mapping of the key, well-exposed western range indicates that the felsic volcanics are mainly crop out in the southerly, frontal part of the range, separated from the latest Cretaceous-Paleogene basaltic volcanics farther north by a thrust. New U-Pb zircon dating of the felsic volcanics indicates a primary age of c. 74.0 Ma (Late Campanian). The felsic volcanics are characterised by evolved compositions that were probably generated in an extensional subduction-related setting. Their relatively low Nb and Y but high Rb concentrations, together with characteristic Th/Ta ratios (6-20), suggest a mature continental arc setting. The latest Cretaceous-Paleogene basaltic volcanics have mainly within-plate chemical characteristics (in the east), although some have a subordinate subduction influence; e.g. negative Nb (in the west). Sr-Nd-Hf isotopic signatures (i.e. high positive $\varepsilon Nd(t)$ and $\varepsilon Hf(t)$ values) suggest derivation of the basalts from several OIB-like mantle sources, with probable involvement of a crustal (recycled) component (i.e. elevated Nb/Y ratios). Comparisons with SE Turkey, where Late Cretaceous arc-related granitic rocks are widely developed, suggest that the Kyrenia Range igneous rocks may have originated to the south of the Alanya metamorphic massif (N of Cyprus) and correlative continental units in SE Turkey. The latest Cretaceous-Paleogene basaltic volcanics in N Cyprus and SE Turkey (Maden Complex) are interpreted to represent incipient marginal basin formation, possibly in an oblique-convergent setting, prior to Miocene suturing with Arabia. In the light of alternatives, we infer genesis of the N Cyprus Late Cretaceous and Paleogene volcanic rocks related to stages in the development of the northerly active continental margin of the Southern Neotethys.

Highlights

- Felsic volcanics erupted at c. 74 Ma in an active continental margin arc setting
- Some within-plate basalts (c. dated at 70-45 Ma) were affected by subduction
- The basalts are interpreted to represent incipient marginal basin formation
- The volcanism provides new evidence of subduction in the E Mediterranean region
- Northward subduction is supported by coeval arc magmatism in SE Turkey

Evidence from Late Cretaceous-Paleogene volcanic rocks of the Kyrenia Range, northern Cyprus for the northern, active continental margin of the Southern Neotethys

Guohui Chen[1]*, Alastair H. F. Robertson[1]

[1]School of GeoSciences, University of Edinburgh, West Mains Road, Edinburgh EH9 3JW, UK

*Current Address: State Key Laboratory of Lithospheric Evolution, Institute of Geology and Geophysics, Chinese Academy of Sciences, P.O. Box 9825, Beijing 100029, China

Corresponding author: Guohui Chen (Guohui.Chen@live.cn)

Abstract

Late Cretaceous felsic and latest Cretaceous-Paleogene basaltic volcanic rocks are exposed throughout the Kyrenia Range, N Cyprus. Field mapping of the key, well-exposed western range indicates that the felsic volcanics are mainly crop out in the southerly, frontal part of the range, separated from the latest Cretaceous-Paleogene basaltic volcanics farther north by a thrust. New U-Pb zircon dating of the felsic volcanics indicates a primary age of c. 74.0 Ma (Late Campanian). The felsic volcanics are characterised by evolved compositions that were probably generated in an extensional subduction-related setting. Their relatively low Nb and Y but high Rb concentrations, together with characteristic Th/Ta ratios (6-20), suggest a mature continental arc setting. The latest Cretaceous-Paleogene basaltic volcanics have mainly within-plate chemical characteristics (in the east), although some have a subordinate subduction influence; e.g. negative Nb (in the west). Sr-Nd-Hf isotopic signatures (i.e. high positive εNd(t) and εHf(t) values) suggest derivation of the basalts from several OIB-like mantle sources, with probable involvement of a crustal (recycled) component (i.e. elevated Nb/Y ratios). Comparisons with SE Turkey, where Late Cretaceous arc-related granitic rocks are widely developed, suggest that the Kyrenia Range igneous rocks may have originated to the south of the Alanya metamorphic massif (N of Cyprus) and correlative continental units in SE Turkey. The latest Cretaceous-Paleogene basaltic volcanics in N Cyprus and SE Turkey (Maden Complex) are interpreted to represent incipient marginal basin formation, possibly in an oblique-convergent setting, prior to Miocene suturing with Arabia. In the light of alternatives, we infer genesis of the N Cyprus Late Cretaceous and Paleogene volcanic rocks related to stages in the development of the northerly active continental margin of the Southern Neotethys.

Keywords: Late Cretaceous-Paleogene; Volcanic rocks; Kyrenia Range; Arc magmatism; Marginal basin formation; Southern Neotethys

1. Introduction

Continental margin magmatism is a key feature of subduction at convergent plate margins (Dewey, 1969; Şengör and Natal'In, 1996). Information concerning the field relations, age, petrology and geochemistry are essential to understand the growth and demise of arcs, and are critical to reconstruct paleogeography and to test alternative tectonic hypotheses (e.g. Trehu et al., 1994; Tatsumi and Kogiso, 2003; Bowman et al., 2019).

The Eastern Mediterranean region, situated between the North African-Arabian and Anatolian (Eurasian) plates, includes tectonically emplaced remnants of Neotethys that developed from the preceding Paleotethys farther north (e.g. Le Pichon, 1982; Şengör et al., 1984; Robertson and Dixon, 1984; Stampfli and Borel, 2002). Much of the arc magmatism in the north, in the Pontides, of Jurassic-Eocene age (Fig. 1), relates to long-lived northward subduction of the Northern Neotethys (İzmir-Ankara-Erzincan ocean) (Adamia et al., 1977; Dercourt et al., 1993; Ustaömer and Robertson, 1997; Rice et al., 2006). Subduction of the Southern Neotethys resulted in both continental margin and oceanic magmatism that ranges, overall, from Late Cretaceous to Paleogene (Fig. 1). Here, we focus on evidence of Late Cretaceous and Paleogene volcanism in the Kyrenia Range of northern Cyprus, representing the most westerly known occurrence of arc-type magmatism that can be related to subduction of the Southern Neotethys (Fig. 1) (Moore, 1960; Ducloz, 1972; Pearce, 1975; Baroz, 1979, 1980; Robertson and Woodcock, 1986; Huang et al., 2007; Robertson et al., 2012b).

Our specific objectives here are: (1) to understand the tectono-stratigraphy of two, contrasting, felsic and basaltic volcanic units in relation to associated sedimentary units; (2) to determine the eruptive ages of both of the volcanic units directly, using geochronology. Previously, the volcanics were dated indirectly using microfossils within interbedded pelagic carbonates (Baroz, 1979; Robertson et al., 2012b); (3) to determine whether there is any petrological or geochemical variation (including isotopic variation) along the Kyrenia Range (c. 100 km) and, if so, the implications; (4) to infer the magmatic-tectonic setting of eruption, compared with the evidence of arc volcanism, especially in southeast Turkey; (5) to test alternative tectono-magmatic hypotheses bearing in mind that arc magmatism plays a key role in plate tectonic interpretations.

2. Volcanism in the Kyrenia Range

Rifting of the Southern Neotethys during Late Permian and Early-Middle Triassic was followed by continental break-up during the Late Triassic-Early Jurassic (Robertson and Woodcock, 1979; Şengör and Yılmaz, 1981; Robertson and Dixon, 1984; Garfunkel, 1998; Robertson et al., 2020). The Kyrenia Range then formed part of a carbonate platform that slowly subsided during Jurassic-Early Cretaceous in a passive margin setting (Robertson and Woodcock, 1986). The carbonate platform was deformed and metamorphosed under greenschist facies during the Late Cretaceous, extensionally exhumed, and then unconformably overlain by basic extrusive igneous rocks of latest Cretaceous-Paleogene age (Figs. 2-3) (Ducloz, 1972; Baroz, 1979; Robertson and Woodcock, 1986). In addition, felsic volcanics and tuffs are exposed as thrust slices at a low structural level in the south of the range (Figs. 2b, 3) (Robertson et al., 2012b). These volcanic rocks have no exposed base and are directly overlain by a much larger thrust sheet that includes the mainly basic extrusive igneous rocks.

Baroz (1979, 1980) mapped the volcanic rocks and carried out petrographic and whole-rock chemical analysis of major elements. He reported the presence of a lower stratigraphic sequence of basalt, dolerite, trachybasalt, trachyandesite, dacite and rhyolitic tuff, and interpreted this as a bimodal basic-acidic calc-alkaline suite, related to a Late Maastrichtian volcanic arc. In contrast, the Paleogene volcanic assemblage was suggested to have erupted stratigraphically above in a post-collisional (intra-continental) strike-slip setting (Baroz, 1980). However, a thrust was later mapped between the mainly felsic and mainly basic suites (Robertson et al., 2012b), complicating this simple stratigraphy.

Chemical analysis of the Paleogene basaltic lavas, including immobile trace elements, initially suggested an alkaline, within-plate eruptive setting (Pearce, 1975). Subsequent chemical analysis, including some immobile elements, confirmed this mainly alkaline within-plate setting but also revealed some evidence of a subduction influence (e.g. negative Nb anomaly) (Robertson and Woodcock, 1986). The Paleogene lavas were inferred by these authors to have erupted in a transtensional setting along the northern, active margin of the 'Troodos ocean'. Huang et al. (2007) carried out additional chemical analysis of the Paleogene basaltic lavas, mainly from the eastern and western Kyrenia Range, with emphasis on immobile elements, and proposed a Late Cretaceous-Paleogene back-arc setting related to northward subduction.

The felsic rocks of the lowermost thrust sheet, known as the Fourkovouno (Selvilitepe)[1] Formation, up to 400 m thick, begin with marine water-lain felsic tuffs and subaqueous felsic debris-flow deposits and culminate in laterally discontinuous, thick-bedded to massive rhyolitic lava flows (Fig. 3) (Moore, 1960; Baroz, 1979; Huang et al., 2007; Robertson et al., 2012b). The felsic rocks are locally cut by small (meter-sized) basaltic/doleritic intrusions (not studied). A Late Cretaceous age (Late Campanian) was suggested for the felsic lavas, based on sparse planktic foraminifera (*Globotruncana sp.*) that were recognised in a chalky interbed near the top of the

[1] For simplicity, we use the traditional stratigraphy for the formation names (more recent Turkish equivalents are mentioned initially). However, we use current the Turkish names (e.g. for settlements); pre-existing names are mentioned initially.

succession (Baroz, 1979).

The Late Cretaceous and Paleogene basaltic igneous rocks have been divided into two formations, namely the Maastrichtian Melounda (Mallıdağ) Formation and the Paleocene-Middle Eocene Ayios Nikolaos (Yamaçköy) Formation (Fig. 2a).

The Melounda Formation, c. 300 m thick, unconformably overlies the exhumed Mesozoic platform carbonates of the Trypa (Tripa) Group or, in places, unmetamorphosed terrigenous turbidites of the Kiparisso Vouno (Alevkaya Tepe) Member of the Melounda Formation (Baroz, 1979; Robertson and Woodcock, 1986; Robertson et al., 2012b). The basaltic lavas of the Melounda Formation are commonly intercalated with pinkish pelagic limestones (Fig. 2a). The succession locally includes lenticular, lithoclastic breccias and finer-grained clastic facies that were reworked from the underlying meta-platform carbonates (Fig. 2a) (Robertson and Woodcock, 1986; Robertson et al., 2012b). Planktic foraminifera from pelagic carbonates between the lavas indicate a Late Maastrichtian age (Baroz, 1979; Robertson et al., 2012b).

The overlying Ayios Nikolaos Formation, 300-400 m thick, comprises basaltic volcanics that are variably interbedded with pelagic carbonates. Calciturbidites, calcareous debris-flow deposits and carbonate-rock breccias appear above the lavas, towards the top of the overall succession (Baroz, 1979; Robertson and Woodcock, 1986; Robertson et al., 2012b, 2014) (Fig. 2a). Planktic foraminifera from pelagic carbonates that are interbedded with the lavas indicate a Late Paleocene to Mid-Eocene age range (Baroz, 1979; Robertson et al., 2012b).

3. Methods

The Kyrenia Range is a complex thrust belt and therefore it was essential to remap the western Kyrenia Range, where felsic and basaltic volcanic rocks are exposed together (Moore, 1960; Baroz, 1979; Robertson et al., 2012b). In addition, sedimentary logs were measured and correlated to produce a composite stratigraphy of the volcanogenic successions that are exposed in two superimposed thrust sheets.

Optical microscopy was carried out on the samples collected. For the felsic lithologies, 13 samples were studied from the western range. For the basaltic lithologies, we used a combination of our samples (n=29) and also some that were previously collected for paleomagnetic study (n=26) throughout the Kyrenia Range (Morris et al., 2015).

Whole-rock major and trace element concentrations of the volcanic rocks were measured by X-ray fluorescence (XRF) on fused glass beads and pressed powder pellets at the School of GeoSciences, University of Edinburgh, using the well-known methods of Fitton et al. (1998) and Fitton and Godard (2004). Accuracy and precision are typically c. 5%. For representative samples, additional trace and rare earth element (REE) analysis was carried out by inductively coupled plasma-mass spectrometry (ICP-MS) at the ACME Analytical Laboratories, Vancouver. Major element contents were determined from a $LiBO_2$ fusion by ICP-ES, using 5 g of sample pulp. Trace element contents were determined from a $LiBO_2$ fusion by ICP-MS, again using 5 g of sample pulp. Detection limits range between 0.01 and 0.04 wt% for major oxides, 0.01 and 0.1 ppm for trace and rare earth elements. The relative standard deviation for the REE is ~5% and for all other trace elements is up to 10%, with quality control using international geostandards (see http://acmelab.com).

In addition, Sr-Nd-Hf isotopic analysis was performed on a Neptune Plus multi-collector (MC)-ICP-MS at Wuhan SampleSolution Analytical Technology Co., Ltd., China, as reported by Li et al. (2012). Whole procedural blanks were <100 pg for Sr, <50 pg for Nd and <50 pg for Hf. $^{87}Sr/^{86}Sr$, $^{143}Nd/^{144}Nd$ and $^{176}Hf/^{177}Hf$ ratios were normalised to $^{86}Sr/^{88}Sr = 0.1194$, $^{146}Nd/^{144}Nd = 0.7219$ and $^{179}Hf/^{177}Hf = 0.7325$, using the exponential law. Standard analysis yielded $^{87}Sr/^{86}Sr = 0.710240 \pm 11$ (2SD, n = 4) for NBS987, $^{143}Nd/^{144}Nd = 0.512440 \pm 8$ (2SD, n = 8) for GSB 04-3258-2015, and

$^{176}Hf/^{177}Hf$ = 0.282224 ± 6 (2SD, n = 6) for Alfa Hf. In addition, USGS reference materials BCR-2 and RGM-2 were also analysed for Sr–Nd–Hf isotopes, and gave ratios of 0.705039 ± 8 and 0.704169 ± 11 for $^{87}Sr/^{86}Sr$, 0.512644 ± 6 and 0.512808 ± 9 for $^{143}Nd/^{144}Nd$ and 0.282864 ± 6 and 0.283016 ± 7 for $^{176}Hf/^{177}Hf$, which is within error of recommended values (Thirlwall, 1991; Weis et al., 2006, 2007). The analytical data for the major, trace and rare earth elements/isotope ratio of the felsic and basaltic volcanics are listed in the Supplementary Table S1, S2, respectively.

In addition, two polished thin sections of basalt (no. 02 and 21) that contain relatively fresh feldspar and pyroxene crystals were selected for analysis of major elements using a Cameca SX100 electron microprobe at the School of GeoSciences, University of Edinburgh. Details of the analytical conditions and methods are given by Hayward (2011) and by Hartley and Thordarson (2013). The accuracy of major element determinations is <± 1% of total value. Analytical data for feldspar and pyroxene are given in Supplementary Table S3, S4, respectively.

For dating, zircon crystals within 30-160 μm fraction were separated from crushed felsic tuffaceous rock and rhyolitic lava (no. 14-18, 14-19 and 14-20; c. 5 kg each). A Wilfley table, Frantz Isodynamic magnetic separator and a high-density solution (lithium polytungstate; 2.85 g/ml) were used to aid separation. The zircon grains were randomly handpicked under a binocular microscope, mounted in epoxy resin and polished sufficiently to expose the centre of the grains. Internal structures were studied with a scanning electron microscope using cathodoluminescence (CL) at the School of GeoSciences, University of Edinburgh. U-Pb analysis was then performed using a Cameca IMS-1270 secondary ion mass spectrometer (SIMS) at the School of GeoSciences, University of Edinburgh, using the methods reported by Kelly et al. (2008) and Ustaömer et al. (2012). Errors of the reported ages are ± 1σ. Related geochronological plots were produced using ISOPLOT (Ludwig, 2012). Analytical results are listed in the Supplementary Table S5.

4. Results

4.1. Volcanic successions

The felsic volcanics, mainly crop out in the western part of the Kyrenia Range in two thrust sheets (Figs. 3-4). The lower of these, which is relatively intact, extends from Geçitköy (Panagra) eastwards to Selvilitepe (Fourkovouno) (Fig. 5a-e). The second, structurally higher unit, comprises discontinuous exposures extending from north of Geçitköy, to southwest of Karsıyaka (Vasileia) and west of Alevkaya Tepe (Kiparisso Vouno) (Fig. 5f-j). Farther west, in the Kayalar (Orga) area (Fig. 3a), a small thrust slice exposes coarse-grained felsic tuff and a felsic debris-flow deposit. Small (tens of m-sized) outcrops of felsic volcanogenic rocks also occur farther east; e.g. northeast of Aşağı Dikmen (Kato Dikomon), between thrust sheets of Mesozoic meta-carbonate rocks (Baroz, 1979). Small exposures are also intersliced with Late Cretaceous pelagic carbonates of the Melounda Formation to the north of Ergenekon (Agios Khariton) (Fig. 3a) (Robertson et al., 2012b).

The local successions are restored as a lower thrust sheet and an upper thrust sheet. The succession in the lower thrust sheet, c. 90 m thick, begins with weakly-bedded, white felsic tuff (beds <0.5 m thick) (Fig. 5a, c-e), followed by thick layers of matrix-supported felsic breccia-conglomerate (c. 10 m thick) that we interpret as debris-flow deposits (Fig. 5a, c, e). The succession passes upwards into massive, vitreous, rhyolitic lava flows, individually up to 10 m thick (Figs. 5a, Supplementary Figure S1). Localised normal grading; e.g. northeast of Geçitköy, indicates that the succession is the right way up, stratigraphically (Fig. 5a-b). In places, steeply dipping, irregularly shaped basaltic or doleritic intrusions, up to 2 m across, cut the felsic layering (Figs. 5a, Supplementary Figure S1). Adjacent to these intrusions, poorly consolidated tuffaceous sediments have undergone contact metamorphism to form hard, dark grey, flint-like, recrystallised felsic rock (Robertson et al., 2012b). There is no evidence of similar intrusions in the structurally overlying basalts, which is in keeping with the mapped tectonic contact between the two units. The succession in the upper thrust sheet begins with greyish to greenish, tuffaceous matrix-supported conglomerates, including clasts of silicified rhyolite, chalk and basalt (Supplementary Figure S1). The estimated thickness ranges from c. 40 m north of Geçitköy (Fig. 5f), to c. 80 m southwest of Karsıyaka (Fig. 5g-h), to 30 m west of the Alevkaya Tepe (Fig. 5i-j).

Contrasting field relations facilitate mapping of the Late Cretaceous versus the Paleogene formations (Baroz, 1979; Robertson and Woodcock, 1986; Hakyemez et al., 2000; Robertson et al., 2012b). In the far east of the Kyrenia Range, the Karpas Peninsula (Fig. 3a), both pillowed and massive basalt are widely exposed near Balalan (Platanissos). Interpillow carbonate and lenticular interbeds of pelagic carbonate (< 1 m thick) (Figs. 3a, Supplementary Figure S2) contain Late Maastrichtian microfossils (Robertson et al., 2012b). In the eastern range, basaltic rocks of the Melounda Formation contain abundant pelagic carbonate and are overlain by massive basalts of the Ayios Nikolaos Formation; i.e. from Ağıllar (Mandres) to Mallıdağ (Melounda) (Fig. 3a) (Baroz, 1979; Robertson and Woodcock, 1986; Hakyemez et al., 2000; Robertson et al., 2012b). In the central range, pillow lava with interbedded pelagic carbonate of the Melounda Formation occurs in two settings. The first is directly above the Upper Cretaceous basal unconformity, with the meta-carbonate platform rock beneath; e.g. near Tirmen (Trypimeni). The second setting is as one (or several), small thrust sheets along the southern flank of the range; e.g. Değirmenlik (Kythrea), Boğaz (Bogaz) and southwest of Alevkaya Tepe (Figs. 3a, Supplementary Figure S2). Basalt with some interbedded pelagic carbonate of the Ayios Nikolaos Formation is exposed higher in the succession (within a shear zone), near Tirmen, Arapköy (Klepini) and İncesu (Motides) (Baroz, 1979). In the western range, basaltic lavas interbedded with pelagic carbonates of the Melounda Formation are exposed in a thrust sheet along the southern margin of the range; e.g. Geçitköy (Figs. 3, Supplementary Figure S2). Similar basaltic lavas with pelagic carbonates and local carbonate breccias are exposed along the northern margin of the range; e.g. near Karşıyaka and farther west (Baroz, 1979; Hakyemez et al., 2000; Robertson et al., 2012b). In addition, basaltic lava interbedded with pelagic chalk of the Ayios Nikolaos Formation occurs higher in the succession (southward-younging) along the eastern side of Geçitköy road (Huang et al., 2007; Robertson et al., 2012b).

In summary, the Late Maastrichtian basalts (Melounda Formation) are typically pillowed, forming repeated flows (individually up to c. 10 m thick), reaching a maximum of > 90 m in the east (near Balalan). The lavas include pink pelagic carbonate as interstitial sediment and discontinuous layers. In contrast, the Paleogene basalts (Ayios Nikolaos Formation) are commonly massive, especially in the eastern range, where individual lava flows reach c. 45 m thick, with relatively few pelagic intercalations (Supplementary Figure S2). In the central and western ranges, thinner lava flows (<10m) are intercalated with pelagic carbonates and reddish chert (formed by diagenetic replacement). During this work, we identified geochemical differences between the Late Cretaceous-Paleogene basaltic lavas of similar age along the far-eastern, eastern, central and western Kyrenia Range (see below).

4.2. Petrography

The felsic rocks are porphyritic, composed of quartz, plagioclase and sanidine, together with subordinate biotite and rare hornblende. Large sanidine crystals (0.3-1 mm) show simple twinning, whereas plagioclase commonly has lamellar twinning (Supplementary Figure S3). Biotite laths (0.3-0.8 mm in length) are preferentially orientated parallel to flow layering. Rare quartz phenocrysts (<1%, 0.2-0.5 mm) are commonly fragmented, probably related to quenching during eruption; i.e. explosive fragmentation (Supplementary Figure S3). The groundmass comprises microcrystalline quartz and feldspar, together with minor muscovite, biotite and rare hornblende (c. 60 μm). In some samples (e.g. nos. 14-19 and 14-20), the groundmass is cryptocrystalline, almost glassy (Supplementary Figure S3).

The basaltic rocks of both Late Cretaceous and Paleogene age generally fall into two groups in terms of mineral composition and texture. The first group (most common) is porphyritic with subhedral to euhedral clinopyroxene phenocrysts (30-40%), up to 0.6 mm long, that occur interstitially or are intergrown with subhedral feldspar (Supplementary Figure S4, Table S3). Feldspar (45-60%) forms elongate, acicular laths, up to 1 mm long. Olivine is relatively rare (<5%). The second group is ophitic, as locally observed in the western Kyrenia Range with abundant anhedral to subhedral augite phenocrysts (up to 0.6 mm in size). Most plagioclase is acicular, enclosed or surrounded by augite (Supplementary Figure S4).

Most samples are slightly to moderately altered. Amygdales and veins are infilled with secondary minerals such as calcite and zeolite. Alteration is variable, for example, pyroxene and plagioclase are heavily altered to chlorite and clay minerals (e.g. smectite/sericite). The relatively high loss on ignition values result from secondary processes, which need to be taken into account prior to rock identification and tectonic discrimination.

4.3. Whole-rock chemistry

Major-element oxides (K_2O, Na_2O and CaO) and trace elements (e.g. Rb, Sr and Ba) exhibit a relatively wide compositional range, consistent with the effects of alteration (see Supplementary Table S1-S2). Alteration can be inferred from variable LOI values that range between 0.3-5.4 wt% for the felsic volcanics and 4.09-14.57 wt% for the basaltic rocks. This is consistent with the presence of considerable amounts of water- and/or carbonate dioxide-bearing minerals, for example chlorite and calcite, as observed petrographically (see Supplementary Figure S3, S4). Trace elements such as Ti, Zr, Y, Nb, Ta, V, Co, Th and REEs tend to be immobile during weathering and/or metamorphism below amphibole facies are, therefore, preferred for rock-type identification and tectonic discrimination (e.g. Pearce and Cann, 1973; Rollinson, 1993). For basaltic rocks, samples with high crystal contents (cumulate composition or highly porphyritic) should be discounted from geochemical discrimination (Pearce, 1996). In general, samples with immobile element Al_2O_3 > 20 wt% (concentrated in feldspar), Sc > 50 ppm (concentrated in clinopyroxene), or Ni > 200 ppm (concentrated in olivine) are predicted to contain high amounts of cumulated minerals (Pearce, 1996). On this basis, basaltic rocks nos. 14-66, 14-50, 14-51, 14-58, 14-68, 08, 16, 25 and 28 are discounted.

The more felsic assemblage is mainly rhyolitic in the classification of Winchester and Floyd (1977) but shows a trachytic affinity in the revised Zr/Ti vs. Nb/Y (Fig. 6a) diagram of Pearce (1996). Relatively high abundances of Th (>14 ppm) but low Co concentrations (<12 ppm) are consistent with high-K and shoshonitic affinities (Fig. 6b). Primitive mantle-normalised multi-element plots (Fig. 6c) show variable enrichments and depletions in large-ion lithophile elements (LILEs; e.g. Cs, Rb, Ba, K and Sr) that are influenced by alteration. The samples show negative anomalies of Nb, Zr and Ti, coupled with marked positive anomalies of Th/U, Pb, Nd and probably Sm (Fig. 6c). Total REE contents of the felsic assemblage (Fourkovouno Formation) vary from 115 to 173 ppm. La ranges from 29-44 ppm, $(La/Yb)_N$=12.63-18.98, suggestive of an alkalic affinity. The ratios $(La/Sm)_N$=6.13-7.22 and $(Gd/Yb)_N$=1.26-1.68 suggest a large LREE fractionation but low to moderate HREE fractionation (Fig. 6d). Pronounced negative Eu anomalies (Eu/Eu*=0.32-0.48) are consistent with plagioclase crystallization, as seen petrographically (see Supplementary Figure S3). In general, the samples are comparable to upper continental crust (UCC).The basaltic rocks plot in the fields of basalt and alkali basalt, with intermediate degrees of fractionation (Zr/Ti=0.01-0.02) and moderate alkalinity (Nb/Y=0.1-1.8) on the rock-type discrimination plot (Fig. 7a). The basalts have a calc-alkaline affinity, except for samples from Mallıdağ (no. 01), Tirmen (no. 19-51), Değirmenlik (no. 14-64) and İncesu (no. 19-67) that exhibit high-K and shoshonitic affinities (Fig. 7b). The trace element compositions of the basaltic rocks exhibit wide ranges of Sr, Ba, Rb, Th, Ta, Nb and Ce. However, Zr, Hf, Sm, Ti and Y generally comparable with enriched mid-ocean ridge basalt (E-MORB) and oceanic island basalt (OIB) (Fig. 8a-c).

The basaltic rocks are characterised by variable REE concentrations (67.2-239.4 ppm) and light REE enrichments ($(La/Yb)_N$=3.18-19.35) (Fig. 8d). Samples from the central range, at Değirmenlik and Tirmen, show much higher total REE contents and steeper REE patterns. Westwards in the Kyrenia Range, the patterns become smoother, with less pronounced enrichment in LREEs. In general, no marked Eu anomaly (~1) is observed.

4.4. Whole-rock Sr-Nd-Hf isotopes

The selected basaltic samples have relatively uniform whole-rock Sr-Nd-Hf isotopic characteristics. Adopting a Late Cretaceous eruption age based on the paleontological dating (Robertson et al., 2012b), the calculated initial $^{87}Sr/^{86}Sr$ ratios range from 0.705054 to 0.705701, with εNd(t) values of 2.27 to 5.76. Initial $^{176}Hf/^{177}Hf$ and εHf(t) values are 0.282934-0.283017, 7.36-10.14, respectively (see Supplementary Table S2).

4.5. Zircon U-Pb geochronology

Zircon crystals separated from the felsic rocks are typically angular to sub-angular, 30-160 μm long. The grains have variable internal textures, including banded zoning (e.g. zircon 1), concentric zoning (nos. 2, 4, 5 and 12), and minor sector zoning (nos.

10, 11; Fig. 9a). Fractures (or depressions) and some inherited cores are affected by fluid-related chemical alteration (nos. 6 and 8) (Fig. 9a). The zircon grains have high Th/U ratios (0.19-1.24), suggestive of a magmatic origin (Rubatto, 2002). Twelve zircon grains were analysed with concordance levels ranging from 99-105%. The calculated $^{206}Pb/^{238}U$ age with the generally lowest possible error was used for age determination. The much older zircon grain (no. 4) is subhedral with a patchy xenocrystic texture, suggestive of a recycled origin (Fig. 9a). The concordant or nearly concordant data (100-102%) with a young age distribution yielded weighted mean $^{206}Pb/^{238}U$ gave ages of 74.0±0.6 Ma, 74.0±0.4 Ma and 71.7±0.7 Ma (Fig. 9b-d).

5. Discussion

5.1. Genetic type/source characteristics

For the felsic rocks, the high LREE/HREE (e.g. $(La/Yb)_N$=12.63-18.98) and negative Eu anomalies, resemble model UCC but with depletion in Eu, Sr and P (Fig. 6c-d). The A/CNK (molar ratio of $Al_2O_3/(CaO+Na_2O+K_2O)$) ratio is useful to identify the source of felsic rocks (Chappell and White, 1992) but is questionable for altered rocks like those of the Kyrenia Range. SiO_2, P_2O_5 and Th can also be used as indices of the fractional crystallization of a felsic melt (Chappell and White, 1992), but again may be affected by alteration (specially SiO_2). In our samples, P_2O_5 deceases with increasing SiO_2 and Th (Fig. 10a-b), trends that are indicative of I (igneous)- or A (anorogenic)-type granites. The relatively low contents of Zr, Nb, Y, La, Ce, Zn and Ga further characterise these rocks as I-type (Fig. 10c-d). The abundances of Th and Co, in particular hint at a shoshonitic composition (Hastie et al., 2007).

The trace element patterns of the basaltic rocks show a wider range of variation (Fig. 8). E-MORB and OIB-type basalts were derived from relatively enriched sources, specifically for the basalts of the Karpas Peninsula, eastern range and most of the central range. The lesser enrichment of Nb within the basalts of the central range at Ergenekon (no. 31), Arapköy (no. 14-62) and Alevkaya Tepe (no. 14-49), and the western range at Karsıyaka (no. 14) and Geçitköy (no. 10), can be explained by a relatively depleted mantle source, together with subduction modification. There is little evidence of the addition of radiogenic Sr from seawater, either to the source melt or during post-magmatic alteration. The Sr vs. Nd isotope correlation diagram (Fig. 11a) does not show a significant shift towards higher initial $^{87}Sr/^{86}Sr$ ratios as would be expected in both of these cases.

The basalts all have positive εNd(t) values (+2.27 - +5.76), consistent with derivation from an OIB-like source mantle (Fig. 11a). The samples plot directly on the terrestrial array, overlapping with the Nd isotope compositions of Etna and the Aeolian Arc, but intermediate between these settings in Hf isotopes (Fig. 11b). The samples that show trace element evidence of a subduction-modified source, based on relatively flat MORB-normalised multi-element patterns and negative Nb anomalies (no. 10, Geçitköy), plot in the Aeolian Arc-type mantle field. Conversely, samples from the Karpas Peninsular, at Balalan, plot close to the field of Etna and exhibit less subduction modification (Fig. 11b). The trace element and isotopic data, therefore, yield consistent results.

The involvement of a crustal component is also suggested by incompatible element ratio plots, on which the basalts exhibit two distinct trends. The samples with relatively strong subduction signatures plot away from the MORB array (Fig. 12a), fingerprinting a subduction-related lithospheric mantle end member. A probable lower crust input is suggested by relatively higher La/Nb and Ba/Nb ratios (e.g. Wang et al., 2004). In contrast, an OIB-like mantle component dominated most of the other basalt samples, as indicated by relatively low La/Nb, Zr/Nb but high Nb/Y ratios (Fig. 12b). The ratios of highly incompatible elements with small distribution coefficients (e.g.

Zr/Nb, Nb/Th, Nb/La) are sensitive indicators of mantle source heterogeneity (Saunders et al., 1988; Condie, 2003; Pearce and Stern, 2006). The samples from the western locations fall in the fields of an enriched component and upper continental crust (Fig. 12c), which could represent mantle mixing with continental sediments (subducted) or crustal contamination. In contrast, the samples from the easterly locations resemble those of the OIB/recycled component, and cluster around a different batch-melting trajectory (10-20%) (Fig. 12c) that is representative of recycled oceanic lithosphere (Saunders et al., 1988). We, therefore, infer that the basalts are likely to have been derived from multiple sources (i.e. two or more source components were involved).

5.2. Tectonic discrimination

On the Nb vs.Y diagram (Fig. 13a), the felsic volcanics show similarities with volcanic arc granites and syn-collisional granites. One sample from Geçitköy (no. 16-08), with relatively high Nb and Y concentrations, plots near the field of within-plate granite. On the Th/Yb vs. Ta/Yb diagram (Fig. 13b), the volcanics mainly erupted on active continental margins. An active continental margin setting is therefore inferred for the felsic volcanics.

Basalts of the Kyrenia Range (e.g. easterly locations) mostly exhibit a within-plate affinity (Fig. 8). However, some samples, especially in the west, have a subduction-related signature (e.g. negative Nb anomalies) (Fig. 8b-c) akin to volcanic arc basalts. Most samples have a within-plate affinity on the Zr/Y vs. Zr (Fig. 13c) diagram, except for two samples, from Ergenekon and Arapköy (central range), that straddle the island arc and MORB fields. The basalts overlap the MORB and back-arc basin basalt fields on the Ti vs. V plot (Fig. 13d). Clinopyroxene compositions, as shown in the ternary TiO_2-MnO-Na_2O plot (see Supplementary Figure S5), indicate a dominantly within-plate affinity. The relatively high TiO_2 contents of the clinopyroxenes point to an enriched MORB-related source (see Supplementary Figure S5). Overall, the inferred subduction contribution decreases from west to east along the range.

5.3. Global comparison of the Kyrenia Range volcanic rocks

Global comparisons (see Supplementary Figure S6) lend support to our interpretation of the Kyrenia Range volcanic rocks as being subduction-related. In particular, within the Late Cretaceous felsic rocks, the enrichment of Rb, Th and Sm versus the depletion of Ti, Ba, Nb, P compared to primitive mantle, are characteristic of volcanic arc granites (Fig. 6c) (Pearce et al., 1984).

The Kyrenia Range Maastrichtian and Paleogene basalts of within-plate affinities (e.g. Balalan, eastern range) mainly have MORB-normalised spider patterns that are similar to the Pliocene-Quaternary OIB-type basalts of the Tyrrhenian Sea, W Mediterranean (Peccerillo, 2017). The MORB-normalised patterns of these basalts suggest a within-plate eruptive setting, with a small sub-crustal lithosphere metasomatic influence (Kastens et al. 1988; Peccerillo, 2017).

Back-arc basalts of the Early Cretaceous Sarmiento Complex, southern Chile (Saunders et al., 1979) and the Miocene Japan Sea (Tamaki et al., 1990) resemble a minority of the Kyrenia Range basalts (c. 10%; e.g. Geçitköy, western range), although with lower abundances of K, Rb, Ba, Th, Ta and Nb. The relative depletion of these elements is characteristic of eruption in a relatively wide, evolved back-arc basin (e.g. Bransfield Strait; Weaver et al., 1979). However, another possible setting is eruption in a back-arc basin that was influenced by oblique extension (e.g. Guaymas pull-apart basin; Brune et al., 2012). The relatively flat MORB-normalised patterns, akin to E-MORB, of both the Bransfield Strait and Guaymas back-arc basin basalts (e.g. Saunders et al., 1982; Keller et al., 2002) point to substantial involvement of depleted

MORB sources.

5.4. Comparison with the adjacent Tethyan region

Late Cretaceous and Paleogene arc-related rocks; i.e. similar in age of those in the Kyrenia Range are critical to any regional magmatic-tectonic interpretation.

In western Cyprus, a Late Cretaceous arc-derived volcanogenic succession (Kannaviou Formation) overlies the Troodos ophiolite. The volcaniclastic sediments were derived from intermediate-felsic eruptions, c. 6 Ma before the felsic eruptions in the Kyrenia Range (c. 80 vs. 74 Ma). Grain size and textural evidence suggest that, depending on prevailing wind direction and strength, the eruptive centers are likely to have been <100 km away (Chen and Robertson, 2019). The centers for the Kannaviou Formation were located to the south of the Kyrenia Range or its lateral extension, areas that are not now exposed. The Kyrenia Range was affected by south-directed thrusting during Mid-Eocene and Late Miocene-earliest Pliocene (Baroz, 1979; Robertson et al., 2012b, 2014; McCay and Robertson, 2013; Robertson and Kinnaird, 2016), such that the distal (southerly) edge of the inferred over-riding active margin (see below) could have been subducted, structurally over-ridden or eroded. In other words, additional arc units could have existed to the south of their present location in the Kyrenia Range.

To the northeast (c. 200 km), the Misis-Andırın Range in southern Turkey is an extension of the Kyrenia lineament (Robertson et al., 2004). The outcrop, known as the Misis-Andırın Complex, includes massive basalts, pillow lavas, lava breccias and volcaniclastic debris-flows. These lithologies were previously inferred to be Miocene (Floyd et al., 1991, 1992). However, inter-lava sediments there have been dated as Campanian-Maastrichtian (Robertson et al., 2004), similar in age to the oldest basaltic rocks in the Kyrenia Range. The Miocene sediments are structurally intercalated. The basalts of the Misis-Andırın Complex are tholeiitic, with mildly enriched, subduction-related characteristics (e.g. moderate La/Nb ratios), and are interpreted as of back-arc basin origin (Floyd et al., 1991, 1992), which is consistent with our interpretation of the Kyrenia Range basalts (Fig. 14a-b, Supplementary Figure S6).

The Kyrenia Range is backed to the north by the Alanya Massif (Fig. 1), which has been interpreted as a continental fragment, separate from the Tauride carbonate platform to the north (Robertson et al., 2012a; Çetinkaplan et al., 2016). The Alanya Massif is represented by the Late Precambrian-Mesozoic, mainly meta-sedimentary rocks. High pressure-low temperature (HP-LT) metamorphics document Late Cretaceous (82-80 Ma) subduction/exhumation (Oberhänsli et al., 2010, 2013). This is inferred to have taken place along the northern, active margin of the Southern Neotethys (Çetinkaplan et al., 2016; Robertson and Parlak, 2020). The felsic volcanics (Fourkovouno Formation) in the Kyrenia Range could have erupted along the southern (trailing) margin of the Alanya microcontinent where they could have escaped metamorphism. However, they could also represent a separate more southerly unit.

Late Cretaceous continental margin arc-type magmatic rocks also occur extensively farther east, in SE Turkey, as two separate belts.

The most southerly, known Late Cretaceous arc rocks in SE Turkey are exposed in the Helete area, part of a zone of frontal thrust sheets (Yıldırım, 2015; Nurlu et al., 2016) (Fig. 1). Two thrust assemblages are exposed, both cut by granites that have been radiometrically dated at 93-83 Ma (Cenomanian-Campanian) (Nurlu et al., 2016). The lower of the assemblages, the Helete volcanics, comprises arc-related basaltic andesite, andesite, dacite, rhyolite and common tuffaceous rocks. The upper of the two thrust assemblages is a dismembered Late Cretaceous supra-subduction zone-type ophiolite (Meydan ophiolite) (Yıldırım, 2015; Nurlu et al., 2016). The cross-cutting intrusive rocks sealed the thrust sheets during the Late Cretaceous. The granitic rocks are interpreted as a calc-alkaline, subduction-related suite that formed by mixing of mantle and crustal sources, as suggested by Sr-Nd-Pb isotopic data (Nurlu et al., 2016). The granitic rocks exhibit relatively flat chondrite-normalised REE patterns, similar to E-MORB (Nurlu et al., 2016) (Supplementary Figure S6). In contrast, the chondrite-normalised REE patterns of the Kyrenia Range felsic rocks are similar to UCC (Fig. 6c), suggesting a more continentally-influenced setting.

The second belt of arc-related magmatism is located up to c. 100 km farther north and north-east, in the Keban (Malatya), Göksun (Kahramanmaraş) and Baskil (Elazığ) regions (Fig. 1) (Yazgan and Chessex, 1991; Parlak, 2006; Rızaoğlu et al., 2009; Karaoğlan et al., 2013, 2016). Arc-granitic rocks (Baskil intrusives) cut the Late Cretaceous Göksun ophiolite and equivalents (i.e. Berit meta-ophiolite (=North Berit ophiolite), Kömürhan ophiolite and İspendere ophiolite) that are inferred to have formed above a northward-dipping subduction zone (Parlak, 2006). Similar arc granites also cut the structurally over-riding Malayta metamorphic unit, which is interpreted as the southern part of the Tauride microcontinent. The Göksun ophiolite (and equivalents) and the Malayta metamorphic (Tauride) units were juxtaposed along an active continental margin when the arc-granitic rocks were intruded (Robertson et al., 2006; Rızaoğlu et al., 2009; Karaoğlan et al., 2013, 2016).

The extrusive rocks of the Göksun and related ophiolites can also be broadly correlated with widespread assemblages of basic igneous rocks and volcanogenic sediments in the Malatya-Elazığ region, known as the Yüksekova Complex (Perincek and Özkaya, 1981; Aktaş and Robertson, 1984). The basalts have a tholeiitic to tholeiitic-transitional character, variable Zr/Y (1.5-6) ratios and mantle-array-aligned Sr-Nd isotopes (Ural et al., 2015). These basic volcanics were derived from a depleted mantle source without a significant crustal contribution; i.e. from an intra-oceanic setting within the Southern Neotethys (Ural et al., 2015).

The arc rocks that cut both the Göksun (and related) ophiolites and the Malatya Metamorphics (Baskil intrusives) in the northern belt are mainly hornblende-biotite granodiorites and ‘normal’ granites, dated radiometrically at 88-82 Ma (Santonian-

Campanian) (Parlak, 2006; Rızaoğlu et al., 2009; Karaoğlan et al., 2016); i.e. up to c. 5 Ma younger than Helete area granites in the south. These southerly granitic rocks have I-type, calc-alkaline arc affinities, with both mantle and crustal-derivation features (Nurlu et al., 2016). The Baskil intrusions of the northern belt are relatively enriched in LREE (Parlak, 2006; Rızaoğlu et al., 2009) compared to the Helete granites of the south, which suggests a more crustally influenced source during magma genesis for the former. Similarly, the Kyrenia Range basalts have relatively high Zr/Y (2.8-7.7) and Nb/Y (Figs. 12b, 13c), suggestive of a magmatic contribution from continental crust or subducted continentally derived sediments (Zindler and Hart, 1986; Pearce, 1996).

The northerly arc has been explained by northward subduction of Mesozoic oceanic basin (Berit ocean) that was located between two continental units; i.e. the Bitlis and Püturge massifs in the south and the Tauride continent represented by the Malatya Metamorphics in the north (Robertson et al., 2012a; Karaoğlan et al., 2013, 2016; Barrier et al., 2018). The Late Cretaceous arc-related intrusive magmatism of the northern belt in SE Turkey (Baskil intrusives) evolved towards collisional, including shoshonitic compositions (74-72 Ma), which are interpreted to indicate continental and post-collisional settings (Kuşcu et al., 2013; Erturk et al., 2018; Sar et al., 2019). The shoshonitic compositions of some of the granitic rocks, together with the evidence of HP/LT metamorphism, are consistent with the collision of the Tauride carbonate platform (i.e. Malatya Metamorphics) to the north with the Bitlis and Pütürge continental units to the south. However, the origins of shoshonites remain controversial because the necessary partial melting of mantle and interaction with subduction-related fluids can take place in a variety of pre-, syn- and post-collisional settings (e.g. Campbell et al., 2014).

Several authors have correlated the Late Cretaceous Göksun and related ophiolites in the north with the Meydan ophiolite (Berit meta-ophiolite of Yılmaz et al., 1993) in the south. If correct, the granitic intrusives in both belts originated as different parts of a single arc lineament that straddled the northerly active continental margin of the oceanic basin. The southerly arc and ophiolitic rocks (Helete-Meydan) were emplaced southwards during the latest Cretaceous, although further southward thrusting took place, mainly during the Eocene and Miocene (Perinçek and Kozlu, 1984; Yılmaz et al., 1993).

In many reconstructions, oceanic crust still remained between the Bitlis-Püturge continental units and Arabia until the Miocene (Yılmaz, 1993; Robertson et al., 2012a; Barrier et al., 2018; van Hinsbergen et al., 2020). The Bitlis and Püturge massifs have been generally correlated with the Alanya metamorphic massif to the north of Cyprus (with or without a direct continuation) (Çetinkaplan et al., 2016). If correct, the Late Cretaceous Kyrenia Range felsic arc volcanism (and that of the Kannaviou Formation) could have been located to south of the Alanya continent, with a possible eastward continuation to south of the Bitlis and Püturge continental units.

Paleogene magmatic rocks are also present in SE Turkey. Eocene volcanic rocks and associated minor intrusions, known as the Maden Complex, unconformably overlie and cut the Pütürge and Bitlis metamorphosed continental units (Fig. 1) (Hempton, 1985; Yazgan and Chessex, 1991; Aktaş and Robertson, 1984, 1990; Yılmaz, 1993; Elmas and Yılmaz, 2003; Robertson et al., 2006; Erturk et al., 2018). The volcanics show enrichment in LILEs and relative depletion in Nb, Ta and Ti compared to MORB (Erturk et al., 2018), similar to a minority of the subduction-related volcanics in the Kyrenia Range (see Supplementary Figure S6). The Eocene Maden Complex magmatism is widely proposed to relate to back-arc rifting of the (Eurasian) active continental margin during the later stages of northward subduction of the Southern Neotethys, in keeping with the widespread view that collision with Arabia was delayed until the Miocene (Aktaş and Robertson, 1984, 1990; Yılmaz, 1993; Yılmaz et al., 1993; Yiğitbaş and Yılmaz, 1996; Robertson et al., 2006, 2007; van Hinsbergen et al., 2020). Oblique convergence, proposed by several authors (Aktaş and Robertson, 1990;

Elmas and Yılmaz, 2003), could have resulted in along-strike variation in the geochemical signatures of extension versus subduction in the Kyrenia Range, although more geochemical work is needed, regionally and globally to test this hypothesis.

Farther north, Eocene granitic rocks locally cut the continental Malatya metamorphic unit (Doğanşehir region) (Perinçek and Kozlu, 1984; Karaoğlan et al., 2013, 2016). However, no extrusive equivalents are known and, as noted above, the magmatic rocks in this lineament are unlikely to correlate directly with the Kyrenia Range.

During the Miocene, the active continental margin bordering the remnant Southern Neotethys collided with the Arabian passive continental margin to the south. In both the Kyrenia Range and SE Turkey, the Late Cretaceous and Paleogene magmatic rocks are exposed close the thrust front (Eurasia), implying that at least tens of kms of fore-arc crust have been lost (subducted or overridden), potentially removing additional frontal arc-related crust, both Late Cretaceous and Paleogene. Thus, the Kyrenia, Kannaviou (W Cyprus) and Maden Complex magmatism could all represent surviving products of a regional active continental margin.

5.5. Tectono-magmatic hypotheses

In the light of the regional setting, the felsic volcanics (Fourkovouno Formation, c. 74 Ma), with continental margin arc affinities, are interpreted to have resulted from northward subduction beneath continental crust, possibly the Alanya continental unit to the north (Çetinkaplan et al., 2016; Robertson et al., 2020). The felsic volcanism is characteristic of relatively advanced subduction, suggesting that earlier eruptive centers existed along the active continental margin. The early volcanism is likely to be represented by the Campanian (c. 80 Ma) arc-derived volcanogenic sediments

(Kannaviou Formation) in western Cyprus (Robertson, 1977; Gilbert and Robertson, 2013; Chen and Robertson, 2019). The underlying mantle wedge (sub-continental lithosphere) was metasomatically enriched during the Late Cretaceous subduction, with implications for the subsequent basaltic volcanism.

For the Maastrichtian to Late Eocene basaltic volcanics, there are three alternative tectono-magmatic models. The first model envisages a marginal basin setting related to northward subduction. Compared to typical back-arc basin basalts (Fig. 14a-b), the Kyrenia Range basalts have relatively high Th/Nb but low La/Nb ratios. The high abundances of Th are likely to reflect a continental crust influence (Floyd et al., 1991). The variation in La/Nb ratios of the basalts could reflect the influence of a within-plate mantle source (i.e. easterly basalts) and/or the arc maturity; i.e. the arc-like western basalts could have erupted closer to the distal (oceanward) edge of the convergent margin. However, a problem with this model is the absence of evidence for a Paleogene volcanic arc to the south. There is no evidence of arc-derived fallout tuff or volcaniclastic sediments in the Maastrichtian-Paleogene basaltic succession, in contrast with, for example, the SW Pacific Mariana and Tonga marginal basins (Clift, 1994; Bryan et al., 2004).

The second model involves an extensional (or transtensional) setting. In this interpretation, the Late Maastrichtian and Paleogene ‘enriched’ within-plate volcanism was triggered by strike-slip (or transtension) along the active continental margin. One option is that the volcanism was linked to the anticlockwise paleorotation of the Troodos ophiolite to the south during Late Campanian-Early Eocene (Clube et al., 1985; Clube and Robertson, 1986; Morris et al., 2006, 2015; Hodgson et al., 2010). More generally, oblique convergence of the African plate with respect to Eurasia could have resulted in segmentation of the South Neotethyan active margin into subducting segments with arc magmatism, and also strike-slip segments without arc magmatism (Aktaş and Robertson, 1990). A modern example is the Andaman Sea where oblique convergence between the Asian and the Australian plates resulted in segmented arc magmatism (e.g. Curray et al., 2005). However, there is limited information from different modern settings to test this hypothesis.

The third, preferred, scenario is that both the felsic and the basaltic volcanism are related to northward subduction during stages in the closure of the Mesozoic ocean basin to the south. The Late Cretaceous magmatism can then be explained by regional northward subduction (nearly orthogonal) resulting in continental margin arc volcanism. Slab-derived and residual slab components (fluid, melt) were released into the upper mantle lithosphere (e.g. Pearce, 1983; Harangi et al., 2007). The Late Maastrichtian and Paleogene basaltic volcanics then erupted in an extensional (or transtensional) setting, perhaps related to slab rollback and incipient marginal basin formation. Several different mantle sources are likely to have contributed along the Kyrenia Range. The variable subduction-related signatures were inherited from the previously modified mantle lithosphere in this interpretation. Examples of subduction-influenced settings that were affected by later extension-related melting include the Rio Grande Rift, west USA (e.g. Riecker, 1979) and the Neogene north Aegean-west Anatolia volcanic province (e.g. Şengör and Yılmaz, 1981; Ersoy and Palmer, 2013). In summary, the available evidence is consistent with Late Maastrichtian-Paleogene incipient marginal basin formation along the northern, active margin of an ocean basin (Southern Neotethys) that did not close until the Miocene.

5.6. Testing alternative tectonic models

Finally, the Late Cretaceous-Paleogene volcanism in N Cyprus and SE Turkey can be used to test alternative plate tectonic models, including those by Robertson et al. (2012a), Karaoğlan et al. (2013, 2016), Maffione et al. (2017), Barrier et al. (2018), McPhee and van Hinsbergen (2019) and van Hinsbergen et al. (2020), as summarised in Figure 15.

In Reconstruction 1 (Fig. 15a-c) (Robertson et al., 2012a), the Southern Neotethys rifted in the Triassic, while Paleotethys evolved into the Northern Neotethys (İzmir-Ankara-Erzincan ocean). The Kyrenia Range is restored to the northern passive margin of the Southern Neotethys. Both intra-oceanic and continental margin subduction zones (northward-dipping) were active in the Southern Neotethys during the Late Cretaceous. The continental margin arc volcanism was constructed on, or to the south of one, or more, continental blocks (microcontinents), represented by the Kyrenia-Alanya-Püturge-Bitlis lineament in the south and the Malatya-Keban lineament farther north. This reconstruction is compatible with our new evidence.

Reconstruction 2 (Fig. 15d-f) (Barrier et al., 2018) has many common features with (1), in particular the arc volcanism along the northern margin of the Southern Neotethys. However, the Kyrenia, Malatya and Pütürge-Bitlis massifs are restored as a single elongate continental unit rather than as microcontinents, as in (1). Also, little or no oceanic crust is inferred between the southerly continental unit and the Tauride carbonate platform to the north (i.e. Göksun and related ophiolites). This is difficult to reconcile with the Late Cretaceous and Eocene granitic magmatism cutting the Mesozoic Malatya (Keban) platform unless large-scale strike-slip and terrane duplication has taken place for which there is little supporting evidence.

In Reconstruction 3 (Fig. 15g-h) (Maffione et al., 2017; van Hinsbergen et al., 2020), the Kyrenia Range is restored to the southern passive margin of the Mesozoic Tethyan ocean. Late Cretaceous ophiolites that are presently located in several c. E-W, sub-parallel belts (i.e. N and S of the Bitlis and Pütürge massifs) originated above a single subduction zone that originated within Neotethys, dipping generally to the east or northeast (Stampfli and Borel, 2002; Moix et al., 2008). The subduction zone rolled back generally westwards until it collided with the Tauride and Arabian continents. In the south, the subduction zone broke through the oceanic gap between the African and Tauride continents, ‘invaded’ and replaced the Southern Neotethys with Late

Cretaceous supra-subduction zone fore-arc crust. Fore-arc ophiolites were then obducted generally northwards and southwards over the opposing continents (van Hinsbergen et al., 2020). Two alternatives are suggested; in one, the Bitlis and Pütürge continental units are correlated with Arabia (Maffione et al., 2017), whereas in the other these units are correlated with the southern margin of the Tauride continent (van Hinsbergen et al., 2020). The Kyrenia Range (Trypa Group) is placed on the N African continental margin in both alternatives. The metamorphism of the Mesozoic carbonate platform in the Kyrenia Range (Trypa Group) resulted from northeastward underthrusting/subduction beneath the obducted forearc Troodos ophiolite (van Hinsbergen et al., 2020). However, there are several problematic aspects: (1) seismic tomography in the Eastern Mediterranean supports generally northward subduction (e.g. Hafkenscheid et al., 2006), without evidence of a relict southward-dipping slab, as implied by the inferred northward emplacement of some Late Cretaceous ophiolites in S Turkey; (2) it does not allow for the tens to hundreds of km of subduction required to produce the Late Cretaceous arc magmatism in N Cyprus and SE Turkey. The Malatya metamorphic unit, cut by Late Cretaceous granites, is instead restored to the lower, downgoing plate (i.e. beneath the south margin of the Tauride continent) implying northward subduction; (3) the model (van Hinsbergen et al., 2020) does not allow for any Late Cretaceous continental arc-related magmatism in northern Cyprus, SE Turkey or Iran (e.g. Agard et al., 2011); (4) in this model, the proposed Late Eocene-Miocene (post 45 Ma) northward subduction is too young to explain the Late Cretaceous-Paleogene magmatic rocks in the Kyrenia Range and SE Turkey; (5) arc magmatism of Oligocene-Miocene age in S Turkey is absent, although this would be expected if significant northward subduction took place during this time, as in model 3.

6. Conclusions

- Latest Cretaceous mainly felsic volcanic rocks and latest Cretaceous-Paleogene mainly basaltic volcanic rocks are exposed throughout the Kyrenia Range, separated by a thrust.
- Mapping and logging of the key, well-exposed western Kyrenia Range segment shows that the Late Cretaceous felsic arc volcanics occur as variably dismembered thrust sheets in the southerly, frontal part of thrust belt.
- The primary eruptive age of the felsic arc volcanics (Fourkovouno Formation) is c. 74.0 Ma (Late Campanian), based on U-Pb dating of zircons.
- The latest Cretaceous-Paleogene basalts vary geochemically along the Kyrenia Range (E-W). The volcanics in the east resemble normal rift products. In contrast, the volcanics in the west have a subordinate subduction-related signature (e.g. negative Nb anomaly).
- Sr-Nd-Hf isotopic data for the latest Cretaceous-Paleogene basalts suggest that they were derived from several OIB-like mantle sources, with the involvement of a crustally-derived (recycled) component.
- The Kyrenia Range felsic volcanics show some geochemical similarities with the late Cretaceous arc-related rocks in S Turkey (Helete granite; 93-83 Ma). These felsic volcanics are interpreted to represent a fragment of a mature magmatic arc that was active along a regional-scale active continental margin. Regional reconstructions suggest that the Helete granites and related ophiolitic rocks were emplaced southwards from an oceanic basin (Berit ocean) to the north.
- The latest Cretaceous-Paleogene volcanics in the Kyrenia Range have geochemical similarities with the Middle Eocene (c. 47 Ma) basaltic rocks in S Turkey (Maden Complex), suggesting an along-strike continuation of the same active continental margin.

- The latest Cretaceous-Paleogene basaltic volcanics in the Kyrenia Range are interpreted as the products of an incipient marginal basin that developed during northward subduction, possibly related to oblique convergence, prior to collision with Arabia during the Miocene.
- In the light of alternative regional tectonic models, the Late Cretaceous and Paleogene magmatic rocks of N Cyprus are interpreted to represent stages in the development of the northerly active continental margin of the Southern Neotethys.

Acknowledgements

We thank Richard Hinton, Steffen Kutterolf and Dick Kroon for scientific discussion. Mike Hall is thanked for thin section and polished blocks preparation. Nick Odling kindly assisted with the XRF analysis. Antony Morris is thanked for providing the samples of basalt from drill cores that were originally collected for paleomagnetic studies. Rory McKavney kindly assisted with the fieldwork in northern Cyprus. The first author gratefully acknowledges the receipt of a joint studentship of the Principal's Career Development PhD Scholarship and Edinburgh Global Research Scholarship. The authors are grateful for financial support via the Natural Environment Research Council Ion Microprobe Facility (to A.H.F. Robertson) to carry out the secondary ion mass spectrometry U-Pb dating of detrital zircons. Fieldwork and geochemical analysis were aided by financial support from the International Association of Sedimentologists [Postgraduate Grant Scheme], the Mineralogical Society of Great Britain and Ireland [Postgraduate Student Bursary Awards], and the Edinburgh Geological Society [Clough Fund], all to the first author. Additional financial support was provided by the John Dixon Memorial Fund. Osman Parlak is thanked for discussion of SE Turkey geology. The manuscript benefitted from comments by Pamela Kempton, Fatih Karaoğlan and the editor, Greg Shellnutt.

References

Adamia, S.A., Lordkipanidze, M., Zakariadze, G., 1977. Evolution of an active continental margin as exemplified by the Alpine history of the Caucasus. Tectonophysics 40, 183-199.

Agard, P., Omrani, J., Jolivet, L., Whitechurch, H., Vrielynck, B., Spakman, W., Monié, P., Meyer, B., Wortel, R., 2011. Zagros orogeny: a subduction-dominated process. Geological Magazine 148, 692-725.

Aktaş, G., Robertson, A.H.F., 1984. The Maden Complex, SE Turkey: evolution of a Neotethyan active margin, in: Dixon, J.E., Robertson, A.H.F. (Eds.), The Geological Evolution of the Eastern Mediterranean. Geological Society of London, Special Publications 17, pp. 375-402.

Aktaş, G., Robertson, A.H.F., 1990. Tectonic evolution of the Tethys suture zone in SE Turkey: evidence from the petrology and geochemistry of Late Cretaceous and Middle Eocene extrusives, in: Malpas, J., Moores, E.M., Panayiotou, A., Xenophontos, C. (Eds.), Ophiolites-Oceanic Crustal Analogues. Proceedings of the International Symposium ‘Troodos 1987’. Cyprus Geological Survey Department, Nicosia, pp. 311-329.

Baroz, F., 1979. Etude géologique dans le Pentadaktylos et la Mesaoria (Chypre Septentrionale). Doctor of Science Thesis (Published). Université de Nancy, France (434 pp).

Baroz, F., 1980. Volcanism and continent-island arc collision in the Pentadaktylos range, Cyprus, in: Panayiotou, A. (Ed.), Ophiolites: Proceedings of the International Ophiolite Symposium. Cyprus Ministry of Agriculture and Natural Resources, Geology Survey Department, Nicosia, Cyprus, pp. 73-85.

Barrier, E., Vrielynck, B., Brouillet, J.F., Brunet, M.F., 2018. Paleotectonic Reconstruction of the Central Tethyan Realm. Tectono-Sedimentary-Palinspastic Maps from Late Permian to Pliocene. Atlas of 20 maps (scale 1/15000000).

CCGM/CGMW, Paris.

Beccaluva, L., Macciotta, G., Piccardo, G., Zeda, O., 1989. Clinopyroxene composition of ophiolite basalts as petrogenetic indicator. Chemical Geology 77, 165-182.

Bowman, N., Van Otterloo, J., Cairns, C., Taylor, D., Cas, R., 2019. Complex evolution of volcanic arcs: The lithofacies and palaeogeography of the Cambrian Stavely Arc, Delamerian Fold Belt, Western Victoria. Journal of Volcanology and Geothermal Research 373, 120-132.

Brune, S., Popov, A.A., Sobolev, S.V., 2012. Modeling suggests that oblique extension facilitates rifting and continental break-up. Journal of Geophysical Research: Solid Earth 117. doi: 10.1029/2011JB008860

Bryan, S., Cook, A., Evans, J., Colls, P., Wells, M., Lawrence, M., Jell, J., Greig, A., Leslie, R., 2004. Pumice rafting and faunal dispersion during 2001–2002 in the Southwest Pacific: record of a dacitic submarine explosive eruption from Tonga. Earth and Planetary Science Letters 227, 135-154.

Campbell, I.H., Stepanov, A.S., Liang, H.-Y., Allen, C.M., Norman, M.D., Zhang, Y.-Q., Xie, Y.-W., 2014. The origin of shoshonites: new insights from the Tertiary high-potassium intrusions of eastern Tibet. Contributions to Mineralogy and Petrology 167. doi: 10.1007/s00410-014-0983-9

Çetinkaplan, M., Pourteau, A., Candan, O., Koralay, O.E., Oberhänsli, R., Okay, A.I., Chen, F., Kozlu, H., Şengün, F., 2016. P–T–t evolution of eclogite/blueschist facies metamorphism in Alanya Massif: time and space relations with HP event in Bitlis Massif, Turkey. International Journal of Earth Sciences 105, 247-281.

Chappell, B.W., White, A.J.R., 1992. I- and S-type granites in the Lachlan Fold Belt. Earth and Environmental Science Transactions of the Royal Society of Edinburgh 83, 1-26.

Chen, G., Robertson, A.H.F., 2019. Provenance and magmatic-tectonic setting of Campanian-aged volcaniclastic sandstones of the Kannaviou Formation in western Cyprus: Evidence for a South-Neotethyan continental margin volcanic arc.

Sedimentary Geology 388, 114-138.

Chen, S.-s., Liu, J.-q., Chen, S.-s., Guo, Z.-f., Sun, C.-q., 2015. Variations in the geochemical structure of the mantle wedge beneath the northeast Asian marginal region from pre- to post-opening of the Japan Sea. Lithos 224-225, 324-341.

Clift, P., 1994. Controls on the Sedimentary and Subsidence History of an Active Plate Margin: An Example from the Tonga Arc (Southwest Pacific), in: Hawkins, J., Parson, L., Allan, J. (Eds.), Proceedings of the Ocean Drilling Program, Scientific Results. Ocean Drilling Program 135, College Station, TX, pp. 173–189.

Clube, T.M.M., Creer, K.M., Robertson, A.H.F., 1985. Palaeorotation of the Troodos microplate, Cyprus. Nature 317, 522-525.

Clube, T.M.M., Robertson, A.H.F., 1986. The palaeorotation of the Troodos microplate, Cyprus, in the Late Mesozoic-Early Cenozoic plate tectonic framework of the Eastern Mediterranean. Surveys in Geophysics 8, 375-437.

Condie, K.C., 2003. Incompatible element ratios in oceanic basalts and komatiites: tracking deep mantle sources and continental growth rates with time. Geochemistry, Geophysics, Geosystems 4, 1005. doi:10.1029/2002GC000333

Condie, K.C., 2005. High field strength element ratios in Archean basalts: a window to evolving sources of mantle plumes? Lithos 79, 491-504.

Curray, J.R., 2005. Tectonics and history of the Andaman Sea region. Journal of Asian Earth Sciences 25, 187-232.

Dercourt, J., Ricou, L.E., Vrielynck, B., 1993. Atlas of Peri-Tethys Palaeogeographical Maps. CCGM/CGMW, Paris (268 pp).

Dewey, J.F., 1969. Evolution of the Appalachian/Caledonian orogen. Nature 222, 124-129.

Ducloz, C., 1972. The geology of the Bellapais-Kythrea area of the Central Kyrenia Range. Bulletin of the Geological Survey Department 6, Nicosia, Cyprus (75 pp).

Elmas, A., Yılmaz, Y., 2003. Development of an oblique subduction zone-tectonic evolution of the Tethys suture zone in southeast Turkey. International Geology

Review 45, 827-840.

Ersoy, E.Y., Palmer, M.R., 2013. Eocene-Quaternary magmatic activity in the Aegean: implications for mantle metasomatism and magma genesis in an evolving orogeny. Lithos 180, 5-24.

Erturk, M.A., Beyarslan, M., Chung, S.L., Lin, T.H., 2018. Eocene magmatism (Maden Complex) in the Southeast Anatolian Orogenic Belt: Magma genesis and tectonic implications. Geoscience Frontiers 9, 1829-1847.

Fitton, J.G., Godard, M., 2004. Origin and evolution of magmas on the Ontong Java Plateau, in: Fitton, J.G., Mahoney, J.J., Wallace, P.J., Saunders, A.D. (Eds.), Origin and Evolution of the Ontong Java Plateau. Geological Society of London, Special Publications 229, pp. 151-178.

Fitton, J.G., Saunders, A.D., Larsen, L.M., Hardarson, B.S., Norry, M.J., 1998. Volcanic rocks from the southeast Greenland margin at 63°N: composition, petrogenesis and mantle sources, in: Saunders, A.D., Larsen, H.C., Wise, S.W. (Eds.), Proceedings of the Ocean Drilling Program, Scientific Results. Ocean Drilling Program 152, College Station, TX, pp. 331-350.

Floyd, P., Kelling, G., Gökçen, S., Gökçen, N., 1991. Geochemistry and tectonic environment of basaltic rocks from the Misis ophiolitic mélange, south Turkey. Chemical Geology 89, 263-280.

Floyd, P., Kelling, G., Gökçen, S., Gökçen, N., 1992. Arc-related origin of volcaniclastic sequences in the Misis Complex, Southern Turkey. The Journal of Geology 100, 221-230.

Garfunkel, Z., 1998. Constrains on the origin and history of the Eastern Mediterranean basin. Tectonophysics 298, 5-35.

Gilbert, M.F., Robertson, A.H.F., 2013. Field relations, geochemistry and origin of the Upper Cretaceous volcaniclastic Kannaviou Formation in western Cyprus: evidence of a southerly Neotethyan volcanic arc, in: Robertson, A.H.F., Parlak, O., Ünlügenç, U.C. (Eds.), Geological Development of Anatolia and the Easternmost

Mediterranean Region. Geological Society of London, Special Publications 372, pp. 273-298.

Gorton, M.P., Schandl, E.S., 2000. From continents to island arcs: a geochemical index of tectonic setting for arc-related and within-plate felsic to intermediate volcanic rocks. The Canadian Mineralogist 38, 1065-1073.

Hafkenscheid, E., Wortel, M., Spakman, W., 2006. Subduction history of the Tethyan region derived from seismic tomography and tectonic reconstructions. Journal of Geophysical Research: Solid Earth 111, B08401. doi: 10.1029/2005JB003791

Hakyemez, Y., Turhan, N., Sönmez, I., Sümengen, M., 2000. Kuzey Kıbrıs Türk Cumhuriyeti'nin Jeolojisi (Geology of the Turkish Republic of Northern Cyprus). Genel Müdürlüğü Jeoloji Etütleri Diaresi, Maden Tektik ve Arama, Ankara (44 pp).

Harangi, S., Downes, H., Thirlwall, M., Gmeling, K., 2007. Geochemistry, Petrogenesis and Geodynamic Relationships of Miocene Calc-alkaline Volcanic Rocks in the Western Carpathian Arc, Eastern Central Europe. Journal of Petrology 48, 2261-2287.

Hartley, M.E., Thordarson, T., 2013. The 1874-1876 volcano-tectonic episode at Askja, North Iceland: Lateral flow revisited. Geochemistry, Geophysics, Geosystems 14, 2286-2309.

Hastie, A.R., Kerr, A.C., Pearce, J.A., Mitchell, S.F., 2007. Classification of Altered Volcanic Island Arc Rocks using Immobile Trace Elements: Development of the Th–Co Discrimination Diagram. Journal of Petrology 48, 2341-2357.

Hayward, C., 2011. High spatial resolution electron probe microanalysis of tephras and melt inclusions without beam-induced chemical modification. The Holocene 22, 119-125.

Hempton, M.R., 1985. Structure and deformation history of the Bitlis suture near Lake Hazar, southeastern Turkey. Geological Society of America Bulletin 96, 233-243.

Hodgson, E., Morris, A., Anderson, M., Robertson, A., 2010. First palaeomagnetic results from the Kyrenia Range terrane of northern Cyprus and their implication for the regional plate tectonic evolution of the eastern Mediterranean, EGU General Assembly Conference Abstracts, Vienna, Austria, p. 6449.

Hu, Z., Gao, S., 2008. Upper crustal abundances of trace elements: a revision and update. Chemical Geology 253, 205-221.

Huang, K., Malpas, J., Xenophontos, C., 2007. Geological studies of igneous rocks and their relationships along the Kyrenia Range, in: Moumani, K., Shawabkeh, K., Al-Malabeh, A., Abdelghafoor, M. (Eds.), 6th International Congress of Eastern Mediterranean Geology, Amman, Jordan, p. 53.

Karaoğlan, F., Parlak, O., Hejl, E., Neubauer, F., Kloetzli, U., 2016. The temporal evolution of the active margin along the Southeast Anatolian Orogenic Belt (SE Turkey): Evidence from U–Pb, Ar–Ar and fission track chronology. Gondwana Research 33, 190-208.

Karaoğlan, F., Parlak, O., Robertson, A., Thöni, M., Klötzli, U., Koller, F., Okay, A.İ., 2013. Evidence of Eocene high-temperature/high-pressure metamorphism of ophiolitic rocks and granitoid intrusion related to Neotethyan subduction processes (Doğanşehir area, SE Anatolia), in: Robertson, A.H.F., Parlak, O., Ünlügenç, U.C. (Eds.), Geological Development of Anatolia and the Easternmost Mediterranean Region. Geological Society of London, Special Publications 372, pp. 249-272.

Keller, R.A., Fisk, M.R., Smellie, J.L., Strelin, J.A., Lawver, L.A., 2002. Geochemistry of back arc basin volcanism in Bransfield Strait, Antarctica: Subducted contributions and along-axis variations. Journal of Geophysical Research: Solid Earth 107. doi: 10.1029/2001JB000444

Kelly, N., Hinton, R., Harley, S., Appleby, S., 2008. New SIMS U–Pb zircon ages from the Langavat Belt, South Harris, NW Scotland: implications for the Lewisian terrane model. Journal of the Geological Society 165, 967-981.

Kempton, P.D., Downes, H., Lustrino, M., 2018. Pb and Hf isotope evidence for mantle enrichment processes and melt interactions in the lower crust and lithospheric mantle in Miocene orogenic volcanic rocks from Monte Arcuentu (Sardinia, Italy). Geosphere 14, 926-950.

Kuşcu, İ., Tosdal, R.M., Gencalioğlu-Kuşcu, G., Friedman, R., Ullrich, T.D., 2013. Late Cretaceous to Middle Eocene Magmatism and Metallogeny of a Portion of the Southeastern Anatolian Orogenic Belt, East-Central Turkey. Economic Geology 108, 641-666.

Le Pichon, X., 1982. Land-locked oceanic basins and continental collision: the Eastern Mediterranean as a case example, in: Hsü, K.J. (Ed.), Mountain building processes. Academic Press, New York, pp. 201-211.

Li, C.-F., Li, X.-H., Li, Q.-L., Guo, J.-H., Li, X.-H., Yang, Y.-H., 2012. Rapid and precise determination of Sr and Nd isotopic ratios in geological samples from the same filament loading by thermal ionization mass spectrometry employing a single-step separation scheme. Analytica Chimica Acta 727, 54-60.

Ludwig, K.R., 2012. Users manual for Isoplot 3.75. A geochronological toolkit for Microsoft Excel. Berkeley Geochronology Centre, Special Publication No. 5, Berkeley.

Maffione, M., van Hinsbergen, D.J., de Gelder, G.I., van der Goes, F.C., Morris, A., 2017. Kinematics of Late Cretaceous subduction initiation in the Neo-Tethys Ocean reconstructed from ophiolites of Turkey, Cyprus, and Syria. Journal of Geophysical Research: Solid Earth 122, 3953-3976.

McCay, G.A., Robertson, A.H.F., 2013. Upper Miocene–Pleistocene deformation of the Girne (Kyrenia) Range and Dar Dere (Ovgos) lineaments, northern Cyprus: role in collision and tectonic escape in the easternmost Mediterranean region, in: Robertson, A.H.F., Parlak, O., Ünlügenç, U.C. (Eds.), Geological Development of Anatolia and the Easternmost Mediterranean Region. Geological Society of London, Special Publications 372, pp. 421-445.

McCay, G.A., Robertson, A.H.F., Kroon, D., Raffi, I., Ellam, R.M., Necdet, M., 2013. Stratigraphy of Cretaceous to Lower Pliocene sediments in the northern part of Cyprus based on comparative $^{87}Sr/^{86}Sr$ isotopic, nannofossil and planktonic foraminiferal dating. Geological Magazine 150, 333-359.

McPhee, P.J., van Hinsbergen, D.J., 2019. Tectonic reconstruction of Cyprus reveals Late Miocene continental collision of Africa and Anatolia. Gondwana Research 68, 158-173.

Moix, P., Beccaletto, L., Kozur, H.W., Hochard, C., Rosselet, F., Stampfli, G.M., 2008. A new classification of the Turkish terranes and sutures and its implication for the paleotectonic history of the region. Tectonophysics 451, 7-39.

Moore, T.A., 1960. The geology and mineral resources of the Astromeritis-Kormakiti area. Geological Survey Department, Memoir 6, Nicosia, Cyprus (96 pp).

Morris, A., Anderson, M.W., Inwood, J., Robertson, A.H., 2006. Palaeomagnetic insights into the evolution of Neotethyan oceanic crust in the eastern Mediterranean, in: Robertson, A.H.F., Mountrakis, D. (Eds.), Tectonic Development of the Eastern Mediterranean Region. Geological Society of London, Special Publications 260, pp. 351-372.

Morris, A., Robertson, A.H.F., Anderson, M.W., Hodgson, E., 2015. Did the Kyrenia Range of northern Cyprus rotate with the Troodos–Hatay microplate during the tectonic evolution of the eastern Mediterranean? International Journal of Earth Sciences 105, 399-415.

Nisbet, E.G. Pearce, J.A., 1977. Clinopyroxene composition in mafic lavas from different tectonic settings. Contributions to Mineralogy and Petrology 63, 149-160.

Nurlu, N., Parlak, O., Robertson, A.H.F., von Quadt, A., 2016. Implications of Late Cretaceous U–Pb zircon ages of granitic intrusions cutting ophiolitic and volcanogenic rocks for the assembly of the Tauride allochthon in SE Anatolia (Helete area, Kahramanmaraş Region, SE Turkey). International Journal of Earth Sciences 105, 283-314.

Oberhänsli, R., Candan, O., Bousquet, R., Rimmele, G., Okay, A., Goff, J., 2010. Alpine high pressure evolution of the eastern Bitlis complex, SE Turkey, in: Sosson, M., Kaymakci, N., Stephenson, R.A., Bergerat, F., Starostenko, V. (Eds.), Sedimentary Basin Tectonics from the Black Sea and Caucasus to the Arabian Platform. Geological Society of London, Special Publications 340, pp. 461-483.

Oberhänsli, R., Koralay, E., Candan, O., Pourteau, A., Bousquet, R., 2013. Late Cretaceous eclogitic high-pressure relics in the Bitlis Massif. Geodinamica Acta 26, 175-190.

Parlak, O., 2006. Geodynamic significance of granitoid magmatism in the southeast Anatolian orogen: geochemical and geochronogical evidence from Göksun–Afşin (Kahramanmaraş, Turkey) region. International Journal of Earth Sciences 95, 609-627.

Pearce, J.A., 1975. Basalt geochemistry used to investigate past tectonic environments on Cyprus. Tectonophysics 25, 41-67.

Pearce, J.A., 1983. Role of the sub-continental lithosphere in magma genesis at active continental margins, in: Hawkersworth, C.J., Norry, M.J. (Eds.), Continental Basalts and Mantle Xenoliths. Shiva, Cheshire, UK, pp. 230-249.

Pearce, J.A., 1996. A user’s guide to basalt discrimination diagrams, in: Wyman, D.A. (Ed.), Trace Element Geochemistry of Volcanic Rocks: Applications for Massive Sulphide Exploration. Geological Association of Canada, Short Course Notes 12, pp. 79-113.

Pearce, J.A., Cann, J., 1973. Tectonic setting of basic volcanic rocks determined using trace element analyses. Earth and Planetary Science Letters 19, 290-300.

Pearce, J.A., Harris, N.B., Tindle, A.G., 1984. Trace element discrimination diagrams for the tectonic interpretation of granitic rocks. Journal of Petrology 25, 956-983.

Pearce, J.A., Norry, M.J., 1979. Petrogenetic implications of Ti, Zr, Y, and Nb variations in volcanic rocks. Contributions to Mineralogy and Petrology 69, 33-47.

Peccerillo, A., 2017. Cenozoic Volcanism in the Tyrrhenian Sea Region. Springer

International Publishing, Cham (399 pp).

Perinçek, D., Kozlu, H., 1984. Stratigraphy and structural relations of the units in the Afşin-Elbistan-Doğanşehir region (Eastern Taurus), in: Tekeli, O., Göncüoğlu, M.C. (Eds.), Geology of the Taurus Belt: Proceedings of the International Symposium. Maden Tetkik ve Arama Enstitüsü, Ankara, pp. 181-198.

Perinçek, D., Özkaya, İ., 1981. Tectonic evolution of the northern margin of Arabian plate. Bulletin of Institute of Earth Science, Hacettepe University 8, 91-101.

Rice, S.P., Robertson, A.H.F., Ustaömer, T., 2006. Late Cretaceous-Early Cenozoic tectonic evolution of the Eurasian active margin in the Central and Eastern Pontides, northern Turkey, in: Robertson, A.H.F., Mountrakis, D. (Eds.), Tectonic Development of the Eastern Mediterranean Region. Geological Society of London, Special Publications 260, pp. 413-445.

Riecker, R.E., 1979. Rio Grande Rift: Tectonics and Magmatism. American Geophysical Union, Washington, DC (438 pp).

Rızaoğlu, T., Parlak, O., Höck, V., Koller, F., Hames, W.E., Billor, Z., 2009. Andean-type active margin formation in the eastern Taurides: Geochemical and geochronogical evidence from the Baskil granitoid (Elazığ, SE Turkey). Tectonophysics 473, 188-207.

Robertson, A.H.F., 1977. The Kannaviou Formation, Cyprus: volcaniclastic sedimentation of a probable Late Cretaceous volcanic arc. Journal of the Geological Society 134, 269-292.

Robertson, A.H.F., Dixon, J.E., 1984. Introduction: aspects of the geological evolution of the Eastern Mediterranean, in: Dixon, J.E., Robertson, A.H.F. (Eds.), The Geological Evolution of the Eastern Mediterranean. Geological Society of London, Special Publications 17, pp. 1-74.

Robertson, A.H.F., Kinnaird, T.C., 2016. Structural development of the central Kyrenia Range (north Cyprus) in its regional setting in the eastern Mediterranean region. International Journal of Earth Sciences 105, 417-437.

Robertson, A.H.F., Parlak, O., 2020. Late Cretaceous-Palaeocene subduction-collision-exhumation of a microcontinent along the northern, active margin of South Neotethys: evidence from the Alanya Massif and the adjacent Antalya Complex (S Turkey). Journal of Asian Earth Sciences, 104467. doi: 10.1016/j.jseaes.2020.104467

Robertson, A.H.F., Parlak, O., Kinnaird, T.C., Taslı, K., Dumitrica, P., 2020. Cambrian-Eocene pre-rift, pulsed rift, passive margin and emplacement processes along the northern margin of the Southern Neotethys: Evidence from the Antalya Complex in the Alanya Window (S Turkey). Journal of Asian Earth Sciences: X 3, 100026. doi: 10.1016/j.jaesx.2020.100026

Robertson, A.H.F., Parlak, O., Rizaoğlu, T., Ünlügenç, Ü., İnan, N., Tasli, K., Ustaömer, T., 2007. Tectonic evolution of the South Tethyan ocean: evidence from the Eastern Taurus Mountains (Elazığ region, SE Turkey), in: Ries, A.C., Butler, R.W.H., Graham, R.H. (Eds.), Deformation of the Continental Crust: The Legacy of Mike Coward. Geological Society of London, Special Publications 272, pp. 231-270.

Robertson, A.H.F., Parlak, O., Ustaömer, T., 2012a. Overview of the Palaeozoic-Neogene evolution of Neotethys in the Eastern Mediterranean region (southern Turkey, Cyprus, Syria). Petroleum Geoscience 18, 381-404.

Robertson, A.H.F., Tasli, K., İnan, N., 2012b. Evidence from the Kyrenia Range, Cyprus, of the northerly active margin of the Southern Neotethys during Late Cretaceous–Early Cenozoic time. Geological Magazine 149, 264-290.

Robertson, A.H.F., Unlügenç, Ü.C., İnan, N., Tasli, K., 2004. The Misis-Andırın Complex: a Mid-Tertiary melange related to late-stage subduction of the Southern Neotethys in S Turkey. Journal of Asian Earth Sciences 22, 413-453.

Robertson, A.H.F., Ustaömer, T., Parlak, O., Ünlügenç, U.C., Taşlı, K., İnan, N., 2006. The Berit transect of the Tauride thrust belt, S Turkey: Late Cretaceous-Early Cenozoic accretionary/collisional processes related to closure of the Southern

Neotethys. Journal of Asian Earth Sciences 27, 108-145.

Robertson, A.H.F., Woodcock, N.H., 1979. Mamonia Complex, southwest Cyprus: Evolution and emplacement of a Mesozoic continental margin. Geological Society of America Bulletin 90, 651-665.

Robertson, A.H.F., Woodcock, N.H., 1986. The role of the Kyrenia Range Lineament, Cyprus, in the geological evolution of the eastern Mediterranean area. Philosophical Transactions of the Royal Society of London. Series A, Mathematical and Physical Sciences 317, 141-177.

Rollinson, H.R., 1993. Using Geochemical Data: Evaluation, Presentation, Interpretation. Routledge, London (384 pp).

Rubatto, D., 2002. Zircon trace element geochemistry: partitioning with garnet and the link between U–Pb ages and metamorphism. Chemical Geology 184, 123-138.

Rudnick, R.L., Gao, S., 2003. Composition of the continental crust, in: Holland, H.D., Turekian, K.K. (Eds.), Treatise on geochemistry. Elsevier-Pergamon 3, Oxford, pp. 1-64.

Sar, A., Ertürk, M.A., Rizeli, M.E., 2019. Genesis of Late Cretaceous intra-oceanic arc intrusions in the Pertek area of Tunceli Province, eastern Turkey, and implications for the geodynamic evolution of the southern Neo-Tethys: Results of zircon U–Pb geochronology and geochemical and Sr–Nd isotopic analyses. Lithos 350-351, 105263. doi: 10.1016/j.lithos.2019.105263

Saunders, A.D., Fornari, D.J., Joron, J., Tarney, J., Treuil, M., 1982. Geochemistry of basic igneous rocks, Gulf of California, Deep Sea Drilling Project Leg 64, in: Curray, J.R., Moore, D.G., Kelts, K. (Eds.), Initial Reports of the Deep Sea Drilling Project. Ocean Drilling Program 64, College Station, TX, pp. 595-642.

Saunders, A.D., Tarney, J., Stern, C.R., Dalziel, I.W., 1979. Geochemistry of Mesozoic marginal basin floor igneous rocks from southern Chile. Geological Society of America Bulletin 90, 237-258.

Şengör, A.M.C., Natal'in, B.A., 1996. Turkic-type orogeny and its role in the making of the continental crust. Annual Review of Earth and Planetary Sciences 24, 263-337.

Şengör, A.M.C., Yılmaz, Y., 1981. Tethyan evolution of Turkey: a plate tectonic approach. Tectonophysics 75, 181-241.

Şengör, A.M.C., Yılmaz, Y., Sungurlu, O., 1984. Tectonics of the Mediterranean Cimmerides: nature and evolution of the western termination of Palaeo-Tethys, in: Dixon, J.E., Robertson, A.H.F. (Eds.), The Geological Evolution of the Eastern Mediterranean. Geological Society of London, Special Publications 17, pp. 77-112.

Shervais, J.W., 1982. Ti-V plots and the petrogenesis of modern and ophiolitic lavas. Earth and Planetary Science Letters 59, 101-118.

Stampfli, G.M., Borel, G., 2002. A plate tectonic model for the Paleozoic and Mesozoic constrained by dynamic plate boundaries and restored synthetic oceanic isochrons. Earth and Planetary Science Letters 196, 17-33.

Sun, S.-s., McDonough, W.F., 1989. Chemical and isotopic systematics of oceanic basalts: implications for mantle composition and processes, in: Saunders, A.D., Norry, M.J. (Eds.), Magmatism in the Ocean Basins. Geological Society of London, Special Publications 42, pp. 313-345.

Tamaki, K., Pisciotto, K., Allan, J., Alexandrovich, J.M., Barnes, D.A., Boggs, S., Brumsack, H., Brunner, C.A., Cramp, A., Jolivet, L., Kawka, O.E., Koizumi, I., Kuramoto, S.i., Langseth, M.G., McEvoy, J., Meredith, J.A., Mertz, K.A., Murray, R.W., Nobes, D.C., Rahman, A., Schaar, R., Stewart, K.P., Tada, R., Thy, P., Vigliotti, L., White, L.D., Wippern, J., Yamashita, S., 1990. Proceedings of the Ocean Drilling Program, Initial Reports vol. 127. Ocean Drilling Program.

Tatsumi, Y., Kogiso, T., 2003. The subduction factory: its role in the evolution of the Earth's crust and mantle, in: Larter, R.D., Leat, P.T. (Eds.), Intra-Oceanic Subduction Systems: Tectonic and Magmatic Processes. Geological Society of London, Special Publications 219, pp. 55-80.

Thirlwall, M., 1991. Long-term reproducibility of multicollector Sr and Nd isotope ratio analysis. Chemical Geology 94, 85-104.

Trehu, A., Asudeh, I., Brocher, T., Luetgert, J., Mooney, W., Nabelek, J., Nakamura, Y., 1994. Crustal architecture of the Cascadia forearc. Science 266, 237-243.

Ural, M., Arslan, M., Göncüoglu, M., Tekin, U., Kürüm, S., 2015. Late Cretaceous arc and back-arc formation within the southern Neotethys: Whole-rock, trace element and Sr-Nd-Pb isotopic data from basaltic rocks of the Yüksekova Complex (Malatya- Elazığ, SE Turkey). Ofioliti 40, 52-72.

Ustaömer, P.A., Ustaömer, T., Robertson, A.H.F., 2012. Ion probe U-Pb dating of the Central Sakarya basement: a peri-Gondwana terrane intruded by late Lower Carboniferous subduction/collision-related granitic rocks. Turkish Journal of Earth Sciences 21, 905-932.

Ustaömer, T., Robertson, A.H.F., 1997. Tectonic-sedimentary evolution of the North-Tethyan active margin in the Central Pontides of Northern Turkey, in: Robinson, A.G. (Ed.), Regional and Petroleum Geology of the Black Sea and Surrounding Region. AAPG Memoirs 68, pp. 255-290.

van Hinsbergen, D.J., Torsvik, T.H., Schmid, S.M., Maţenco, L.C., Maffione, M., Vissers, R.L., Gürer, D., Spakman, W., 2020. Orogenic architecture of the Mediterranean region and kinematic reconstruction of its tectonic evolution since the Triassic. Gondwana Research 81, 79-229.

Wang, Y., Fan, W., Zhang, Y., Guo, F., Zhang, H., Peng, T., 2004. Geochemical, 40Ar/39Ar geochronological and Sr–Nd isotopic constraints on the origin of Paleoproterozoic mafic dikes from the southern Taihang Mountains and implications for the ca. 1800Ma event of the North China Craton. Precambrian Research 135, 55-77.

Weaver, S.D., Saunders, A.D., Pankhurst, R.J., Tarney, J., 1979. A geochemical study of magmatism associated with the initial stages of back-arc spreading. Contributions to Mineralogy and Petrology 68, 151-169.

Weis, D., Kieffer, B., Hanano, D., Nobre Silva, I., Barling, J., Pretorius, W., Maerschalk, C., Mattielli, N., 2007. Hf isotope compositions of US Geological Survey reference materials. Geochemistry, Geophysics, Geosystems 8, 57-77.

Weis, D., Kieffer, B., Maerschalk, C., Barling, J., De Jong, J., Williams, G.A., Hanano, D., Pretorius, W., Mattielli, N., Scoates, J.S., 2006. High-precision isotopic characterization of USGS reference materials by TIMS and MC-ICP-MS. Geochemistry, Geophysics, Geosystems 7, Q08006. doi: 10.1029/2006GC001283

Whalen, J.B., Currie, K.L., Chappell, B.W., 1987. A-type granites: geochemical characteristics, discrimination and petrogenesis. Contributions to Mineralogy and Petrology 95, 407-419.

Winchester, J., Floyd, P., 1977. Geochemical discrimination of different magma series and their differentiation products using immobile elements. Chemical Geology 20, 325-343.

Yazgan, E., Chessex, R., 1991. Geology and Tectonic Evolution of the Southeastern Taurides in the Region of Malatya. Turkish Association of Petroleum Geologists 3, 1-42.

Yiğitbaş, E., Yılmaz, Y., 1996. Post-Late Cretaceous strike-slip tectonics and its implications for the Southeast Anatolian orogen, Turkey. International Geology Review 38, 818-831.

Yıldırım, E., 2015. Geochemistry, petrography and tectonic significance of the ophiolitic rocks, felsic intrusions and Eocene volcanic rocks of an imbrication zone (Helete area, Southeast Turkey). Journal of African Earth Sciences 107, 89-107.

Yılmaz, Y., 1993. New evidence and model on the evolution of the southeast Anatolian orogen. Geological Society of America Bulletin 105, 251-271.

Yılmaz, Y., Yiğitbaş, E., Genç, Ş.C., 1993. Ophiolitic and metamorphic assemblages of southeast Anatolia and their significance in the geological evolution of the orogenic belt. Tectonics 12, 1280-1297.

Zhang, Y., Wang, Y., Geng, H., Zhang, Y., Fan, W., Zhong, H., 2013. Early

Neoproterozoic (~850Ma) back-arc basin in the Central Jiangnan Orogen (Eastern South China): Geochronological and petrogenetic constraints from meta-basalts. Precambrian Research 231, 325-342.

Zindler, A., Hart, S., 1986. Chemical geodynamics. Annual Review of Earth and Planetary Sciences 14, 493-571.

Listing of Figures

Fig. 1 Outline tectonic map of the Eastern Mediterranean region, including the main volcanic units mentioned in the text. The tectonic framework is modified after Robertson et al. (2012a). Note the location of the Kyrenia Range in northern Cyprus (red box). Jurassic, Cretaceous and Eocene igneous rocks are shown in blue, red and yellow, respectively (see the text for literature sources).

Fig. 2 Successions shown in two main thrust sheets exposed in the Kyrenia Range, northern Cyprus. (a) Simplified log of the succession in the largest thrust sheet including the latest Cretaceous-Paleogene volcanics (Melounda Formation); (b) Restored log of the small, dismembered frontal thrust sheets that expose the Late Cretaceous felsic volcanics (Fourkovouno Formation) (data from Baroz, 1979; Robertson et al., 2012b and this study).

Fig. 3 (a) Outline geological map of the Kyrenia Range (modified from Robertson et al., 2012b). Locations from which basalts were collected are numbered on the map, with small yellow boxes. Karpas Peninsula: 1-Balalan (Platanissos); Eastern Range: 2-Ağıllar (Mandres), 3-Çınarlı (Platani), 4-Mallıdağ (Melounda); Central Range: 5-Tirmen (Trypimeni), 6-Ergenekon (Agios Khariton), 7-Değirmenlik (Kythrea), 8-Arapköy (Klepini), 9-Beylerbeyi (Bellapais), 10-Boğaz (Bogaz), 11-Pınarbaşı (Krini), 12-İncesu (Motides), 13-Alevkaya Tepe (Kiparisso Vouno); Western Range, 14-Karşıyaka (Vasileia), 15-Geçitköy (Panagra); (b) Geological map of the western Kyrenia Range, northern Cyprus made during this study (based on mapping by Baroz, 1979). Locations of cross sections (AA', BB' and CC') are indicated. Note that the two contrasting, mainly felsic and mainly basaltic volcanic units are separated by a thrust fault (Robertson et al., 2012b; this study; see Fig. 2).

Fig. 4 (a) A-A' cross section of Geçitköy that is dominated by a south-verging, recumbent anticline (Late Miocene-earliest Pliocene); (b) B-B' cross-section of Selvilitepe showing southward imbrication of basalt/pelagic chalk and felsic volcanogenic rocks; (c) C-C' cross-section showing imbricated felsic volcanogenic rocks.

Fig. 5 Measured stratigraphic logs of partial successions in the felsic volcanics and structurally associated units. The structural lower unit (logs a-e) is relatively intact, whereas the higher unit (logs f-j) is characterised by the thrust intercalations with the Trypa Group.Fig. 6 (a) Zr/Ti vs. Nb/Y diagram (after Pearce, 1996) and (b) Th vs. Co diagram (after Hastie et al., 2007) for the Kyrenia Range felsic rocks; (c) Primitive mantle-normalised multi-element spider diagram and (d) chondrite-normalised rare earth element (REE) patterns of the felsic volcanics with reference data for upper continental crust (UCC) and lower continental crust (LCC). Normalising values of primitive mantle and chondrite after Sun and McDonough (1989), upper continental crust (UCC) and lower continental crust (LCC) data are from Rudnick and Gao (2003), and Hu and Gao (2008). The Chile volcanic arc granite data are after Pearce et al. (1984).

Fig. 7 (a) Zr/Ti vs. Nb/Y diagram (after Pearce, 1996) and (b) Th vs. Co diagram (after Hastie et al., 2007) for the basaltic volcanics. Red symbols: Karpas Peninsula and eastern range; green symbols: central range; blue symbols: western range. Paleogene basalt samples are indicated by thick magenta-outlined symbols.

Fig. 8 Mid-ocean ridge basalt (MORB)-normalised multi-element spider diagram for basalts from the Karpas Peninsula and the eastern (a), central (b) and western (c) Kyrenia Range. MORB-normalised data are from Pearce et al. (1983); (d) Chondrite-normalised REE patterns of selected basalts. Chondrite, OIB and E-MORB data are from Sun and McDonough (1989). Paleogene basalt samples are indicated by solid black lines and magenta-outlined symbols.

Fig. 9 (a) Cathodoluminescence images of zircon grains separated from the samples of Geçitköy. Red circles mark inconsistent analyses that were omitted from the weighted mean $^{206}Pb/^{238}U$ age calculation. Locations of the ion probe analysis spots and the corresponding ages ($^{206}Pb/^{238}U$ ± 1σ) are indicated. Scale bar = 20 μm; (b-d) Wetherill Concordia diagram for the zircons analyses from sample 14-18 (b), 14-19 (c) and 14-20 (d).

Fig. 10 (a-b) Plots of P_2O_5 vs. SiO_2 and Th, respectively, show that all of the samples follow the I–type granite trend; (c) Zr vs. 10000×Ga/Al, and (d) Nb vs. 10000×Ga/Al discrimination diagrams of Whalen et al. (1987), showing the I-, S (sedimentary)- and M (depleted mantle source)-type nature of the Late Cretaceous felsic volcanics.

Fig. 11 (a) εNd(t) vs. εSr(t) diagram for the basaltic rocks analysed. The samples are mainly Late Cretaceous (n=4); Paleogene basalt samples (n=2) are indicated by magenta-outlined symbols. Comparative compositions are from Zindler and Hart (1986); (b) εHf(t) vs. εNd(t) plot showing rocks for Kyrenia Range, northern Cyprus relative to other volcanic rocks of the western Mediterranean (after Kempton et al., 2018).

Fig. 12 (a) Ba/Nb versus La/Nb diagram (after Zhang et al., 2013); (b) Nb/Y versus Zr/Y diagram (after Condie, 2005), arrows in (b) indicate the effects of batch melting (F) and the probable effect of fluids derived from subduction (SUB); (c) Zr/Nb vs. Nb/Th diagram (modified after Condie, 2003). Abbreviations: PM, primitive mantle; DM, shallow depleted mantle; HIMU, high mμ (U/Pb) source; EMI and EMII, enriched mantle sources; ARC, arc-related basalt; N-MORB, normal ocean ridge basalt; OIB, oceanic island basalt; DEP, deep depleted mantle; EN, enriched component; REC, recycled component; UCC, upper upper continental crust; LCC, lower continental crust; BM, batch melting trajectory with percent melting noted. Numbers on mixing lines are percents.

Fig. 13 (a) Nb vs. Y diagram (Pearce et al., 1984) and (b) Th/Yb vs. Ta/Yb (Gorton and Schandl, 2000) for the felsic volcanics; (c) Zr/Y vs. Zr diagram (after Pearce and Norry, 1979) and (d) V vs. Ti discrimination diagram (after Shervais, 1982) for the basaltic rocks. Abbreviations: WPG, within-plate granite; VAG, volcanic arc granite; syn-COLG, syn-collisional granite; ORG, ocean ridge granite; WPB, within-plate basalt; MORB, mid-ocean ridge basalt; BABB, back-arc basin basalt; ARC, arc-related basalt; OFB, oceanic floor basalt.

Fig. 14 (a) Th/Nb vs. La/Nb and (b) La/Nb versus Y diagrams (after Floyd et al., 1991). Abbreviations: IAT, island arc tholeiite; BABB, back-arc basin basalt; OFB, oceanic flood basalt; FAPB, fore-arc platform basalt; T/E-MORB, T-type/enriched-mid-ocean ridge basalt.

Fig. 15 Alternative tectonic models of Tethys in the Eastern Mediterranean region. (a-c) Northward subduction with continental fragments rifted from Gondwana (Robertson et al., 2012a); (d-f) Northward subduction and marginal basin formation (Barrier et al., 2018); (g-h) Genesis of Late Cretaceous supra-subduction ophiolites at a single subduction zone to the NE followed by roll-back of segments including the Southern Neotethys (Maffione et al., 2017; McPhee and van Hinsbergen, 2019; van Hinsbergen et al., 2020). Based on discussion (see text), model 1 is generally favoured.

Listing of Supplementary Figure

Supplementary Figure S1 Field photographs of the felsic volcanics. (a) Exposure in Geçitköy. Samples 14-18 and 14-19 are from this location; (b) Irregular-shaped doleritic intrusion (hammer for scale); (c) Localised occurrence of greyish to greenish, rhyolitic debris-flow unit, north of Geçitköy; (d) Greenish rhyolitic debris-flow unit with angular rhyolitic clasts (pen for scale).

Supplementary Figure S2 Field photographs of the basaltic volcanics. (a) Pillow lavas and interstitial pink pelagic carbonate; roadcut c. 200 m north of Balalan; (b) basalt interbedded with pelagic carbonate; thrust sheet above Miocene siliciclastic sediment; c. 800 m northwest of Değirmenlik; (c) Basaltic volcanics intercalated with pelagic carbonates and small slices of meta-platform carbonates of the Trypa Group along the southern flank of the range, 800 m north of Boğaz; (d) Basalt-pelagic carbonate intercalation, south of Karşıyaka.

Supplementary Figure S3 Photomicrographs of felsic volcanics. (a) Subhedral sanidine (Sa), plagioclase (Pl) and biotite (Bt), in a groundmass of devitrified glassy volcanic shards (cross-polarised light); (b) felsic glass groundmass (Vg) with microcrystalline quartz, irregular-shaped quartz (Q) and feldspar (Pl) (cross-polarised light). Sample number is indicated in the bottom-left corner.

Supplementary Figure S4 Photomicrographs of basalts. (a) Intersertal basalt with euhedral granular augite (Px), elongate plagioclase laths (Pl) and opaque grains (Op) (cross-polarised light); (b) Basalt with intersertal texture, in which randomly-oriented plagioclase generally enclose pyroxenes (plane-polarised light); (c) Porphyrictic basalt with euhedral plagioclase and strongly altered olivine phenocrysts (cross-polarised light); (d) Ophitic basalt with plagioclase phenocrysts, augite occurs as an inclusion within individual plagioclase crystals (cross-polarised light). Sample number is indicated in the bottom-left corner. Samples no. 21, 14-51 and 14-69 are from the Melounda Formation, whereas sample no. 19-51 is from the Ayios Nikolaos Formation.

Supplementary Figure S5 Tectonic discrimination plots. (a) TiO_2-MnO-Na_2O ternary diagram (after Nisbet and Pearce, 1977) for clinopyroxenes in basalt; (b) TiO_2-SiO_2-Na_2O diagram (after Beccaluva et al., 1989) for clinopyroxenes in basalt. Abbreviations: VAB, volcanic arc basalt; OFB, ocean-floor basalt; WPA, within-plate alkali basalt; WPT, within-plate tholeiitic basalt; BON, boninite; IAT, island-arc tholeiite; WPB, within-plate basalt.

Supplementary Figure S6 (a) Chondrite-normalised REE comparison patterns of the Kyrenia Range felsic rocks and the Helete granites in SE Turkey (data after Nurlu et al., 2016). Chondrite data after Sun and McDonough (1989); (b)-(c) MORB-normalised multi-element spider diagrams for basalts. For comparison, the coloured fields show the composition variations of basalts from the Kyrenia Range (this study), the Misis Complex, S Turkey (Floyd et al., 1991), the Maden Complex, S Turkey (Erturk et al., 2018), the Japan Sea (Chen et al., 2015), the Sarmiento Complex, Chile (Saunders et al., 1979), the Bransfield Strait, Antarctic (Keller et al., 2002), the Guaymas Basin, Caribbean (Saunders et al., 1982) and the Tyrrhenian Sea, Italy (Peccerillo, 2017). MORB-normalised data are from Pearce et al. (1983). N-MORB, E-MORB and OIB data are from Sun and McDonough (1989). Specifically, two representative basalts of different affinities (within-plate vs. volcanic arc) from the Kyrenia Range are indicated.

Listing of Supplementary Tables

Supplementary Table S1. Major element oxides, trace and rare earth elements for the Late Cretaceous Fourkovouno (Selvilitepe) Formation.

Supplementary Table S2. Major element oxides, trace and rare earth element analyses for the latest Cretaceous-Paleogene basaltic volcanics.

Supplementary Table S3. Electron microprobe analyses of feldspar in the latest Cretaceous-Paleogene basaltic volcanics.

Supplementary Table S4. Electron microprobe analyses of pyroxene in the latest Cretaceous-Paleogene basaltic volcanics.

Supplementary Table S5. SIMS zircon U-Pb analyses of the zircon grains separated from the Late Cretaceous Fourkovouno (Selvilitepe) Formation.

Evidence from Late Cretaceous-Paleogene volcanic rocks of the Kyrenia Range, northern Cyprus for the northern, active continental margin of the Southern Neotethys

Guohui Chen[1]*, Alastair H. F. Robertson[1]

[1]School of GeoSciences, University of Edinburgh, West Mains Road, Edinburgh EH9 3JW, UK

*Current Address: State Key Laboratory of Lithospheric Evolution, Institute of Geology and Geophysics, Chinese Academy of Sciences, P.O. Box 9825, Beijing 100029, China

Corresponding author: Guohui Chen (Guohui.Chen@live.cn)

Abstract

Late Cretaceous felsic and latest Cretaceous-Paleogene basaltic volcanic rocks are exposed throughout the Kyrenia Range, N Cyprus. Field mapping of the key, well-exposed western range indicates that the felsic volcanics are mainly crop out~~exposed~~ in the southerly, frontal part of the range, separated from the latest Cretaceous-Paleogene basaltic volcanics farther north by a thrust. New U-Pb zircon dating of the felsic volcanics indicates a primary age of c. 74.0 Ma (Late Campanian). The felsic volcanics are characterised by evolved ~~high potassium and shoshonitic~~ compositions, that were probably generated in an extensional subduction-related setting.~~–~~ Their relatively low Nb and~~,~~ Y but high Rb concentrations, together with characteristic Th/Ta ratios (6-20), suggest a mature continental arc setting. The latest Cretaceous-Paleogene basaltic volcanics have mainly within-plate chemical characteristics (in the east), although some have a subordinate subduction influence; e.g. negative Nb (in

Formatted: Font color: Auto

Formatted: Font color: Auto

the west). Sr-Nd-Hf isotopic signatures (i.e. high positive εNd(t) and εHf(t) values) suggest derivation of the basalts from several OIB-like mantle sources, with probable involvement of a crustal (recycled) component (i.e. elevated Nb/Y ratios). Comparisons with SE Turkey, where Late Cretaceous arc-related granitic rocks are widely developed, suggest that the Kyrenia Range igneous rocks may have originated to the south of the Alanya metamorphic massif (N of Cyprus) and correlative continental units in SE Turkey. T~~ The Kyrenia Range Late Cretaceous felsic volcanics are comparable with rare Late Cretaceous granitic rocks in the front of the over-riding Tauride thrust belt in SE Turkey (Helete unit). They are also comparable with Late Cretaceous arc-related magmatic rocks higher in the regional tectono-stratigraphy in SE Turkey, although these may relate to a different continental margin arc. We propose that the Late Cretaceous felsic volcanics in N Cyprus record mature arc magmatism, as in SE Turkey. In contrast, t~~he latest Cretaceous-Paleogene basaltic volcanics in N Cyprus and SE Turkey (Maden Complex) are interpreted to represent incipient marginal basin formation, possibly in an oblique-convergent setting, prior to Miocene suturing with Arabia. In the light of alternatives, we infer genesis of the N Cyprus Late Cretaceous and Paleogene volcanic rocks related to stages in the development of the northerly active continental margin of the Southern Neotethys.

Keywords: Late Cretaceous-Paleogene; Volcanic rocks; Kyrenia Range; Arc magmatism; Marginal basin formation; Southern Neotethys

1. Introduction

Continental margin magmatism is a key feature of subduction at convergent plate margins (Dewey, 1969; Şengör and Natal'In, 1996). Information concerning the field relations, age, petrology and geochemistry are essential to understand the growth and demise of arcs, and are critical to reconstruct paleogeography and to test alternative tectonic hypotheses (e.g. Trehu et al., 1994; Tatsumi and Kogiso, 2003; Bowman et al., 2019).

The Eastern Mediterranean region, situated between the North African-Arabian and Anatolian (Eurasian) plates, includes tectonically emplaced remnants of Neotethys that developed from the preceding~~, larger~~ Paleotethys farther north (e.g. Le Pichon, 1982; Şengör et al., 1984; Robertson and Dixon, 1984; Stampfli and Borel, 2002). Much of the arc magmatism in the north, in the Pontides, of Jurassic-Eocene age (Fig. 1), relates to long-lived northward subduction of the Northern Neotethys (İzmir-Ankara-Erzincan ocean) (Adamia et al., 1977; Dercourt et al., 1993; Ustaömer and Robertson, 1997; Rice et al., 2006). Subduction of the Southern Neotethys ~~also took place during the Late Cretaceous (95-90 Ma), ~~resulted~~ing~~ in both continental margin and oceanic magmatism that ranges, overall, from Late Cretaceous to Paleogene (Fig. 1). Here, we focus on evidence of Late Cretaceous and Paleogene volcanism in the Kyrenia Range of northern Cyprus, representing the most westerly known occurrence of arc-type magmatism that can be related to subduction of the Southern Neotethys (Fig. 1) (Moore, 1960; Ducloz, 1972; Pearce, 1975; Baroz, 1979, 1980; Robertson and Woodcock, 1986; Huang et al., 2007; Robertson et al., 2012b).

Our specific objectives here are: (1) to understand the tectono-stratigraphy of two, contrasting, felsic and basaltic volcanic units in relation to associated sedimentary units; (2) to determine ~~directly~~ the eruptive ages of both of the volcanic units directly, using geochronology. Previously, the volcanics~~ These~~ were ~~previously~~ dated indirectly using microfossils within interbedded pelagic carbonates (Baroz, 1979; Robertson et al., 2012b); (3) to ~~investigate~~ determine whether there is any petrological or geochemical variation (including isotopic variation) along the Kyrenia Range (c. 100 km) and, if so, the implications; (4) to infer the magmatic-tectonic setting of eruption, compared with the evidence of arc volcanism ~~globally~~, ~~and~~ especially in southeast Turkey; (5) to test alternative tectono-magmatic hypotheses bearing in mind that arc magmatism plays ~~has~~ a key role in plate tectonic interpretations~~s~~.

~~2. Methods~~

~~The Kyrenia Range is a complex thrust belt, and therefore it was essential initially, to remap the western Kyrenia Range, where felsic and basaltic volcanic rocks are exposed together (Moore, 1960; Baroz, 1979; Robertson et al., 2012b). In addition, sedimentary logs were measured and correlated to produce a composite stratigraphy of the volcanogenic successions that are exposed in two superimposed thrust sheets.~~

~~Optical microscopy was carried out on the samples collected. For the felsic lithologies, 13 samples were studied from the western range. For the basaltic lithologies, we used a combination of new samples (n=29) and also samples that were previously collected for paleomagnetic study (n=26) (Morris et al., 2015) throughout the Kyrenia Range.~~

~~Whole-rock major and trace element concentrations of the volcanic rocks were measured by X-ray fluorescence (XRF) on fused glass beads and pressed powder pellets at the School of GeoSciences, University of Edinburgh, using the well-known methods of Fitton et al. (1998) and Fitton and Godard (2004). Accuracy and precision are typically c. 5%. For representative samples, additional trace and rare earth element (REE) analysis was carried out by inductively coupled plasma-mass spectrometry (ICP-MS) at the ACME Analytical Laboratories, Vancouver. Major element contents were determined from a $LiBO_2$ fusion by ICP-ES by using 5 g of sample pulp. Trace~~

element contents were determined from a $LiBO_2$ fusion by ICP-MS by using 5 g of sample pulp. Detection limits range between 0.01 and 0.04 wt% for major oxides, 0.01 and 0.1 ppm for trace and rare earth elements. The relative standard deviation for the REE is ~5% and for all other trace elements is up to 10%, with quality control using international geostandards (see http://acmelab.com).

In addition, Sr-Nd-Hf isotopic analysis was performed on a Neptune Plus multi-collector (MC)-ICP-MS at Wuhan SampleSolution Analytical Technology Co., Ltd., China, as reported by Li et al. (2012). Whole procedural blanks were <100 pg for Sr, <50 pg for Nd and <50 pg for Hf. $^{87}Sr/^{86}Sr$, $^{143}Nd/^{144}Nd$ and $^{176}Hf/^{177}Hf$ ratios were normalised to $^{86}Sr/^{88}Sr = 0.1194$, $^{146}Nd/^{144}Nd = 0.7219$ and $^{179}Hf/^{177}Hf = 0.7325$, using the exponential law. Standard analysis yielded $^{87}Sr/^{86}Sr = 0.710240 \pm 11$ (2SD, n = 4) for NBS987, $^{143}Nd/^{144}Nd = 0.512440 \pm 8$ (2SD, n = 8) for GSB 04- 3258- 2015, and $^{176}Hf/^{177}Hf = 0.282224 \pm 6$ (2SD, n = 6) for Alfa Hf. In addition, USGS reference materials BCR-2 and RGM-2 were also analysed for Sr–Nd–Hf isotopes, and gave ratios of 0.705039 ± 8 and 0.704169 ± 11 for $^{87}Sr/^{86}Sr$, 0.512644 ± 6 and 0.512808 ± 9 for $^{143}Nd/^{144}Nd$ and 0.282864 ± 6 and 0.283016 ± 7 for $^{176}Hf/^{177}Hf$, which is within error of recommended values (Thirlwall, 1991; Weis et al., 2006, 2007). The analytical data for the major, trace and rare earth elements/isotope ratio of the felsic and basaltic volcanics are listed in the Supplementary Table S1, S2, respectively.

Furthermore, two polished thin sections of basalt (no. 02 and 21) that contain relatively fresh feldspar and pyroxene crystals were selected for analysis of major elements using a Cameca SX100 electron microprobe at the School of GeoSciences, University of Edinburgh. Details of the analytical conditions and methods are given by Hayward (2011) and by Hartley and Thordarson (2013). The accuracy of major element determinations is <± 1% of total value. Analytical data for feldspar and pyroxene are given in Supplementary Table S3, S4, respectively.

~~Zircon crystals within 30-160 µm fraction were separated from crushed felsic tuffaceous rock and rhyolitic lava (no. 14-18, 14-19 and 14-20; c. 5 kg each). A Wilfley table, Frantz Isodynamic magnetic separator and a high-density solution (lithium polytungstate; 2.85 g/ml) were used to aid separation. Zircon grains were randomly handpicked under a binocular microscope, mounted in epoxy resin and polished sufficiently to expose the center of the grains. Internal structures were studied with a scanning electron microscope using cathodoluminescence (CL) at the School of GeoSciences, University of Edinburgh. U-Pb analysis was then performed using a Cameca IMS-1270 secondary ion mass spectrometer (SIMS) at the School of GeoSciences, University of Edinburgh, using the methods reported by Kelly et al. (2008) and Ustaömer et al. (2012). Errors of the reported ages are ± 1σ. Related geochronological plots were produced using ISOPLOT (Ludwig, 2012). Analytical results are listed in the Supplementary Table S5.~~

~~3~~2. Volcanism in the Kyrenia Range

Rifting of the Southern Neotethys during Late Permian and Early-Middle Triassic was followed by continental break-up during the Late Triassic-Early Jurassic (Robertson and Woodcock, 1979; Şengör and Yılmaz, 1981; Robertson and Dixon, 1984; Garfunkel, 1998; Robertson et al., 2020). The Kyrenia Range then formed part of a carbonate platform that slowly subsided during Jurassic-~~ and ~~Early Cretaceous in a ~~along a ~~passive margin ~~of the Southern Neotethys~~setting (Robertson and Woodcock, 1986). The carbonate platform was deformed and metamorphosed under greenschist facies during the Late Cretaceous, extensionally exhumed, and then unconformably overlain by basic extrusive igneous rocks of latest Cretaceous-~~ and ~~Paleogene age (Figs. 2-3) (Ducloz, 1972; Baroz, 1979; Robertson and Woodcock, 1986). In addition, felsic volcanics and tuffs are exposed as thrust slices at a low structural level in the south of the range (Figs. 2b, 3) (Robertson et al., 2012b). These volcanic rocks have no exposed base and are directly overlain by ~~the~~ a much larger thrust sheet that includes the mainly basic extrusive igneous rocks.

Baroz (1979, 1980) mapped the volcanic rocks and carried out petrographic and whole-rock chemical analysis of major elements. He reported the presence of a lower stratigraphic sequence of basalt, dolerite, trachybasalt, trachyandesite, dacite and rhyolitic tuff, and interpreted this as a bimodal basic-acidic calc-alkaline suite, related to a Late Maastrichtian volcanic arc. In contrast, the Paleogene volcanic assemblage was suggested to have erupted stratigraphically above in a post-collisional (intra-continental) strike-slip setting (Baroz, 1980). However, a thrust was later mapped between the mainly felsic and mainly basic suites (Robertson et al., 2012b), complicating this simple stratigraphy.

Chemical analysis of the Paleogene basaltic lavas, including immobile trace elements, initially suggested an alkaline, within-plate eruptive setting (Pearce, 1975). Subsequent chemical analysis, including some immobile elements, confirmed this~~a~~ mainly alkaline within-plate setting but also revealed some evidence of a subduction influence (e.g. negative Nb anomaly) (Robertson and Woodcock, 1986). The Paleogene lavas were ~~at that time~~ inferred by these authors to have erupted in a transtensional setting along the northern, active margin of the ‘Troodos ocean’. Huang et al. (2007) carried out additional chemical analysis of the Paleogene basaltic lavas, mainly from the eastern and western Kyrenia Range, with emphasis on immobile elements, and proposed a Late Cretaceous-Paleogene back-arc setting related to northward subduction.

The felsic rocks of the lowermost thrust sheet, known as the Fourkovouno (Selvilitepe)[1] Formation, ~~(~~up to 400 m thick~~)~~, begin with marine water-lain felsic tuffs

---

[1] For simplicity, w~~W~~e use the traditional stratigraphy for the formation names (more recent Turkish equivalents are mentioned initially). However, we use current the ~~the~~ Turkish names

and subaqueous felsic debris-flow deposits and culminate in laterally discontinuous, thick-bedded to massive rhyolitic lava flows (Fig. 3) (Moore, 1960; Baroz, 1979; Huang et al., 2007; Robertson et al., 2012b). The felsic rocks are locally cut by small (meter-sized) basaltic/doleritic intrusions (~~that were~~ not studied). A Late Cretaceous age (Late Campanian) was ~~previously~~ suggested for the felsic lavas, based on sparse planktic foraminifera (*Globotruncana sp.*) that were recognised in a chalky interbed near the top of the succession (Baroz, 1979).

The Late Cretaceous and Paleogene basaltic igneous rocks have been divided into ~~three~~ two formations, namely the Maastrichtian Melounda (Mallıdağ) Formation and~~,~~ the Paleocene-Middle Eocene Ayios Nikolaos (Yamaçköy) Formation (Fig. 2a).

The Melounda Formation, c. 300 m thick, unconformably overlies the exhumed Mesozoic platform carbonates of the Trypa (Tripa) Group or, in places, unmetamorphosed terrigenous turbidites of the Kiparisso Vouno (Alevkaya Tepe) Member of the Melounda Formation (Baroz, 1979; Robertson and Woodcock, 1986; Robertson et al., 2012b). The basaltic lavas of the Melounda Formation are commonly intercalated with pinkish pelagic limestones (Fig. 2a). The succession locally includes lenticular, lithoclastic breccias and finer-grained clastic facies that were reworked from the underlying meta-platform carbonates (Fig. 2a) (Robertson and Woodcock, 1986; Robertson et al., 2012b). Planktic foraminifera from ~~the~~ pelagic carbonates between the lavas indicate a Late Maastrichtian age (Baroz, 1979; Robertson et al., 2012b).

The overlying Ayios Nikolaos Formation, 300-400 m thick, comprises basaltic volcanics that are variably interbedded with pelagic carbonates. Calciturbidites, calcareous debris-flow deposits and carbonate-rock breccias appear above the lavas, towards the top of the overall succession (Baroz, 1979; Robertson and Woodcock,

---

(e.g. for~~that are currently in use (e.g. for~~ settlements); pre-existing names are mentioned ~~only~~ initially~~)~~.

1986; Robertson et al., 2012b, 2014) (Fig. 2a). Planktic foraminifera from pelagic carbonates that are interbedded with the lavas indicate a maximum Late Paleocene to Mid-Eocene age range (Baroz, 1979; Robertson et al., 2012b).

3. Methods

The Kyrenia Range is a complex thrust belt and therefore it was essential to remap the western Kyrenia Range, where felsic and basaltic volcanic rocks are exposed together (Moore, 1960; Baroz, 1979; Robertson et al., 2012b). In addition, sedimentary logs were measured and correlated to produce a composite stratigraphy of the volcanogenic successions that are exposed in two superimposed thrust sheets.

Optical microscopy was carried out on the samples collected. For the felsic lithologies, 13 samples were studied from the western range. For the basaltic lithologies, we used a combination of our samples (n=29) and also some that were previously collected for paleomagnetic study (n=26) throughout the Kyrenia Range (Morris et al., 2015).

Whole-rock major and trace element concentrations of the volcanic rocks were measured by X-ray fluorescence (XRF) on fused glass beads and pressed powder pellets at the School of GeoSciences, University of Edinburgh, using the well-known methods of Fitton et al. (1998) and Fitton and Godard (2004). Accuracy and precision are typically c. 5%. For representative samples, additional trace and rare earth element (REE) analysis was carried out by inductively coupled plasma-mass spectrometry (ICP-MS) at the ACME Analytical Laboratories, Vancouver. Major element contents were determined from a $LiBO_2$ fusion by ICP-ES, using 5 g of sample pulp. Trace element contents were determined from a $LiBO_2$ fusion by ICP-MS, again using 5 g of sample pulp. Detection limits range between 0.01 and 0.04 wt% for major oxides, 0.01 and 0.1 ppm for trace and rare earth elements. The relative standard deviation for the

Formatted: Indent: First line: 2 ch

REE is ~5% and for all other trace elements is up to 10%, with quality control using international geostandards (see http://acmelab.com).

In addition, Sr-Nd-Hf isotopic analysis was performed on a Neptune Plus multi-collector (MC)-ICP-MS at Wuhan SampleSolution Analytical Technology Co., Ltd., China, as reported by Li et al. (2012). Whole procedural blanks were <100 pg for Sr, <50 pg for Nd and <50 pg for Hf. $^{87}Sr/^{86}Sr$, $^{143}Nd/^{144}Nd$ and $^{176}Hf/^{177}Hf$ ratios were normalised to $^{86}Sr/^{88}Sr$ = 0.1194, $^{146}Nd/^{144}Nd$ = 0.7219 and $^{179}Hf/^{177}Hf$ = 0.7325, using the exponential law. Standard analysis yielded $^{87}Sr/^{86}Sr$ = 0.710240 ± 11 (2SD, n = 4) for NBS987, $^{143}Nd/^{144}Nd$ = 0.512440 ± 8 (2SD, n = 8) for GSB 04-3258-2015, and $^{176}Hf/^{177}Hf$ = 0.282224 ± 6 (2SD, n = 6) for Alfa Hf. In addition, USGS reference materials BCR-2 and RGM-2 were also analysed for Sr–Nd–Hf isotopes, and gave ratios of 0.705039 ± 8 and 0.704169 ± 11 for $^{87}Sr/^{86}Sr$, 0.512644 ± 6 and 0.512808 ± 9 for $^{143}Nd/^{144}Nd$ and 0.282864 ± 6 and 0.283016 ± 7 for $^{176}Hf/^{177}Hf$, which is within error of recommended values (Thirlwall, 1991; Weis et al., 2006, 2007). The analytical data for the major, trace and rare earth elements/isotope ratio of the felsic and basaltic volcanics are listed in the Supplementary Table S1, S2, respectively.

In addition, two polished thin sections of basalt (no. 02 and 21) that contain relatively fresh feldspar and pyroxene crystals were selected for analysis of major elements using a Cameca SX100 electron microprobe at the School of GeoSciences, University of Edinburgh. Details of the analytical conditions and methods are given by Hayward (2011) and by Hartley and Thordarson (2013). The accuracy of major element determinations is <± 1% of total value. Analytical data for feldspar and pyroxene are given in Supplementary Table S3, S4, respectively.

For dating, zircon crystals within 30-160 μm fraction were separated from crushed felsic tuffaceous rock and rhyolitic lava (no. 14-18, 14-19 and 14-20; c. 5 kg each). A Wilfley table, Frantz Isodynamic magnetic separator and a high-density solution (lithium polytungstate; 2.85 g/ml) were used to aid separation. The zircon grains were randomly handpicked under a binocular microscope, mounted in epoxy resin and polished sufficiently to expose the centre of the grains. Internal structures were studied with a scanning electron microscope using cathodoluminescence (CL) at the School of GeoSciences, University of Edinburgh. U-Pb analysis was then performed using a Cameca IMS-1270 secondary ion mass spectrometer (SIMS) at the School of GeoSciences, University of Edinburgh, using the methods reported by Kelly et al. (2008) and Ustaömer et al. (2012). Errors of the reported ages are ± 1σ. Related geochronological plots were produced using ISOPLOT (Ludwig, 2012). Analytical results are listed in the Supplementary Table S5.

4. Results

4.1. ~~Restored v~~Volcanic successions

The felsic volcanics, mainly crop out in the western part of the Kyrenia Range in two thrust sheets (Figs. 3-4). The lower of these, which is relatively intact, extends from Geçitköy (Panagra) eastwards to Selvilitepe (Fourkovouno) (Fig. 5a-e). The second, structurally higher unit, comprises discontinuous exposures extending from north of Geçitköy, to southwest of Karsıyaka (Vasileia) and west of Alevkaya Tepe (Kiparisso Vouno) (Fig. 5f-j). Farther west, in the Kayalar (Orga) area (Fig. 3a), a small thrust slice exposes ~~of~~ coarse-grained felsic tuff and a felsic debris-flow ~~deposits~~ deposit~~are exposed~~. Small (tens of m-sized) outcrops of felsic volcanogenic rocks also occur farther east; e.g. northeast of Aşağı Dikmen (Kato Dikomon), between thrust sheets of ~~the~~ Mesozoic meta-carbonate rocks (Baroz, 1979). Small exposures are also intersliced with Late Cretaceous pelagic carbonates of the Melounda Formation to the north of Ergenekon (Agios Khariton) (Fig. 3a) (Robertson et al., 2012b).

The ~~restored~~ local successions are restored as a ~~in the~~ lower thrust sheet and an upper thrust sheet. The succession in the lower thrust sheet, c. 90 m thick, begins with weakly-bedded, white felsic tuff (beds <0.5 m thick) (Fig. 5a, c-e), followed by thick layers of matrix-supported felsic breccia-conglomerate (c. 10 m thick) that we~~are~~ interpret~~ed~~ as debris-flow deposits (Fig. 5a, c, e). The succession passes upwards into massive, vitreous, rhyolitic lava flows, individually up to 10 m thick (Figs. 5a, Supplementary Figure S1). Localised normal grading; e.g. northeast of Geçitköy, indicates that the succession is~~, stratigraphically~~ the right way up, stratigraphically (Fig. 5a-b). In places, steeply dipping, irregularly shaped basaltic or doleritic intrusions, up to 2 m ~~thick~~across, cut the felsic layering (Figs. 5a, Supplementary Figure S1). ~~In contact with~~Adjacent to these intrusions, poorly consolidated tuffaceous sediments have undergone contact metamorphism to form hard, dark grey, flint-like, recrystallised felsic rock (Robertson et al., 2012b). There is no evidence of similar intrusions in the structurally overlying basalts, which is in keeping with the mapped tectonic contact between the two units.

The succession in the upper thrust sheet begins with greyish to greenish, tuffaceous matrix-supported conglomerates, including clasts of silicified rhyolite, chalk and basalt (Supplementary Figure S1). The estimated thickness ranges from c. 40 m north of Geçitköy (Fig. 5f), to c. 80 m southwest of Karsıyaka (Fig. 5g-h), to 30 m west of the Alevkaya Tepe (Fig. 5i-j).

Contrasting field relations facilitate mapping of the Late Cretaceous versus the Paleogene formations (Baroz, 1979; Robertson and Woodcock, 1986; Hakyemez et al., 2000; Robertson et al., 2012b). ~~The Late Maastrichtian basalts (Melounda Formation) are typically pillowed, forming repeated flows, up to c. 10 m thick. They include pink pelagic carbonate as interstitial sediment and discontinuous layers (up to 10s cm thick), extending laterally for up to c. 10 m. In contrast, the Paleogene basalts~~

~~(Ayios Nikolaos Formation) are commonly massive, especially in the eastern range, where individual lava flows reach 10s of m thick, with relatively few pelagic intercalations (Supplementary Figure S2). However, in the central and western ranges, the lava flows are mainly thinner (<10m) and are intercalated with pelagic carbonates that contain abundant reddish chert (formed by diagenetic replacement). The contrasting features facilitate mapping of the two formations (Baroz, 1979; Robertson and Woodcock, 1986; Hakyemez et al., 2000; Robertson et al., 2012b).~~

~~During this work, it was found that there are geochemical differences between lavas of similar age along the far-eastern, eastern, central and western Kyrenia Range (see below). We, therefore, give some more specific information on the lavas in these areas.~~

In the far east of the Kyrenia Range, the Karpas Peninsula (Fig. 3a), both pillowed and massive basalt are widely exposed near Balalan (Platanissos). ~~The lavas include i~~Interpillow carbonate and lenticular interbeds of pelagic carbonate (< 1 m thick) (Figs. 3a, Supplementary Figure S2) contain~~with~~ Late Maastrichtian microfossils (Robertson et al., 2012b). ~~.~~

In the eastern range, basaltic rocks of the Melounda Formation contain abundant pelagic carbonate and are overlain by massive basalts of the Ayios Nikolaos Formation; i.e. from Ağıllar (Mandres) to Mallıdağ (Melounda) (Fig. 3a) (Baroz, 1979; Robertson and Woodcock, 1986; Hakyemez et al., 2000; Robertson et al., 2012b). ~~.~~

In the central range, pillow lava with interbedded pelagic carbonate of the Melounda Formation occurs in two settings. The first is directly above the Upper Cretaceous basal unconformity, with the~~ underlying~~ meta-carbonate platform rock beneath; e.g. near Tirmen (Trypimeni). The second setting is as one (or several), small thrust sheets along the southern flank of the range; e.g. Değirmenlik (Kythrea), Boğaz (Bogaz) and southwest of Alevkaya Tepe (Figs. 3a, Supplementary Figure S2). Basalt

Formatted: Indent: First line: 2.5 ch with some interbedded pelagic carbonate of the Ayios Nikolaos Formation is exposed higher in the succession (within a shear zone), near Tirmen, Arapköy (Klepini) and İncesu (Motides) (Baroz, 1979).

In the western range, basaltic lavas interbedded with pelagic carbonates of the Melounda Formation are exposed in a thrust sheet along the southern margin of the range; e.g. Geçitköy (Figs. 3, Supplementary Figure S2). Similar basaltic lavas with pelagic carbonates and local carbonate breccias, are exposed along the northern margin of the range; e.g. near Karşıyaka and farther west (Baroz, 1979; Hakyemez et al., 2000; Robertson et al., 2012b). In addition, basaltic lava interbedded with pelagic chalk of the Ayios Nikolaos Formation occurs higher in the succession (southward-younging) along the eastern side of Geçitköy road (Huang et al., 2007; Robertson et al., 2012b).

In summary, the Late Maastrichtian basalts (Melounda Formation) are typically pillowed, forming repeated flows (individually up to c. 10 m thick), reaching a maximum of > 90 m in the east (near Balalan). The lavas include pink pelagic carbonate as interstitial sediment and discontinuous layers. In contrast, the Paleogene basalts (Ayios Nikolaos Formation) are commonly massive, especially in the eastern range, where individual lava flows reach c. 45 m thick, with relatively few pelagic intercalations (Supplementary Figure S2). In the central and western ranges, thinner lava flows (<10m) are intercalated with pelagic carbonates and reddish chert (formed by diagenetic replacement). During this work, we identified geochemical differences between the Late Cretaceous-Paleogene basaltic lavas of similar age along the far-eastern, eastern, central and western Kyrenia Range (see below).

4.2. Petrography

The felsic rocks are porphyritic, composed of quartz, plagioclase and sanidine, together with subordinate biotite and rare hornblende. Large sanidine crystals (0.3-1 mm) show simple twinning, whereas plagioclase commonly has lamellar twinning (Supplementary Figure S3). Biotite laths (0.3-0.8 mm in length) are preferentially orientated parallel to flow layering. Rare quartz phenocrysts (<1%, 0.2-0.5 mm) are commonly fragmented, probably related to quenching during eruption; i.e. explosive fragmentation (Supplementary Figure S3). The groundmass comprises microcrystalline quartz and feldspar, together with minor muscovite, biotite and rare hornblende (c. 60 μm). In some samples (e.g. nos. 14-19 and 14-20), the groundmass is cryptocrystalline, almost glassy (Supplementary Figure S3).

The basaltic rocks of both Late Cretaceous and Paleogene age generally fall into two groups in terms of mineral composition and texture. The first group (most common) is porphyritic with subhedral to euhedral clinopyroxene phenocrysts (30-40%), up to 0.6 mm long, that occur interstitially or are intergrown with subhedral feldspar (Supplementary Figure S4, Table S3). Feldspar (45-60%) forms elongate, acicular laths, up to 1 mm long. Olivine is relatively rare (<5%). The second group is ophitic, as locally observed in the western Kyrenia Range with abundant anhedral to subhedral augite phenocrysts (up to 0.6 mm in size). Most plagioclase is acicular, enclosed or surrounded by augite (Supplementary Figure S4).

Most samples are slightly to moderately altered. Amygdales and veins are infilled with secondary minerals such as calcite and zeolite. Alteration is variable, for example, pyroxene and plagioclase are heavily altered to chlorite and clay minerals (e.g. smectite/sericite). The relatively high loss on ignition values result from secondary processes, which need to be taken into account prior to rock identification and tectonic discrimination.

4.3. Whole-rock chemistry

Major-element oxides (K_2O, Na_2O and CaO) and trace elements (e.g. Rb, Sr and

Ba) exhibit a relatively wide compositional range, consistent with the effects of alteration (see Supplementary Table S1-S2). Alteration can be inferred from variable LOI values that range between 0.3-5.4 wt% for the felsic volcanics and 4.09-14.57 wt% for the basaltic rocks. This is consistent with the presence of considerable amounts of water- and/or carbonate dioxide-bearing minerals, for example chlorite and calcite, as observed petrographically (see Supplementary Figure S3, S4). Trace elements such as Ti, Zr, Y, Nb, Ta, V, Co, Th and REEs tend to be immobile during weathering and/or metamorphism below amphibole facies are, therefore, preferred for rock-type identification and tectonic discrimination (e.g. Pearce and Cann, 1973; Rollinson, 1993). For basaltic rocks, samples with high crystal contents (cumulate composition or highly porphyritic) should be discounted from geochemical discrimination (Pearce, 1996). In general, samples with immobile element Al_2O_3 > 20 wt% (concentrated in feldspar), Sc > 50 ppm (concentrated in clinopyroxene), or Ni > 200 ppm (concentrated in olivine) are predicted to contain high amounts of cumulated minerals (Pearce, 1996). On this basis, basaltic rocks nos. 14-66, 14-50, 14-51, 14-58, 14-68, 08, 16, 25 and 28 are discounted.

The more felsic assemblage is mainly rhyolitic in the classification of Winchester and Floyd (1977) but shows a trachytic affinity in the revised Zr/Ti vs. Nb/Y (Fig. 6a) diagram of Pearce (1996). Relatively high abundances of Th (>14 ppm) but low Co concentrations (<12 ppm) are consistent with high-K and shoshonitic affinities (Fig. 6b). Primitive mantle-normalised multi-element plots (Fig. 6c) show variable enrichments and depletions in large-ion lithophile elements (LILEs; e.g. Cs, Rb, Ba, K and Sr) that are influenced by alteration. The samples show negative anomalies of Nb, Zr and Ti, coupled with marked positive anomalies of Th/U, Pb, Nd and probably Sm (Fig. 6c). Total REE contents of the felsic assemblage (Fourkovouno Formation) vary from 115 to 173 ppm. La ranges from 29-44 ppm, $(La/Yb)_N$=12.63-18.98, suggestive of an alkalic affinity. The ratios $(La/Sm)_N$=6.13-7.22 and $(Gd/Yb)_N$=1.26-1.68 suggest a large LREE fractionation but low to moderate HREE fractionation (Fig. 6d). Pronounced negative Eu anomalies (Eu/Eu*=0.32-0.48) are consistent with plagioclase crystallization, as seen petrographically (see Supplementary Figure S3). In general, the samples are comparable to upper continental crust (UCC).The basaltic rocks plot in the fields of basalt and alkali basalt, with intermediate degrees of fractionation (Zr/Ti=0.01-0.02) and moderate alkalinity (Nb/Y=0.1-1.8) on the rock-type discrimination plot (Fig. 7a). The basalts have a calc-alkaline affinity, except for samples from Mallıdağ (no. 01), Tirmen (no. 19-51), Değirmenlik (no. 14-64) and İncesu (no. 19-67) that exhibit high-K and shoshonitic affinities (Fig. 7b). The trace element compositions of the basaltic rocks exhibit wide ranges of Sr, Ba, Rb, Th, Ta, Nb and Ce. However, Zr, Hf, Sm, Ti and Y generally comparable with enriched mid-ocean ridge basalt (E-MORB) and oceanic island basalt (OIB) (Fig. 8a-c).

The basaltic rocks are characterised by variable REE concentrations (67.2-239.4 ppm) and light REE enrichments ($(La/Yb)_N$=3.18-19.35) (Fig. 8d). Samples from the central range, at Değirmenlik and Tirmen, show much higher total REE contents and steeper REE patterns. Westwards in the Kyrenia Range, the patterns become smoother, with less pronounced enrichment in LREEs. In general, no marked Eu anomaly (~1) is observed.

4.4. Whole-rock Sr-Nd-Hf isotopes

The selected basaltic samples have relatively uniform whole-rock Sr-Nd-Hf isotopic characteristics. Adopting a Late Cretaceous eruption age based on the paleontological dating (Robertson et al., 2012b), the calculated initial $^{87}Sr/^{86}Sr$ ratios range from 0.705054 to 0.705701, with εNd(t) values of 2.27 to 5.76. Initial $^{176}Hf/^{177}Hf$ and εHf(t) values are 0.282934-0.283017, 7.36-10.14, respectively (see Supplementary Table S2).

4.5. Zircon U-Pb geochronology

Zircon crystals separated from the felsic rocks are typically angular to sub-angular, 30-160 μm long. The grains have variable internal textures, including banded zoning (e.g. zircon 1), concentric zoning (nos. 2, 4, 5 and 12), and minor sector zoning (nos. 10, 11; Fig. 9a). Fractures (or depressions) and some inherited cores are affected by fluid-related chemical alteration (nos. 6 and 8) (Fig. 9a). The zircon grains have high Th/U ratios (0.19-1.24), suggestive of a magmatic origin (Rubatto, 2002). Twelve zircon grains were analysed with concordance levels ranging from 99-105%. The calculated $^{206}Pb/^{238}U$ age with the generally lowest possible error was used for age determination. The much older zircon grain (no. 4) is subhedral with a patchy xenocrystic texture, suggestive of a recycled origin (Fig. 9a). The concordant or nearly concordant data (100-102%) with a young age distribution yielded weighted mean $^{206}Pb/^{238}U$ gave ages of 74.0±0.6 Ma, 74.0±0.4 Ma and 71.7±0.7 Ma (Fig. 9b-d).

5. Discussion

5.1. Genetic type/source characteristics

For the felsic rocks, the high LREE/HREE (e.g. $(La/Yb)_N$=12.63-18.98) and negative Eu anomalies, resemble model UCC but with depletion in Eu, Sr and P (Fig. 6c-d). The A/CNK (molar ratio of $Al_2O_3/(CaO+Na_2O+K_2O)$) ratio is useful to identify the source of felsic rocks (Chappell and White, 1992) but is questionable for altered rocks like those of the Kyrenia Range. SiO_2, P_2O_5 and Th can also be used as indices of the fractional crystallization of a felsic melt (Chappell and White, 1992), but again may be affected by alteration (specially SiO_2). In our samples, P_2O_5 deceases with increasing SiO_2 and Th (Fig. 10a-b), trends that are indicative of I (igneous)- or A (anorogenic)-type granites. The relatively low contents of Zr, Nb, Y, La, Ce, Zn and Ga further characterise these rocks as I-type (Fig. 10c-d). The abundances of Th and Co, in particular hint at a shoshonitic composition (Hastie et al., 2007).

The trace element patterns of the basaltic rocks show a wider range of variation (Fig. 8). E-MORB and OIB-type basalts were derived from relatively enriched sources, specifically for the basalts of the Karpas Peninsula, eastern range and most of the central range. The lesser enrichment of Nb within the basalts of the central range at Ergenekon (no. 31), Arapköy (no. 14-62) and Alevkaya Tepe (no. 14-49), and the western range at Karsıyaka (no. 14) and Geçitköy (no. 10), can be explained by a relatively depleted mantle source, together with subduction modification. There is little evidence of the addition of radiogenic Sr from seawater, either to the source melt or during post-magmatic alteration. The Sr vs. Nd isotope correlation diagram (Fig. 11a) does not show a significant shift towards higher initial $^{87}Sr/^{86}Sr$ ratios as would be expected in both of these cases.

The basalts all have positive εNd(t) values (+2.27 - +5.76), consistent with derivation from an OIB-like source mantle (Fig. 11a). The samples plot directly on the terrestrial array, overlapping with the Nd isotope compositions of Etna and the Aeolian Arc, but intermediate between these settings in Hf isotopes (Fig. 11b). The samples that show trace element evidence of a subduction-modified source, based on relatively flat MORB-normalised multi-element patterns and negative Nb anomalies (no. 10, Geçitköy), plot in the Aeolian Arc-type mantle field. Conversely, samples from the Karpas Peninsular, at Balalan, plot close to the field of Etna and exhibit less subduction modification (Fig. 11b). The trace element and isotopic data, therefore, yield consistent results.

The involvement of a crustal component is also suggested by incompatible element ratio plots, on which the basalts exhibit two distinct trends. The samples with relatively strong subduction signatures plot away from the MORB array (Fig. 12a), fingerprinting a subduction-related lithospheric mantle end member. A probable lower crust input is suggested by relatively higher La/Nb and Ba/Nb ratios (e.g. Wang et al., 2004). In contrast, an OIB-like mantle component dominated most of the other basalt samples, as indicated by relatively low La/Nb, Zr/Nb but high Nb/Y ratios (Fig. 12b). The ratios of highly incompatible elements with small distribution coefficients (e.g. Zr/Nb, Nb/Th, Nb/La) are sensitive indicators of mantle source heterogeneity (Saunders et al., 1988; Condie, 2003; Pearce and Stern, 2006). The samples from the western locations fall in the fields of an enriched component and upper continental crust (Fig. 12c), which could represent mantle mixing with continental sediments (subducted) or crustal contamination. In contrast, the samples from the easterly locations resemble those of the OIB/recycled component, and cluster around a different batch-melting trajectory (10-20%) (Fig. 12c) that is, representative of recycled oceanic lithosphere (Saunders et al., 1988). We, therefore, infer that the basalts are likely to have been derived from multiple sources (i.e. two or more source components were involved).

5.2. Tectonic discrimination

On the Nb vs.Y diagram (Fig. 13a), the felsic volcanics show similarities with volcanic arc granites and syn-collisional granites. One sample from Geçitköy (no. 16-08), with relatively high Nb and Y concentrations, plots near the field of within-plate granite. On the Th/Yb vs. Ta/Yb diagram (Fig. 13b), the volcanics mainly erupted on active continental margins. An active continental margin setting is therefore inferred for the felsic volcanics.

Basalts of the Kyrenia Range (e.g. easterly locations) mostly exhibit a within-plate affinity (Fig. 8). However, some samples, especially in the west, have a subduction-related signature (e.g. negative Nb anomalies) (Fig. 8b-c) akin to volcanic arc basalts. Most samples have a within-plate affinity on the Zr/Y vs. Zr (Fig. 13c) diagram, except for two samples, from Ergenekon and Arapköy (central range), that straddle the island arc and MORB fields. The basalts overlap the MORB and back-arc basin basalt fields on the Ti vs. V plot (Fig. 13d). Clinopyroxene compositions, as shown in the ternary TiO_2-MnO-Na_2O plot (see Supplementary Figure S5), indicate a dominantly within-plate affinity. The relatively high TiO_2 contents of the clinopyroxenes point to an enriched MORB-related source (see Supplementary Figure S5). Overall, the inferred subduction contribution decreases from west to east along the range.

5.3. Global comparison of the Kyrenia Range volcanic rocks

Global comparison (see Supplementary Figure S6) lendcomparisons (see Supplementary Figure S6) lend -support to our interpretation of the Kyrenia Range volcanic rocks as being subduction-related. In particular,

Wwithin the Late Cretaceous felsic rocks of the Kyrenia Range, the enrichment of Rb, Th and Sm and versus the depletion of Ti, Ba, Nb, P compared to primitive mantle, are characteristic of volcanic arc granites (Fig. 6c) (Pearce et al., 1984).

The Kyrenia Range Maastrichtian and Paleogene basalts of within-plate affinities (e.g. Balalan, eastern range) mainly, have MORB-normalised spider patterns that are similar to the Pliocene-Quaternary OIB-type basalts of the Tyrrhenian Sea, W Mediterranean (Peccerillo, 2017). The MORB-normalised patterns of these basalts suggest a within-plate eruptive setting, with a small sub-crustal lithosphere metasomatic influence (Kastens et al. 1988; Peccerillo, 2017).

Back-arc basalts of the Early Cretaceous Sarmiento Complex, southern Chile (Saunders et al., 1979) and the Miocene Japan Sea (Tamaki et al., 1990) resemble a minority of the Kyrenia Range basalts (c. 10%; e.g. Geçitköy, western range), but although with lower abundances of K, Rb, Ba, Th, Ta and Nb. The relative depletions depletion of these elements is characteristic of ~~are likely to be representative of~~ eruption in a relatively wide, evolved back-arc basin (e.g. Bransfield Strait; Weaver et al., 1979). However, another possible setting is eruption in a back-arc basin that was influenced by oblique extension (e.g. Guaymas pull-apart basin; Brune et al., 2012). The relatively flat MORB-normalised patterns, akin to E-MORB, of both the Bransfield Strait and Guaymas back-arc basin basalts (e.g. Saunders et al., 1982; Keller et al., 2002) point to substantial involvement of depleted MORB sources.

5.4. Comparison with the adjacent Tethyan region

Late Cretaceous and Paleogene arc-related rocks; i.e. similar in age of those in the Kyrenia Range are critical to any regional magmatic-tectonic interpretation.

In western Cyprus, ~~there is~~ a Late Cretaceous arc-derived volcanogenic succession (Kannaviou Formation) ~~that~~ overlies the Troodos ophiolite. The volcaniclastic sediments ~~there~~ were derived from intermediate-felsic ~~composition~~ eruptions, c. 6 Ma before the felsic eruptions in the Kyrenia Range (c. 80 vs. 74 Ma). Grain size and textural evidence suggest that, depending on prevailing wind direction and strength, the eruptive centers are likely to have been <100 km away (Chen and Robertson, 2019). The centers for the Kannaviou Formation were~~could have been~~ located to the south of the Kyrenia Range or its lateral extension, areas that are not now exposed. The Kyrenia Range was affected by south-directed thrusting during Mid-Eocene and Late Miocene-earliest Pliocene (Baroz, 1979; Robertson et al., 2012b, 2014; McCay and Robertson, 2013; Robertson and Kinnaird, 2016), such that the distal (southerly) edge of the inferred over-riding active margin (see below) could have been subducted, structurally over-ridden or eroded. In other words, additional arc units could have existed to the south of their present location in the Kyrenia Range.

To the northeast (c. 200 km), the Misis-Andırın Range in southern Turkey is an extension of the Kyrenia lineament (Robertson et al., 2004). The outcrop, known as the Misis-Andırın Complex, includes massive basalts, pillow lavas, lava breccias and volcaniclastic debris-flows. These lithologies were previously inferred to be Miocene (Floyd et al., 1991, 1992). However, inter-lava sediments there have been dated as Campanian-Maastrichtian (Robertson et al., 2004), similar in age to the oldest basaltic rocks in the Kyrenia Range. The Miocene sediments are structurally intercalated. The basalts of the Misis-Andırın Complex are tholeiitic, with mildly enriched, subduction-related characteristics (e.g. moderate La/Nb ratios), and are interpreted as of back-arc basin origin (Floyd et al., 1991, 1992), which is consistent with our interpretation of the Kyrenia Range basalts ~~(Floyd et al., 1991, 1992)~~ (Fig. 14a-b, Supplementary Figure S6).

The Kyrenia Range is backed to the north by the Alanya Massif (Fig. 1), which has been interpreted as a continental fragment, separate from the Tauride carbonate platform to the north (Robertson et al., 2012a; Çetinkaplan et al., 2016). The Alanya Massif is represented by the Late Precambrian-Mesozoic, mainly meta-sedimentary rocks. High pressure-low temperature (HP-LT) metamorphics document Late Cretaceous (82-80 Ma) subduction/exhumation (Oberhänsli et al., 2010, 2013). This is inferred to have taken place along the northern, active margin of the Southern Neotethys (Çetinkaplan et al., 2016; Robertson and Parlak, 2020). The felsic volcanics (Fourkovouno Formation) in the Kyrenia Range could have erupted along the southern (trailing) margin of the Alanya microcontinent where they could have escaped metamorphism. However, they could also represent a separate more southerly unit.

Late Cretaceous continental margin arc-type magmatic rocks also occur extensively farther east, in SE Turkey, as two separate belts. ~~The Kyrenia Range volcanics are most comparable with volcanogenic units that occur within an extension of the same (or similar) tectonic lineament; i.e. close to the leading edge of the over-riding Tauride (Eurasian) continent.~~

The most southerly, known Late Cretaceous arc rocks in SE Turkey are exposed in the Helete area, part of a zone of frontal thrust sheets (Yıldırım, 2015; Nurlu et al., 2016) (Fig. 1). Two thrust assemblages are exposed, both cut by granites that have been ~~Arc-related volcanogenic units there comprise basaltic andesite, andesite, dacite, rhyolite and common tuffaceous rocks. Cross-cutting granites have been~~ radiometrically dated at 93-83 Ma (Cenomanian-Campanian) (Nurlu et al., 2016). The lower of the assemblages, the Helete volcanics, comprises arc-related basaltic andesite, andesite, dacite, rhyolite and common tuffaceous rocks. The upper of the two thrust assemblages is a dismembered Late Cretaceous supra-subduction zone-type ophiolite (Meydan ophiolite) (Yıldırım, 2015; Nurlu et al., 2016). The cross-cutting intrusive rocks sealed the thrust sheets during the Late Cretaceous. The granitic rocks ~~The intrusive rocks~~ are interpreted as a calc-alkaline, subduction-related suite that formed by mixing of mantle and crustal sources, as suggested by Sr-Nd-Pb isotopic data (Nurlu et al., 2016). The granitic rocks exhibit relatively flat chondrite-normalised REE patterns, similar to E-MORB (Nurlu et al., 2016) (Supplementary Figure S6). In contrast, the chondrite-normalised REE patterns of the Kyrenia Range felsic rocks are similar to UCC (Fig. 6c), suggesting a more continentally-influenced~~proximal (northerly)~~ setting.

The second belt of arc-related magmatism is located up to c. 100 km ~~located~~ farther north and north-east, in the Keban (Malatya), Göksun (Kahramanmaraş) and Baskil (Elazığ) regions (Fig. 1) (Yazgan and Chessex, 1991; Parlak, 2006; Rızaoğlu et al., 2009; Karaoğlan et al., 2013, 2016). ~~(c. 100 km), where a~~ Arc-granitic rocks (Baskil intrusives) cut ~~both~~ the Late Cretaceous Göksun ophiolite and equivalents (i.e. Berit meta-ophiolite (=North Berit ophiolite), Kömürhan ophiolite and İspendere ophiolite) that are inferred to have formed above a northward-dipping subduction zone (Parlak, 2006). Similar~~the~~ arc granites also cut the structurally over-riding Malayta metamorphic unit, which ~~that~~ is interpreted as the southern part of the Tauride microcontinent. The

Göksun ophiolite (and equivalents) and the Malayta metamorphic (Tauride) units were juxtaposed along an active continental margin when the arc-granitic rocks were intruded (Robertson et al., 2006; Rızaoğlu et al., 2009; Karaoğlan et al., 2013, 2016).

The extrusive rocks of the Göksun and related ophiolites can also be broadly correlated with widespread assemblages of basic igneous rocks and volcanogenic sediments in the Malatya-Elazığ region, known as the Yüksekova Complex (Perincek and Özkaya, 1981; Aktaş and Robertson, 1984). The basalts have a tholeiitic to tholeiitic-transitional character, variable Zr/Y (1.5-6) ratios and mantle-array-aligned Sr-Nd isotopes (Ural et al., 2015). These basic volcanics were derived from a depleted mantle source without a significant crustal contribution; i.e. from an intra-oceanic setting within the Southern Neotethys (Ural et al., 2015).

The arc rocks that cut both the Göksun (and related) ophiolites and the Malatya Metamorphics (Baskil intrusives) in the northern belt are mainly hornblende-biotite granodiorites and 'normal' granites, dated radiometrically at 88-82 Ma (Santonian-Campanian) (Parlak, 2006; Rızaoğlu et al., 2009; Karaoğlan et al., 2016); i.e. up to c. 5 Ma younger than Helete area granites in the south. These southerly granitic rocks have I-type, calc-alkaline arc affinities, with both mantle and crustal-derivation features (Nurlu et al., 2016). The Baskil intrusions of the northern belt are relatively enriched in LREE (Parlak, 2006; Rızaoğlu et al., 2009) compared to the Helete granites of the south, which suggests a more crustally influenced source during magma genesis for the former. Similarly, the Kyrenia Range basalts have relatively high Zr/Y (2.8-7.7) and Nb/Y (Figs. 12b, 13c), suggestive of a magmatic contribution from continental crust or subducted continentally derived sediments (Zindler and Hart, 1986; Pearce, 1996).

The northerly arc has been explained by northward subduction of Mesozoic oceanic basin (Berit ocean) that was located between two continental units; i.e. the Bitlis and Pütürge massifs in the south and the Tauride continent represented by the Malatya Metamorphics in the north (Robertson et al., 2012a; Karaoğlan et al., 2013, 2016; Barrier et al., 2018). The Late Cretaceous arc-related intrusive magmatism of the northern belt in SE Turkey (Baskil intrusives) evolved towards collisional, including shoshonitic compositions (74-72 Ma), which are interpreted to indicate continental and post-collisional settings (Kuşcu et al., 2013; Erturk et al., 2018; Sar et al., 2019). The shoshonitic compositions of some of the granitic rocks, together with the evidence of HP/LT metamorphism, are consistent with the collision of the Tauride carbonate platform (i.e. Malatya Metamorphics) to the north with the Bitlis and Pütürge continental units to the south. However, the origins of shoshonites remain controversial because the necessary partial melting of mantle and interaction with subduction-related fluids can take place in a variety of pre-, syn- and post-collisional settings (e.g. Campbell et al., 2014).

Several authors have correlated the Late Cretaceous Göksun and related ophiolites in the north with the Meydan ophiolite (Berit meta-ophiolite of Yılmaz et al., 1993) in the south. If correct, the granitic intrusives in both belts originated as different parts of a single arc lineament that straddled the northerly active continental margin of the oceanic basin. The southerly arc and ophiolitic rocks (Helete-Meydan) were emplaced southwards during the latest Cretaceous, although further southward thrusting took place, mainly during the Eocene and Miocene (Perinçek and Kozlu, 1984; Yılmaz et al., 1993).

In many reconstructions, oceanic crust still remained between the Bitlis-Püturge continental units and Arabia until the Miocene (Yılmaz, 1993; Robertson et al., 2012a; Barrier et al., 2018; van Hinsbergen et al., 2020). The Bitlis and Püturge massifs have been generally correlated with the Alanya metamorphic massif to the north of Cyprus (with or without a direct continuation) (Çetinkaplan et al., 2016). If correct, the Late Cretaceous Kyrenia Range felsic arc volcanism (and that of the Kannaviou Formation) could have been located to south of the Alanya continent, with a possible eastward continuation to south of the Bitlis and Püturge continental units.~~(Parlak, 2006;~~

Robertson et al., 2006). Examples occur in the Keban (Malatya), Göksun (Kahramanmaraş) and Baskil (Elazığ) regions (Fig. 1) (Yazgan and Chessex, 1991; Parlak, 2006; Rızaoğlu et al., 2009; Karaoğlan et al., 2013, 2016). The arc rocks are mainly hornblende-biotite granodiorites and 'normal' granites that are radiometrically dated as 88-82 Ma (Santonian-Campanian) (Rızaoğlu et al., 2009; Karaoğlan et al., 2016). The granitic rocks have I-type, calc-alkaline arc affinities, with both mantle and crustal-derivation features (Parlak, 2006; Rızaoğlu et al., 2009; Karaoğlan et al., 2013, 2016). The intrusions are relatively enriched in LREE (Parlak, 2006; Rızaoğlu et al., 2009) compared to the Helete granites, which suggests a more crustally influenced source during magma genesis. The above granitic rocks are located in a structurally higher position than the Kyrenia and Helete arc rocks (i.e. above the Pütürge metamorphic massif) and are likely to have a different region. The northerly arc have been explained by northward subduction of a small oceanic basin (Berit ocean) that was located between two continental units; i.e. Bitlis-Püturge in the south and the Tauride continent (Malatya) in the north (Robertson et al., 2012a; Karaoğlan et al., 2013, 2016; Barrier et al., 2018).

All of the above extrusive and intrusive felsic arc rocks differ from the Late Cretaceous ophiolitic and oceanic arc rocks in the region. These include a widely exposed assemblage (Malatya-Elazığ region) of basic igneous rocks and volcanogenic sediments, known as the Yüksekova Complex (Perincek and Özkaya, 1981; Aktaş and Robertson, 1984). The basalts have a tholeiitic to tholeiitic-transitional character, variable Zr/Y (1.5-6) ratios and mantle-array-aligned Sr-Nd isotopes (Ural et al., 2015). These basic volcanics were derived from a depleted mantle source without a significant crustal contribution; i.e. from an intra-oceanic setting within the Southern Neotethys (Ural et al., 2015). In contrast, the Kyrenia Range basalts have higher Zr/Y (2.8-7.7) and Nb/Y (Figs. 12b, 13c), suggestive of a magmatic contribution from continental crust or subducted continentally derived sediments (Zindler and Hart, 1986; Pearce, 1996).

Formatted: Font color: Red

Paleogene magmatic rocks are also present in SE Turkey. Eocene volcanic rocks and associated minor intrusions, known as the Maden Complex, unconformably overlie and cut the Pütürge and Bitlis ~~continental metamorphic units~~metamorphosed continental units (Fig. 1) (Hempton, 1985; Yazgan and Chessex, 1991; Aktaş and Robertson, 1984, 1990; Yılmaz, 1993; Elmas and Yılmaz, 2003; Robertson et al., 2006; Erturk et al., 2018). The volcanics show enrichment in LILEs and relative depletion in Nb, Ta and Ti compared to MORB (Erturk et al., 2018), similar to a minority of the subduction-related volcanics in the Kyrenia Range (see Supplementary Figure S6). The Eocene Maden Complex magmatism is widely proposed to relate to back-arc rifting of the (Eurasian) active continental margin during the later stages of northward subduction of the Southern Neotethys, in keeping with the widespread view that collision with Arabia was delayed until the Miocene (Aktaş and Robertson, 1984, 1990; Yılmaz, 1993; Yılmaz et al., 1993; -Yiğitbaş and Yılmaz, 1996; Robertson et al., 2006, 2007; van Hinsbergen et al., 2020). Oblique convergence, ~~as~~ proposed by several authors (Aktaş and Robertson, 1990; Elmas and Yılmaz, 2003), could have resulted in along-strike variation in the geochemical signatures of extension versus subduction in the Kyrenia Range, although more geochemical work ~~in~~ is needed, regionally and globally to test this ~~possibility~~hypothesis.

Farther north, Eocene granitic rocks locally cut the continental Malatya metamorphic unit (Doğanşehir region) (Perinçek and Kozlu, 1984; Karaoğlan et al., 2013, 2016). However, no extrusive equivalents are known and, as noted above, the magmatic rocks in this lineament are unlikely to correlate directly with the Kyrenia Range.

During the Miocene, the active continental margin bordering the remnant Southern Neotethys collided with the Arabian passive continental margin to the south. In both the Kyrenia Range and SE Turkey, the Late Cretaceous and Paleogene magmatic rocks are exposed close the thrust front (Eurasia), implying that at least tens of kms of fore-arc crust have been lost (subducted or overridden), potentially removing additional frontal arc-related crust, both Late Cretaceous and Paleogene. Thus, the Kyrenia, Kannaviou (W Cyprus) and Helete Maden Complex magmatism could all represent surviving products of a regional Late Cretaceousactive continental margin arc.

5.5. Tectono-magmatic hypotheses

In the light of the regional setting, tThe felsic volcanics (Fourkovouno Formation, c. 74 Ma), with continental margin arc affinities, are interpreted to have resulted from northward subduction beneath continental crust, possibly the Alanya continental unit to the north (Çetinkaplan et al., 2016; Robertson et al., 2020). of the Taurides. The felsic volcanism is characteristic of relatively advanced subduction, suggesting that earlier eruptive centers existed along the active continental margin. The early volcanism is likely to be represented by the Campanian (c. 80 Ma) arc-derived volcanogenic sediments (Kannaviou Formation) in western Cyprus (Robertson, 1977; Gilbert and Robertson, 2013; Chen and Robertson, 2019). The underlying mantle wedge (sub-continental lithosphere) was metasomatically enriched during the Late Cretaceous subduction, with implications for the subsequent basaltic volcanism.

For the Maastrichtian to Late Eocene basaltic volcanics, there are three alternative tectono-magmatic models. The first model envisages a marginal basin setting related to northward subduction. The Southern Neotethys remained partly open between the Taurides and the Troodos ophiolite during the Late Cretaceous to Mid-Eocene. Subduction of the remnant ocean gave rise to the basaltic volcanism, including the Misis-Andırın Range. Compared to typical back-arc basin basalts (Fig. 14a-b), the basalts of the Kyrenia Range basalts (and the Misis-Andırın Range) have relatively high Th/Nb but low La/Nb ratios. The high abundances of Th are likely to reflect a continental crust influencenput (Floyd et al., 1991). The variation in La/Nb ratios of the basalts could reflect the influence of a within-plate mantle source (i.e. easterly basalts) and/or the arc maturity; ~~(~~i.e. the arc-like western basalts could have erupted closer to the distal (oceanward) edge of the convergent margin~~)~~. However, a problem with this model is the absence of evidence for a Paleogene volcanic arc to the south. There is no evidence of arc-derived fallout tuff or volcaniclastic sediments in the Maastrichtian-Paleogene basaltic succession, in contrast with, for example, the SW Pacific Mariana and Tonga marginal basins (Clift, 1994; Bryan et al., 2004).

The second model involves an extensional (or transtensional) setting. In this interpretation, the Late Maastrichtian and Paleogene 'enriched' within-plate volcanism was triggered by strike-slip (or transtension) along the ~~South Neotethyan~~ active continental margin. One option is that the volcanism was linked to the anticlockwise paleorotation of the Troodos ophiolite to the south during Late Campanian-Early Eocene (Clube et al., 1985; Clube and Robertson, 1986; Morris et al., 2006, 2015; Hodgson et al., 2010). More generally, oblique convergence of the African plate with respect to Eurasia could have resulted in segmentation of the South Neotethyan active margin into subducting segments with arc magmatism, and also strike-slip segments without arc magmatism (Aktaş and Robertson, 1990). A modern example is the Andaman Sea where oblique convergence between the Asian and the Australian plates resulted in segmented arc magmatism (e.g. Curray et al., 2005). However, there is limited information from different modern settings to test this hypothesis.

The third, preferred, scenario is that both the felsic and the basaltic volcanism are related to northward subduction during stages in the closure of the ~~Southern Neotethys.~~Mesozoic ocean basin to the south. The Late Cretaceous magmatism can then be~~is~~ explained by regional northward subduction (nearly orthogonal) resulting in continental margin arc volcanism. Slab-derived and residual slab components (fluid, melt) were released into the upper mantle lithosphere (e.g. Pearce, 1983; Harangi et al., 2007). The Late Maastrichtian and Paleogene basaltic volcanics then erupted in an extensional (or transtensional) setting, perhaps related to slab rollback and incipient marginal basin formation. Several different mantle sources are likely to have contributed along the Kyrenia Range. The variable subduction-related signatures were inherited from the previously modified mantle lithosphere in this interpretation. Examples of subduction-influenced settings that were affected by later extension-related melting include the Rio Grande Rift, west USA (e.g. Riecker, 1979) and the Neogene north Aegean-west Anatolia volcanic province (e.g. Şengör and Yılmaz, 1981; Ersoy and Palmer, 2013). In summary, the available evidence is consistent with Late Maastrichtian-Paleogene incipient marginal basin formation along the northern, active margin of ~~the Southern Neotethys~~ an ocean basin (Southern Neotethys) that did not close until the Miocene.

5.6. Testing alternative tectonic models

Finally, the Late Cretaceous-Paleogene volcanism in N Cyprus and SE Turkey can be used to test alternative plate tectonic models, including those by Robertson et al. (2012a), Karaoğlan et al. (2013, 2016), Maffione et al. (2017), Barrier et al. (2018), McPhee and van Hinsbergen (2019) and van Hinsbergen et al. (2020), as summarised in Figure 15.

In Reconstruction 1 (Fig. 15a-c) (Robertson et al., 2012a), the Southern Neotethys rifted in the Triassic, while Paleotethys evolved into the Northern Neotethys (İzmir-Ankara-Erzincan ocean). The Kyrenia Range is restored to the northern passive margin of the Southern Neotethys. Both intra-oceanic and continental margin subduction zones (northward-dipping) were active in the Southern Neotethys during the Late Cretaceous. The continental margin arc volcanism was constructed on, or to the south of one, or more, continental blocks (microcontinents), represented by the Kyrenia-Alanya-Püturge-Bitlis lineament in the south and the Malatya-Keban lineament farther north. This reconstruction is compatible with our new evidence~~, while~~

~~prompting questions concerning the implications of two subparallel arc magmatic belts (outside the present scope)~~.

Reconstruction 2 (Fig. 15d-f) (Barrier et al., 2018) has many common features with (1), in particular the arc volcanism along the northern margin of the Southern Neotethys. However, the Kyrenia, Malatya and Pütürge-Bitlis massifs are restored as a single elongate continental unit rather than as microcontinents, as in (1). Also, little or no oceanic crust is inferred between the southerly continental unit and the Tauride carbonate platform to the north (i.e. Göksun and related ophiolites). This is difficult to reconcile with the Late Cretaceous and Eocene granitic magmatism cutting the Mesozoic Malatya (Keban) platform unless large-scale strike-slip and terrane duplication has taken place for which there is little supporting evidence.

In Reconstruction 3 (Fig. 15g-h) (Maffione et al., 2017; van Hinsbergen et al., 2020), the Kyrenia Range is restored to the southern passive margin of the Mesozoic Tethyan ocean. Late Cretaceous ophiolites that are presently located in several c. E-W, sub-parallel belts (i.e. N and S of the Bitlis and Pütürge massifs) originated above a single subduction zone that originated within Neotethys, dipping generally to the east or northeast (Stampfli and Borel, 2002; Moix et al., 2008). The subduction zone rolled back generally westwards until it collided with the Tauride and Arabian continents. In the south, the subduction zone broke through the oceanic gap between the African and Tauride continents, 'invaded' and replaced the Southern Neotethys with Late Cretaceous supra-subduction zone fore-arc crust. Fore-arc ophiolites were then obducted generally northwards and southwards over the opposing continents (van Hinsbergen et al., 2020). Two alternatives ~~have been~~are suggested; in one, the Bitlis and Pütürge continental units are correlated with Arabia (Maffione et al., 2017), whereas in the other these units are correlated with the southern margin of the Tauride ~~continents~~ continent (van Hinsbergen et al., 2020). The Kyrenia Range (Trypa Group) is placed on the N African continental margin in both alternatives. The metamorphism of the Mesozoic carbonate platform in the Kyrenia Range (Trypa Group) resulted from northeastward underthrusting/subduction beneath the obducted forearc Troodos ophiolite (van Hinsbergen et al., 2020). However, there are several problematic aspects: (1) seismic tomography in the Eastern Mediterranean supports generally northward subduction (e.g. Hafkenscheid et al., 2006), without evidence of a relict southward-dipping slab, as implied by the inferred northward emplacement of some Late Cretaceous ophiolites in S Turkey ~~(it is however unclear for how long such a trace would be preserved)~~; (2) it does not allow for the tens to hundreds of km of subduction required to produce the Late Cretaceous arc magmatism in N Cyprus and SE Turkey. ~~Specifically, t~~The ~~magmatically crosscut~~ Malatya metamorphic unit, cut by Late Cretaceous granites, is instead~~is~~ restored to the lower, downgoing plate (i.e. beneath the south~~S~~ margin of the Tauride continent~~s~~) implying ~~suggesting~~ northward subduction; (3) the model (van Hinsbergen et al., 2020) does not allow for any Late Cretaceous continental arc-related magmatism in northern Cyprus, SE Turkey or Iran (e.g. Agard et al., 2011); (4) in this model, the proposed Late Eocene-Miocene (post 45 Ma) northward subduction is ~~also~~ too young to explain the Late Cretaceous-Paleogene magmatic rocks in the Kyrenia Range and SE Turkey; (5) arc magmatism of Oligocene-Miocene age in S Turkey is absent, although this would be expected if significant northward subduction took place during this time, as in model 3.

6. Conclusions

- Latest Cretaceous mainly felsic volcanic rocks and latest Cretaceous-Paleogene mainly basaltic volcanic rocks are exposed throughout the Kyrenia Range, separated by a thrust.
- Mapping and logging of the key, well-exposed ~~segment of the~~ western Kyrenia Range segment~~, N Cyprus~~ shows that the Late Cretaceous felsic arc volcanics

occur as variably dismembered thrust sheets in the southerly, frontal part of thrust belt.

- The primary eruptive age of the felsic arc volcanics (Fourkovouno Formation) is ~~determined as~~ c. 74.0 Ma (Late Campanian), based on U-Pb dating of zircons.
- The latest Cretaceous-Paleogene basalts vary geochemically along the Kyrenia Range (E-W). The volcanics in the east resemble normal rift products. In contrast, the volcanics in the west have a subordinate subduction-related signature (e.g. negative Nb anomaly).
- Sr-Nd-Hf isotopic data for the latest Cretaceous-Paleogene basalts suggest that they were derived from several OIB-like mantle sources, ~~probably~~ with the involvement of a crustally-derived (recycled) component.
- The Kyrenia Range felsic volcanics show some geochemical similarities with the late Cretaceous ~~(93-83 Ma)~~ arc-related rocks in S Turkey (Helete granite; 93-83 Ma). These felsic volcanics are interpreted to represent a fragment of a mature magmatic arc that was active along a regional-scale active continental margin. Regional reconstructions suggest that the Helete granites and related ophiolitic rocks were emplaced southwards from an oceanic basin (Berit ocean) to the north.
- The latest Cretaceous-Paleogene volcanics in the Kyrenia Range have geochemical similarities with the Middle Eocene (c. 47 Ma) basaltic rocks in S Turkey (Maden Complex), suggesting an along-strike continuation of the same active continental margin.~~.~~
- The latest Cretaceous-Paleogene basaltic volcanics in the Kyrenia Range are interpreted as the products of an incipient marginal basin that developed during northward subduction, possibly related to oblique convergence, prior to collision with Arabia during the Miocene.~~.~~

- In the light of alternative regional Having taken account of a range of tectonic models, the Late Cretaceous and- Paleogene magmatic rocks in Kyrenia Range, of N Cyprus are interpreted to represent stages in the development of the northerly active continental margin of the Southern Neotethys.

Acknowledgements

We thank Richard Hinton, Steffen Kutterolf and Dick Kroon for scientific discussion. Mike Hall is thanked for thin section and polished blocks preparation. Nick Odling kindly assisted with the XRF analysis. Antony Morris is thanked for providing the samples of basalt from drill cores that were originally collected for paleomagnetic studies. Rory McKavney kindly assisted with the fieldwork in northern Cyprus. The first author gratefully acknowledges the receipt of a joint studentship of the Principal's Career Development PhD Scholarship and Edinburgh Global Research Scholarship. The authors are grateful for financial support via the Natural Environment Research Council Ion Microprobe Facility (to A.H.F. Robertson) to carry out the secondary ion mass spectrometry U-Pb dating of detrital zircons. Fieldwork and geochemical analysis were aided by financial support from the International Association of Sedimentologists [Postgraduate Grant Scheme], the Mineralogical Society of Great Britain and Ireland [Postgraduate Student Bursary Awards], and the Edinburgh Geological Society [Clough Fund], all to the first author. Additional financial support was provided by the John Dixon Memorial Fund. Osman Parlak is thanked for discussion of SE Turkey geology. The manuscript benefitted from comments by Pamela Kempton, Fatih Karaoğlan and the editor, Greg Shellnutt.

Formatted: Justified, Don't add space between paragraphs of the same style, No widow/orphan control

References

Adamia, S.A., Lordkipanidze, M., Zakariadze, G., 1977. Evolution of an active continental margin as exemplified by the Alpine history of the Caucasus. Tectonophysics 40, 183-199.

Agard, P., Omrani, J., Jolivet, L., Whitechurch, H., Vrielynck, B., Spakman, W., Monié, P., Meyer, B., Wortel, R., 2011. Zagros orogeny: a subduction-dominated process. Geological Magazine 148, 692-725.

Aktaş, G., Robertson, A.H.F., 1984. The Maden Complex, SE Turkey: evolution of a Neotethyan active margin, in: Dixon, J.E., Robertson, A.H.F. (Eds.), The Geological Evolution of the Eastern Mediterranean. Geological Society of London, Special Publications 17, pp. 375-402.

Aktaş, G., Robertson, A.H.F., 1990. Tectonic evolution of the Tethys suture zone in SE Turkey: evidence from the petrology and geochemistry of Late Cretaceous and Middle Eocene extrusives, in: Malpas, J., Moores, E.M., Panayiotou, A., Xenophontos, C. (Eds.), Ophiolites-Oceanic Crustal Analogues. Proceedings of the International Symposium 'Troodos 1987'. Cyprus Geological Survey Department, Nicosia, pp. 311-329.

Baroz, F., 1979. Etude géologique dans le Pentadaktylos et la Mesaoria (Chypre Septentrionale). Doctor of Science Thesis (Published). Université de Nancy, France (434 pp).

Baroz, F., 1980. Volcanism and continent-island arc collision in the Pentadaktylos range, Cyprus, in: Panayiotou, A. (Ed.), Ophiolites: Proceedings of the International Ophiolite Symposium. Cyprus Ministry of Agriculture and Natural Resources, Geology Survey Department, Nicosia, Cyprus, pp. 73-85.

Barrier, E., Vrielynck, B., Brouillet, J.F., Brunet, M.F., 2018. Paleotectonic Reconstruction of the Central Tethyan Realm. Tectono-Sedimentary-Palinspastic Maps from Late Permian to Pliocene. Atlas of 20 maps (scale 1/15000000). CCGM/CGMW, Paris.

Beccaluva, L., Macciotta, G., Piccardo, G., Zeda, O., 1989. Clinopyroxene composition of ophiolite basalts as petrogenetic indicator. Chemical Geology 77, 165-182.

Bowman, N., Van Otterloo, J., Cairns, C., Taylor, D., Cas, R., 2019. Complex evolution of volcanic arcs: The lithofacies and palaeogeography of the Cambrian Stavely Arc, Delamerian Fold Belt, Western Victoria. Journal of Volcanology and Geothermal Research 373, 120-132.

Brune, S., Popov, A.A., Sobolev, S.V., 2012. Modeling suggests that oblique extension facilitates rifting and continental break-up. Journal of Geophysical Research: Solid Earth 117. doi: 10.1029/2011JB008860

Bryan, S., Cook, A., Evans, J., Colls, P., Wells, M., Lawrence, M., Jell, J., Greig, A., Leslie, R., 2004. Pumice rafting and faunal dispersion during 2001–2002 in the Southwest Pacific: record of a dacitic submarine explosive eruption from Tonga. Earth and Planetary Science Letters 227, 135-154.

Campbell, I.H., Stepanov, A.S., Liang, H.-Y., Allen, C.M., Norman, M.D., Zhang, Y.-Q., Xie, Y.-W., 2014. The origin of shoshonites: new insights from the Tertiary high-potassium intrusions of eastern Tibet. Contributions to Mineralogy and Petrology 167. doi: 10.1007/s00410-014-0983-9

Çetinkaplan, M., Pourteau, A., Candan, O., Koralay, O.E., Oberhänsli, R., Okay, A.I., Chen, F., Kozlu, H., Şengün, F., 2016. P–T–t evolution of eclogite/blueschist facies metamorphism in Alanya Massif: time and space relations with HP event in Bitlis Massif, Turkey. International Journal of Earth Sciences 105, 247-281.

Chappell, B.W., White, A.J.R., 1992. I- and S-type granites in the Lachlan Fold Belt. Earth and Environmental Science Transactions of the Royal Society of Edinburgh 83, 1-26.

Chen, G., Robertson, A.H.F., 2019. Provenance and magmatic-tectonic setting of Campanian-aged volcaniclastic sandstones of the Kannaviou Formation in western Cyprus: Evidence for a South-Neotethyan continental margin volcanic arc. Sedimentary Geology 388, 114-138.

Chen, S.-s., Liu, J.-q., Chen, S.-s., Guo, Z.-f., Sun, C.-q., 2015. Variations in the geochemical structure of the mantle wedge beneath the northeast Asian marginal region from pre- to post-opening of the Japan Sea. Lithos 224-225, 324-341.

Clift, P., 1994. Controls on the Sedimentary and Subsidence History of an Active Plate Margin: An Example from the Tonga Arc (Southwest Pacific), in: Hawkins, J., Parson, L., Allan, J. (Eds.), Proceedings of the Ocean Drilling Program, Scientific Results. Ocean Drilling Program 135, College Station, TX, pp. 173–189.

Clube, T.M.M., Creer, K.M., Robertson, A.H.F., 1985. Palaeorotation of the Troodos microplate, Cyprus. Nature 317, 522-525.

Clube, T.M.M., Robertson, A.H.F., 1986. The palaeorotation of the Troodos microplate, Cyprus, in the Late Mesozoic-Early Cenozoic plate tectonic framework of the Eastern Mediterranean. Surveys in Geophysics 8, 375-437.

Condie, K.C., 2003. Incompatible element ratios in oceanic basalts and komatiites: tracking deep mantle sources and continental growth rates with time. Geochemistry, Geophysics, Geosystems 4, 1005. doi:10.1029/2002GC000333

Condie, K.C., 2005. High field strength element ratios in Archean basalts: a window to evolving sources of mantle plumes? Lithos 79, 491-504.

Curray, J.R., 2005. Tectonics and history of the Andaman Sea region. Journal of Asian Earth Sciences 25, 187-232.

Dercourt, J., Ricou, L.E., Vrielynck, B., 1993. Atlas of Peri-Tethys Palaeogeographical Maps. CCGM/CGMW, Paris (268 pp).

Dewey, J.F., 1969. Evolution of the Appalachian/Caledonian orogen. Nature 222, 124-129.

Ducloz, C., 1972. The geology of the Bellapais-Kythrea area of the Central Kyrenia Range. Bulletin of the Geological Survey Department 6, Nicosia, Cyprus (75 pp).

Elmas, A., Yılmaz, Y., 2003. Development of an oblique subduction zone-tectonic evolution of the Tethys suture zone in southeast Turkey. International Geology Review 45, 827-840.

Ersoy, E.Y., Palmer, M.R., 2013. Eocene-Quaternary magmatic activity in the Aegean: implications for mantle metasomatism and magma genesis in an evolving orogeny. Lithos 180, 5-24.

Erturk, M.A., Beyarslan, M., Chung, S.L., Lin, T.H., 2018. Eocene magmatism (Maden Complex) in the Southeast Anatolian Orogenic Belt: Magma genesis and tectonic implications. Geoscience Frontiers 9, 1829-1847.

Fitton, J.G., Godard, M., 2004. Origin and evolution of magmas on the Ontong Java Plateau, in: Fitton, J.G., Mahoney, J.J., Wallace, P.J., Saunders, A.D. (Eds.), Origin and Evolution of the Ontong Java Plateau. Geological Society of London, Special Publications 229, pp. 151-178.

Fitton, J.G., Saunders, A.D., Larsen, L.M., Hardarson, B.S., Norry, M.J., 1998. Volcanic rocks from the southeast Greenland margin at 63°N: composition, petrogenesis and mantle sources, in: Saunders, A.D., Larsen, H.C., Wise, S.W. (Eds.), Proceedings of the Ocean Drilling Program, Scientific Results. Ocean Drilling Program 152, College Station, TX, pp. 331-350.

Floyd, P., Kelling, G., Gökçen, S., Gökçen, N., 1991. Geochemistry and tectonic environment of basaltic rocks from the Misis ophiolitic mélange, south Turkey. Chemical Geology 89, 263-280.

Floyd, P., Kelling, G., Gökçen, S., Gökçen, N., 1992. Arc-related origin of volcaniclastic sequences in the Misis Complex, Southern Turkey. The Journal of Geology 100, 221-230.

Garfunkel, Z., 1998. Constrains on the origin and history of the Eastern Mediterranean basin. Tectonophysics 298, 5-35.

Gilbert, M.F., Robertson, A.H.F., 2013. Field relations, geochemistry and origin of the Upper Cretaceous volcaniclastic Kannaviou Formation in western Cyprus: evidence of a southerly Neotethyan volcanic arc, in: Robertson, A.H.F., Parlak, O., Ünlügenç, U.C. (Eds.), Geological Development of Anatolia and the Easternmost Mediterranean Region. Geological Society of London, Special Publications 372,

pp. 273-298.
Gorton, M.P., Schandl, E.S., 2000. From continents to island arcs: a geochemical index of tectonic setting for arc-related and within-plate felsic to intermediate volcanic rocks. The Canadian Mineralogist 38, 1065-1073.
Hafkenscheid, E., Wortel, M., Spakman, W., 2006. Subduction history of the Tethyan region derived from seismic tomography and tectonic reconstructions. Journal of Geophysical Research: Solid Earth 111, B08401. doi: 10.1029/2005JB003791
Hakyemez, Y., Turhan, N., Sönmez, I., Sümengen, M., 2000. Kuzey Kıbrıs Türk Cumhuriyeti'nin Jeolojisi (Geology of the Turkish Republic of Northern Cyprus). Genel Müdürlüğü Jeoloji Etütleri Diaresi, Maden Tektik ve Arama, Ankara (44 pp).
Harangi, S., Downes, H., Thirlwall, M., Gmeling, K., 2007. Geochemistry, Petrogenesis and Geodynamic Relationships of Miocene Calc-alkaline Volcanic Rocks in the Western Carpathian Arc, Eastern Central Europe. Journal of Petrology 48, 2261-2287.
Hartley, M.E., Thordarson, T., 2013. The 1874-1876 volcano-tectonic episode at Askja, North Iceland: Lateral flow revisited. Geochemistry, Geophysics, Geosystems 14, 2286-2309.
Hastie, A.R., Kerr, A.C., Pearce, J.A., Mitchell, S.F., 2007. Classification of Altered Volcanic Island Arc Rocks using Immobile Trace Elements: Development of the Th–Co Discrimination Diagram. Journal of Petrology 48, 2341-2357.
Hayward, C., 2011. High spatial resolution electron probe microanalysis of tephras and melt inclusions without beam-induced chemical modification. The Holocene 22, 119-125.
Hempton, M.R., 1985. Structure and deformation history of the Bitlis suture near Lake Hazar, southeastern Turkey. Geological Society of America Bulletin 96, 233-243.
Hodgson, E., Morris, A., Anderson, M., Robertson, A., 2010. First palaeomagnetic results from the Kyrenia Range terrane of northern Cyprus and their implication for the regional plate tectonic evolution of the eastern Mediterranean, EGU

General Assembly Conference Abstracts, Vienna, Austria, p. 6449.

Hu, Z., Gao, S., 2008. Upper crustal abundances of trace elements: a revision and update. Chemical Geology 253, 205-221.

Huang, K., Malpas, J., Xenophontos, C., 2007. Geological studies of igneous rocks and their relationships along the Kyrenia Range, in: Moumani, K., Shawabkeh, K., Al-Malabeh, A., Abdelghafoor, M. (Eds.), 6th International Congress of Eastern Mediterranean Geology, Amman, Jordan, p. 53.

Karaoğlan, F., Parlak, O., Hejl, E., Neubauer, F., Kloetzli, U., 2016. The temporal evolution of the active margin along the Southeast Anatolian Orogenic Belt (SE Turkey): Evidence from U–Pb, Ar–Ar and fission track chronology. Gondwana Research 33, 190-208.

Karaoğlan, F., Parlak, O., Robertson, A., Thöni, M., Klötzli, U., Koller, F., Okay, A.İ., 2013. Evidence of Eocene high-temperature/high-pressure metamorphism of ophiolitic rocks and granitoid intrusion related to Neotethyan subduction processes (Doğanşehir area, SE Anatolia), in: Robertson, A.H.F., Parlak, O., Ünlügenç, U.C. (Eds.), Geological Development of Anatolia and the Easternmost Mediterranean Region. Geological Society of London, Special Publications 372, pp. 249-272.

Keller, R.A., Fisk, M.R., Smellie, J.L., Strelin, J.A., Lawver, L.A., 2002. Geochemistry of back arc basin volcanism in Bransfield Strait, Antarctica: Subducted contributions and along-axis variations. Journal of Geophysical Research: Solid Earth 107. doi: 10.1029/2001JB000444

Kelly, N., Hinton, R., Harley, S., Appleby, S., 2008. New SIMS U–Pb zircon ages from the Langavat Belt, South Harris, NW Scotland: implications for the Lewisian terrane model. Journal of the Geological Society 165, 967-981.

Kempton, P.D., Downes, H., Lustrino, M., 2018. Pb and Hf isotope evidence for mantle enrichment processes and melt interactions in the lower crust and lithospheric mantle in Miocene orogenic volcanic rocks from Monte Arcuentu (Sardinia, Italy). Geosphere 14, 926-950.

Kuşcu, İ., Tosdal, R.M., Gencalioğlu-Kuşcu, G., Friedman, R., Ullrich, T.D., 2013. Late Cretaceous to Middle Eocene Magmatism and Metallogeny of a Portion of the Southeastern Anatolian Orogenic Belt, East-Central Turkey. Economic Geology 108, 641-666.

Le Pichon, X., 1982. Land-locked oceanic basins and continental collision: the Eastern Mediterranean as a case example, in: Hsü, K.J. (Ed.), Mountain building processes. Academic Press, New York, pp. 201-211.

Li, C.-F., Li, X.-H., Li, Q.-L., Guo, J.-H., Li, X.-H., Yang, Y.-H., 2012. Rapid and precise determination of Sr and Nd isotopic ratios in geological samples from the same filament loading by thermal ionization mass spectrometry employing a single-step separation scheme. Analytica Chimica Acta 727, 54-60.

Ludwig, K.R., 2012. Users manual for Isoplot 3.75. A geochronological toolkit for Microsoft Excel. Berkeley Geochronology Centre, Special Publication No. 5, Berkeley.

Maffione, M., van Hinsbergen, D.J., de Gelder, G.I., van der Goes, F.C., Morris, A., 2017. Kinematics of Late Cretaceous subduction initiation in the Neo-Tethys Ocean reconstructed from ophiolites of Turkey, Cyprus, and Syria. Journal of Geophysical Research: Solid Earth 122, 3953-3976.

McCay, G.A., Robertson, A.H.F., 2013. Upper Miocene–Pleistocene deformation of the Girne (Kyrenia) Range and Dar Dere (Ovgos) lineaments, northern Cyprus: role in collision and tectonic escape in the easternmost Mediterranean region, in: Robertson, A.H.F., Parlak, O., Ünlügenç, U.C. (Eds.), Geological Development of Anatolia and the Easternmost Mediterranean Region. Geological Society of London, Special Publications 372, pp. 421-445.

McCay, G.A., Robertson, A.H.F., Kroon, D., Raffi, I., Ellam, R.M., Necdet, M., 2013.

Stratigraphy of Cretaceous to Lower Pliocene sediments in the northern part of Cyprus based on comparative $^{87}Sr/^{86}Sr$ isotopic, nannofossil and planktonic foraminiferal dating. Geological Magazine 150, 333-359.

McPhee, P.J., van Hinsbergen, D.J., 2019. Tectonic reconstruction of Cyprus reveals Late Miocene continental collision of Africa and Anatolia. Gondwana Research 68, 158-173.

Moix, P., Beccaletto, L., Kozur, H.W., Hochard, C., Rosselet, F., Stampfli, G.M., 2008. A new classification of the Turkish terranes and sutures and its implication for the paleotectonic history of the region. Tectonophysics 451, 7-39.

Moore, T.A., 1960. The geology and mineral resources of the Astromeritis-Kormakiti area. Geological Survey Department, Memoir 6, Nicosia, Cyprus (96 pp).

Morris, A., Anderson, M.W., Inwood, J., Robertson, A.H., 2006. Palaeomagnetic insights into the evolution of Neotethyan oceanic crust in the eastern Mediterranean, in: Robertson, A.H.F., Mountrakis, D. (Eds.), Tectonic Development of the Eastern Mediterranean Region. Geological Society of London, Special Publications 260, pp. 351-372.

Morris, A., Robertson, A.H.F., Anderson, M.W., Hodgson, E., 2015. Did the Kyrenia Range of northern Cyprus rotate with the Troodos–Hatay microplate during the tectonic evolution of the eastern Mediterranean? International Journal of Earth Sciences 105, 399-415.

Nisbet, E.G. Pearce, J.A., 1977. Clinopyroxene composition in mafic lavas from different tectonic settings. Contributions to Mineralogy and Petrology 63, 149-160.

Nurlu, N., Parlak, O., Robertson, A.H.F., von Quadt, A., 2016. Implications of Late Cretaceous U–Pb zircon ages of granitic intrusions cutting ophiolitic and volcanogenic rocks for the assembly of the Tauride allochthon in SE Anatolia (Helete area, Kahramanmaraş Region, SE Turkey). International Journal of Earth Sciences 105, 283-314.

Oberhänsli, R., Candan, O., Bousquet, R., Rimmele, G., Okay, A., Goff, J., 2010. Alpine high pressure evolution of the eastern Bitlis complex, SE Turkey, in: Sosson, M., Kaymakci, N., Stephenson, R.A., Bergerat, F., Starostenko, V. (Eds.), Sedimentary Basin Tectonics from the Black Sea and Caucasus to the Arabian Platform. Geological Society of London, Special Publications 340, pp. 461-483.

Oberhänsli, R., Koralay, E., Candan, O., Pourteau, A., Bousquet, R., 2013. Late Cretaceous eclogitic high-pressure relics in the Bitlis Massif. Geodinamica Acta 26, 175-190.

Parlak, O., 2006. Geodynamic significance of granitoid magmatism in the southeast Anatolian orogen: geochemical and geochronogical evidence from Göksun–Afşin (Kahramanmaraş, Turkey) region. International Journal of Earth Sciences 95, 609-627.

Pearce, J.A., 1975. Basalt geochemistry used to investigate past tectonic environments on Cyprus. Tectonophysics 25, 41-67.

Pearce, J.A., 1983. Role of the sub-continental lithosphere in magma genesis at active continental margins, in: Hawkersworth, C.J., Norry, M.J. (Eds.), Continental Basalts and Mantle Xenoliths. Shiva, Cheshire, UK, pp. 230-249.

Pearce, J.A., 1996. A user's guide to basalt discrimination diagrams, in: Wyman, D.A. (Ed.), Trace Element Geochemistry of Volcanic Rocks: Applications for Massive Sulphide Exploration. Geological Association of Canada, Short Course Notes 12, pp. 79-113.

Pearce, J.A., Cann, J., 1973. Tectonic setting of basic volcanic rocks determined using trace element analyses. Earth and Planetary Science Letters 19, 290-300.

Pearce, J.A., Harris, N.B., Tindle, A.G., 1984. Trace element discrimination diagrams for the tectonic interpretation of granitic rocks. Journal of Petrology 25, 956-983.

Pearce, J.A., Norry, M.J., 1979. Petrogenetic implications of Ti, Zr, Y, and Nb variations in volcanic rocks. Contributions to Mineralogy and Petrology 69, 33-47.

Peccerillo, A., 2017. Cenozoic Volcanism in the Tyrrhenian Sea Region. Springer International Publishing, Cham (399 pp).

Perinçek, D., Kozlu, H., 1984. Stratigraphy and structural relations of the units in the Afşin-Elbistan-Doğanşehir region (Eastern Taurus), in: Tekeli, O., Göncüoğlu, M.C. (Eds.), Geology of the Taurus Belt: Proceedings of the International Symposium. Maden Tetkik ve Arama Enstitüsü, Ankara, pp. 181-198.

Perinçek, D., Özkaya, İ., 1981. Tectonic evolution of the northern margin of Arabian plate. Bulletin of Institute of Earth Science, Hacettepe University 8, 91-101.

Rice, S.P., Robertson, A.H.F., Ustaömer, T., 2006. Late Cretaceous-Early Cenozoic tectonic evolution of the Eurasian active margin in the Central and Eastern Pontides, northern Turkey, in: Robertson, A.H.F., Mountrakis, D. (Eds.), Tectonic Development of the Eastern Mediterranean Region. Geological Society of London, Special Publications 260, pp. 413-445.

Riecker, R.E., 1979. Rio Grande Rift: Tectonics and Magmatism. American Geophysical Union, Washington, DC (438 pp).

Rızaoğlu, T., Parlak, O., Höck, V., Koller, F., Hames, W.E., Billor, Z., 2009. Andean-type active margin formation in the eastern Taurides: Geochemical and geochronogical evidence from the Baskil granitoid (Elazığ, SE Turkey). Tectonophysics 473, 188-207.

Robertson, A.H.F., 1977. The Kannaviou Formation, Cyprus: volcaniclastic sedimentation of a probable Late Cretaceous volcanic arc. Journal of the Geological Society 134, 269-292.

Robertson, A.H.F., Dixon, J.E., 1984. Introduction: aspects of the geological evolution of the Eastern Mediterranean, in: Dixon, J.E., Robertson, A.H.F. (Eds.), The Geological Evolution of the Eastern Mediterranean. Geological Society of London, Special Publications 17, pp. 1-74.

Robertson, A.H.F., Kinnaird, T.C., 2016. Structural development of the central Kyrenia Range (north Cyprus) in its regional setting in the eastern Mediterranean region. International Journal of Earth Sciences 105, 417-437.

Robertson, A.H.F., Parlak, O., 2020. Late Cretaceous-Palaeocene subduction-collision-exhumation of a microcontinent along the northern, active margin of South Neotethys: evidence from the Alanya Massif and the adjacent Antalya Complex (S Turkey). Journal of Asian Earth Sciences, 104467. doi: 10.1016/j.jseaes.2020.104467

Robertson, A.H.F., Parlak, O., Kinnaird, T.C., Taslı, K., Dumitrica, P., 2020. Cambrian-Eocene pre-rift, pulsed rift, passive margin and emplacement processes along the northern margin of the Southern Neotethys: Evidence from the Antalya Complex in the Alanya Window (S Turkey). Journal of Asian Earth Sciences: X 3, 100026. doi: 10.1016/j.jaesx.2020.100026

Robertson, A.H.F., Parlak, O., Rizaoğlu, T., Ünlügenç, Ü., İnan, N., Tasli, K., Ustaömer, T., 2007. Tectonic evolution of the South Tethyan ocean: evidence from the Eastern Taurus Mountains (Elazığ region, SE Turkey), in: Ries, A.C., Butler, R.W.H., Graham, R.H. (Eds.), Deformation of the Continental Crust: The Legacy of Mike Coward. Geological Society of London, Special Publications 272, pp. 231-270.

Robertson, A.H.F., Parlak, O., Ustaömer, T., 2012a. Overview of the Palaeozoic-Neogene evolution of Neotethys in the Eastern Mediterranean region (southern Turkey, Cyprus, Syria). Petroleum Geoscience 18, 381-404.

Robertson, A.H.F., Tasli, K., İnan, N., 2012b. Evidence from the Kyrenia Range, Cyprus, of the northerly active margin of the Southern Neotethys during Late Cretaceous–Early Cenozoic time. Geological Magazine 149, 264-290.

Robertson, A.H.F., Unlügenç, Ü.C., İnan, N., Tasli, K., 2004. The Misis-Andırın Complex: a Mid-Tertiary melange related to late-stage subduction of the Southern Neotethys in S Turkey. Journal of Asian Earth Sciences 22, 413-453.

Robertson, A.H.F., Ustaömer, T., Parlak, O., Ünlügenç, U.C., Taşlı, K., İnan, N., 2006. The Berit transect of the Tauride thrust belt, S Turkey: Late Cretaceous-Early Cenozoic accretionary/collisional processes related to closure of the Southern Neotethys. Journal of Asian Earth Sciences 27, 108-145.

Robertson, A.H.F., Woodcock, N.H., 1979. Mamonia Complex, southwest Cyprus: Evolution and emplacement of a Mesozoic continental margin. Geological Society of America Bulletin 90, 651-665.

Robertson, A.H.F., Woodcock, N.H., 1986. The role of the Kyrenia Range Lineament, Cyprus, in the geological evolution of the eastern Mediterranean area. Philosophical Transactions of the Royal Society of London. Series A, Mathematical and Physical Sciences 317, 141-177.

Rollinson, H.R., 1993. Using Geochemical Data: Evaluation, Presentation, Interpretation. Routledge, London (384 pp).

Rubatto, D., 2002. Zircon trace element geochemistry: partitioning with garnet and the link between U–Pb ages and metamorphism. Chemical Geology 184, 123-138.

Rudnick, R.L., Gao, S., 2003. Composition of the continental crust, in: Holland, H.D., Turekian, K.K. (Eds.), Treatise on geochemistry. Elsevier-Pergamon 3, Oxford, pp. 1-64.

Sar, A., Ertürk, M.A., Rizeli, M.E., 2019. Genesis of Late Cretaceous intra-oceanic arc intrusions in the Pertek area of Tunceli Province, eastern Turkey, and implications for the geodynamic evolution of the southern Neo-Tethys: Results of zircon U–Pb geochronology and geochemical and Sr–Nd isotopic analyses. Lithos 350-351, 105263. doi: 10.1016/j.lithos.2019.105263

Saunders, A.D., Fornari, D.J., Joron, J., Tarney, J., Treuil, M., 1982. Geochemistry of basic igneous rocks, Gulf of California, Deep Sea Drilling Project Leg 64, in: Curray, J.R., Moore, D.G., Kelts, K. (Eds.), Initial Reports of the Deep Sea Drilling Project. Ocean Drilling Program 64, College Station, TX, pp. 595-642.

Saunders, A.D., Tarney, J., Stern, C.R., Dalziel, I.W., 1979. Geochemistry of Mesozoic marginal basin floor igneous rocks from southern Chile. Geological Society of America Bulletin 90, 237-258.

Şengör, A.M.C., Natal'in, B.A., 1996. Turkic-type orogeny and its role in the making of the continental crust. Annual Review of Earth and Planetary Sciences 24, 263-

337.

Şengör, A.M.C., Yılmaz, Y., 1981. Tethyan evolution of Turkey: a plate tectonic approach. Tectonophysics 75, 181-241.

Şengör, A.M.C., Yılmaz, Y., Sungurlu, O., 1984. Tectonics of the Mediterranean Cimmerides: nature and evolution of the western termination of Palaeo-Tethys, in: Dixon, J.E., Robertson, A.H.F. (Eds.), The Geological Evolution of the Eastern Mediterranean. Geological Society of London, Special Publications 17, pp. 77-112.

Shervais, J.W., 1982. Ti-V plots and the petrogenesis of modern and ophiolitic lavas. Earth and Planetary Science Letters 59, 101-118.

Stampfli, G.M., Borel, G., 2002. A plate tectonic model for the Paleozoic and Mesozoic constrained by dynamic plate boundaries and restored synthetic oceanic isochrons. Earth and Planetary Science Letters 196, 17-33.

Sun, S.-s., McDonough, W.F., 1989. Chemical and isotopic systematics of oceanic basalts: implications for mantle composition and processes, in: Saunders, A.D., Norry, M.J. (Eds.), Magmatism in the Ocean Basins. Geological Society of London, Special Publications 42, pp. 313-345.

Tamaki, K., Pisciotto, K., Allan, J., Alexandrovich, J.M., Barnes, D.A., Boggs, S., Brumsack, H., Brunner, C.A., Cramp, A., Jolivet, L., Kawka, O.E., Koizumi, I., Kuramoto, S.i., Langseth, M.G., McEvoy, J., Meredith, J.A., Mertz, K.A., Murray, R.W., Nobes, D.C., Rahman, A., Schaar, R., Stewart, K.P., Tada, R., Thy, P., Vigliotti, L., White, L.D., Wippern, J., Yamashita, S., 1990. Proceedings of the Ocean Drilling Program, Initial Reports vol. 127. Ocean Drilling Program.

Tatsumi, Y., Kogiso, T., 2003. The subduction factory: its role in the evolution of the Earth's crust and mantle, in: Larter, R.D., Leat, P.T. (Eds.), Intra-Oceanic Subduction Systems: Tectonic and Magmatic Processes. Geological Society of London, Special Publications 219, pp. 55-80.

Thirlwall, M., 1991. Long-term reproducibility of multicollector Sr and Nd isotope ratio analysis. Chemical Geology 94, 85-104.

Trehu, A., Asudeh, I., Brocher, T., Luetgert, J., Mooney, W., Nabelek, J., Nakamura, Y., 1994. Crustal architecture of the Cascadia forearc. Science 266, 237-243.

Ural, M., Arslan, M., Göncüoglu, M., Tekin, U., Kürüm, S., 2015. Late Cretaceous arc and back-arc formation within the southern Neotethys: Whole-rock, trace element and Sr-Nd-Pb isotopic data from basaltic rocks of the Yüksekova Complex (Malatya- Elazığ, SE Turkey). Ofioliti 40, 52-72.

Ustaömer, P.A., Ustaömer, T., Robertson, A.H.F., 2012. Ion probe U-Pb dating of the Central Sakarya basement: a peri-Gondwana terrane intruded by late Lower Carboniferous subduction/collision-related granitic rocks. Turkish Journal of Earth Sciences 21, 905-932.

Ustaömer, T., Robertson, A.H.F., 1997. Tectonic-sedimentary evolution of the North-Tethyan active margin in the Central Pontides of Northern Turkey, in: Robinson, A.G. (Ed.), Regional and Petroleum Geology of the Black Sea and Surrounding Region. AAPG Memoirs 68, pp. 255-290.

van Hinsbergen, D.J., Torsvik, T.H., Schmid, S.M., Maţenco, L.C., Maffione, M., Vissers, R.L., Gürer, D., Spakman, W., 2020. Orogenic architecture of the Mediterranean region and kinematic reconstruction of its tectonic evolution since the Triassic. Gondwana Research 81, 79-229.

Wang, Y., Fan, W., Zhang, Y., Guo, F., Zhang, H., Peng, T., 2004. Geochemical, 40Ar/39Ar geochronological and Sr–Nd isotopic constraints on the origin of Paleoproterozoic mafic dikes from the southern Taihang Mountains and implications for the ca. 1800Ma event of the North China Craton. Precambrian Research 135, 55-77.

Weaver, S.D., Saunders, A.D., Pankhurst, R.J., Tarney, J., 1979. A geochemical study of magmatism associated with the initial stages of back-arc spreading. Contributions to Mineralogy and Petrology 68, 151-169.

Weis, D., Kieffer, B., Hanano, D., Nobre Silva, I., Barling, J., Pretorius, W., Maerschalk, C., Mattielli, N., 2007. Hf isotope compositions of US Geological Survey reference materials. Geochemistry, Geophysics, Geosystems 8, 57-77.

Weis, D., Kieffer, B., Maerschalk, C., Barling, J., De Jong, J., Williams, G.A., Hanano, D., Pretorius, W., Mattielli, N., Scoates, J.S., 2006. High□precision isotopic characterization of USGS reference materials by TIMS and MC□ICP□MS. Geochemistry, Geophysics, Geosystems 7, Q08006. doi: 10.1029/2006GC001283

Whalen, J.B., Currie, K.L., Chappell, B.W., 1987. A-type granites: geochemical characteristics, discrimination and petrogenesis. Contributions to Mineralogy and Petrology 95, 407-419.

Winchester, J., Floyd, P., 1977. Geochemical discrimination of different magma series and their differentiation products using immobile elements. Chemical Geology 20, 325-343.

Yazgan, E., Chessex, R., 1991. Geology and Tectonic Evolution of the Southeastern Taurides in the Region of Malatya. Turkish Association of Petroleum Geologists 3, 1-42.

Yiğitbaş, E., Yılmaz, Y., 1996. Post-Late Cretaceous strike-slip tectonics and its implications for the Southeast Anatolian orogen, Turkey. International Geology Review 38, 818-831.

Yıldırım, E., 2015. Geochemistry, petrography and tectonic significance of the ophiolitic rocks, felsic intrusions and Eocene volcanic rocks of an imbrication zone (Helete area, Southeast Turkey). Journal of African Earth Sciences 107, 89-107.

Yılmaz, Y., 1993. New evidence and model on the evolution of the southeast Anatolian orogen. Geological Society of America Bulletin 105, 251-271.

Yılmaz, Y., Yiğitbaş, E., Genç, Ş.C., 1993. Ophiolitic and metamorphic assemblages of southeast Anatolia and their significance in the geological evolution of the orogenic belt. Tectonics 12, 1280-1297.

Zhang, Y., Wang, Y., Geng, H., Zhang, Y., Fan, W., Zhong, H., 2013. Early Neoproterozoic (~850Ma) back-arc basin in the Central Jiangnan Orogen

(Eastern South China): Geochronological and petrogenetic constraints from meta-basalts. Precambrian Research 231, 325-342.
Zindler, A., Hart, S., 1986. Chemical geodynamics. Annual Review of Earth and Planetary Sciences 14, 493-571.

Listing of Figures

Fig. 1 Outline tectonic map of the Eastern Mediterranean region, including the main volcanic units mentioned in the text. The tectonic framework is modified after Robertson et al. (2012a). Note the location of the Kyrenia Range in northern Cyprus (red box). Jurassic, Cretaceous and Eocene igneous rocks are shown in blue, red and yellow, respectively (see the text for literature sources).

Fig. 2 Successions shown in two main thrust sheets exposed in the Kyrenia Range, northern Cyprus. (a) Simplified log of the succession in the largest thrust sheet including the latest Cretaceous-Paleogene volcanics (Melounda Formation); (b) Restored log of the small, dismembered frontal thrust sheets that expose the Late Cretaceous felsic volcanics (Fourkovouno Formation) (data from Baroz, 1979; Robertson et al., 2012b and this study).

Fig. 3 (a) Outline geological map of the Kyrenia Range (modified from Robertson et al., 2012b). Locations from which basalts were collected are numbered on the map, with small yellow boxes. Karpas Peninsula: 1-Balalan (Platanissos); Eastern Range: 2-Ağıllar (Mandres), 3-Çınarlı (Platani), 4-Mallıdağ (Melounda); Central Range: 5-Tirmen (Trypimeni), 6-Ergenekon (Agios Khariton), 7-Değirmenlik (Kythrea), 8-Arapköy (Klepini), 9-Beylerbeyi (Bellapais), 10-Boğaz (Bogaz), 11-Pınarbaşı (Krini), 12-İncesu (Motides), 13-Alevkaya Tepe (Kiparisso Vouno); Western Range, 14-Karşıyaka (Vasileia), 15-Geçitköy (Panagra); (b) Geological map of the western Kyrenia Range, northern Cyprus made during this study (based on mapping by Baroz, 1979). Locations of cross sections (AA', BB' and CC') are indicated. Note that the two contrasting, mainly felsic and mainly basaltic volcanic units are separated by a thrust fault (Robertson et al., 2012b; this study; see Fig. 2).

Fig. 4 (a) A-A' cross section of Geçitköy that is dominated by a south-verging, recumbent anticline (Late Miocene-earliest Pliocene); (b) B-B' cross-section of Selvilitepe showing southward imbrication of basalt/pelagic chalk and felsic volcanogenic rocks; (c) C-C' cross-section showing imbricated felsic volcanogenic rocks.

Fig. 5 Measured stratigraphic logs of partial successions in the felsic volcanics and structurally associated units. The structural lower unit (logs a-e) is relatively intact, whereas the higher unit (logs f-j) is characterised by the thrust intercalations with the Trypa Group.Fig. 6 (a) Zr/Ti vs. Nb/Y diagram (after Pearce, 1996) and (b) Th vs. Co diagram (after Hastie et al., 2007) for the Kyrenia Range felsic rocks; (c) Primitive mantle-normalised multi-element spider diagram and (d) chondrite-normalised rare earth element (REE) patterns of the felsic volcanics with reference data for upper continental crust (UCC) and lower continental crust (LCC). Normalising values of primitive mantle and chondrite after Sun and McDonough (1989), upper continental crust (UCC) and lower continental crust (LCC) data are from Rudnick and Gao (2003), and Hu and Gao (2008). The Chile volcanic arc granite data are after Pearce et al. (1984).

Fig. 7 (a) Zr/Ti vs. Nb/Y diagram (after Pearce, 1996) and (b) Th vs. Co diagram (after Hastie et al., 2007) for the basaltic volcanics. Red symbols: Karpas Peninsula and eastern range; green symbols: central range; blue symbols: western range. Paleogene basalt samples are indicated by thick magenta-outlined symbols.

Fig. 8 Mid-ocean ridge basalt (MORB)-normalised multi-element spider diagram for basalts from the Karpas Peninsula and the eastern (a), central (b) and western (c) Kyrenia Range. MORB-normalised data are from Pearce et al. (1983); (d) Chondrite-normalised REE patterns of selected basalts. Chondrite, OIB and E-MORB data are from Sun and McDonough (1989). Paleogene basalt samples are indicated by solid black lines and magenta-outlined symbols.

Fig. 9 (a) Cathodoluminescence images of zircon grains separated from the samples of Geçitköy. Red circles mark inconsistent analyses that were omitted from ~~the~~ the weighted mean $^{206}Pb/^{238}U$ age calculation. Locations of the ion probe analysis spots and the corresponding ages ($^{206}Pb/^{238}U$ ± 1σ) are indicated. Scale bar = 20 μm; (b-d) Wetherill Concordia diagram for the zircons analyses from sample 14-18 (b), 14-19 (c) and 14-20 (d).

Fig. 10 (a-b) Plots of P_2O_5 vs. SiO_2 and Th, respectively, show that all of the samples follow the I–type granite trend; (c) Zr vs. 10000×Ga/Al, and (d) Nb vs. 10000×Ga/Al discrimination diagrams of Whalen et al. (1987), showing the I-, S (sedimentary)- and M (depleted mantle source)-type nature of the Late Cretaceous felsic volcanics.

Fig. 11 (a) εNd(t) vs. εSr(t) diagram for the basaltic rocks analysed. The samples are mainly Late Cretaceous (n=4); Paleogene basalt samples (n=2) are indicated by magenta-outlined symbols. Comparative compositions are from Zindler and Hart (1986); (b) εHf(t) vs. εNd(t) plot showing rocks for Kyrenia Range, northern Cyprus relative to other volcanic rocks of the western Mediterranean (after Kempton et al., 2018).

Fig. 12 (a) Ba/Nb versus La/Nb diagram (after Zhang et al., 2013); (b) Nb/Y versus Zr/Y diagram (after Condie, 2005), arrows in (b) indicate the effects of batch melting (F) and the probable effect of fluids derived from subduction (SUB); (c) Zr/Nb vs. Nb/Th diagram (modified after Condie, 2003). Abbreviations: PM, primitive mantle; DM, shallow depleted mantle; HIMU, high mμ (U/Pb) source; EMI and EMII, enriched mantle sources; ARC, arc-related basalt; N-MORB, normal ocean ridge basalt; OIB, oceanic island basalt; DEP, deep depleted mantle; EN, enriched component; REC, recycled component; UCC, upper upper continental crust; LCC, lower continental crust; BM, batch melting trajectory with percent melting noted. Numbers on mixing lines are percents.

Fig. 13 (a) Nb vs. Y diagram (Pearce et al., 1984) and (b) Th/Yb vs. Ta/Yb (Gorton and Schandl, 2000) for the felsic volcanics; (c) Zr/Y vs. Zr diagram (after Pearce and Norry, 1979) and (d) V vs. Ti discrimination diagram (after Shervais, 1982) for the basaltic rocks. Abbreviations: WPG, within-plate granite; VAG, volcanic arc granite; syn-COLG, syn-collisional granite; ORG, ocean ridge granite; WPB, within-plate basalt; MORB, mid-ocean ridge basalt; BABB, back-arc basin basalt; ARC, arc-related basalt; OFB, oceanic floor basalt.

Fig. 14 (a) Th/Nb vs. La/Nb and (b) La/Nb versus Y diagrams (after Floyd et al., 1991). Abbreviations: IAT, island arc tholeiite; BABB, back-arc basin basalt; OFB, oceanic flood basalt; FAPB, fore-arc platform basalt; T/E-MORB, T-type/enriched-mid-ocean ridge basalt.

Fig. 15 Alternative tectonic models of Tethys in the Eastern Mediterranean region. (a-c) Northward subduction with continental fragments rifted from Gondwana (Robertson et al., 2012a); (d-f) Northward subduction and marginal basin formation (Barrier et al., 2018); (g-h) Genesis of Late Cretaceous supra-subduction ophiolites at a single subduction zone to the NE followed by roll-back of segments including the Southern Neotethys (Maffione et al., 2017; McPhee and van Hinsbergen, 2019; van Hinsbergen et al., 2020). Based on discussion (see text), model ~~a~~ 1 is generally favoured.

Listing of Supplementary Figure

Supplementary Figure S1 Field photographs of the felsic volcanics. (a) Exposure in Geçitköy. Samples 14-18 and 14-19 are from this location; (b) Irregular-shaped doleritic intrusion (hammer for scale); (c) Localised occurrence of greyish to greenish, rhyolitic debris-flow unit, north of Geçitköy; (d) Greenish rhyolitic debris-flow unit with angular rhyolitic clasts (pen for scale).

Supplementary Figure S2 Field photographs of the basaltic volcanics. (a) Pillow lavas and interstitial pink pelagic carbonate; roadcut c. 200 m north of Balalan; (b) basalt interbedded with pelagic carbonate; thrust sheet above Miocene siliciclastic sediment; c. 800 m northwest of Değirmenlik; (c) Basaltic volcanics intercalated with pelagic carbonates and small slices of meta-platform carbonates of the Trypa Group along the southern flank of the range, 800 m north of Boğaz; (d) Basalt-pelagic carbonate intercalation, south of Karşıyaka.

Supplementary Figure S3 Photomicrographs of felsic volcanics. (a) Subhedral sanidine (Sa), plagioclase (Pl) and biotite (Bt), in a groundmass of devitrified glassy volcanic shards (cross-polarised light); (b) felsic glass groundmass (Vg) with microcrystalline quartz, irregular-shaped quartz (Q) and feldspar (Pl) (cross-polarised light). Sample number is indicated in the bottom-left corner.

Supplementary Figure S4 Photomicrographs of basalts. (a) Intersertal basalt with euhedral granular augite (Px), elongate plagioclase laths (Pl) and opaque grains (Op) (cross-polarised light); (b) Basalt with intersertal texture, in which randomly-oriented plagioclase generally enclose pyroxenes (plane-polarised light); (c) Porphyrictic basalt with euhedral plagioclase and strongly altered olivine phenocrysts (cross-polarised light); (d) Ophitic basalt with plagioclase phenocrysts, augite occurs as an inclusion within individual plagioclase crystals (cross-polarised light). Sample number is indicated in the bottom-left corner. Samples no. 21, 14-51 and 14-69 are from the Melounda Formation, whereas sample no. 19-51 is from the Ayios Nikolaos Formation.

Supplementary Figure S5 Tectonic discrimination plots. (a) TiO_2-MnO-Na_2O ternary diagram (after Nisbet and Pearce, 1977) for clinopyroxenes in basalt; (b) TiO_2-SiO_2-Na_2O diagram (after Beccaluva et al., 1989) for clinopyroxenes in basalt. Abbreviations: VAB, volcanic arc basalt; OFB, ocean-floor basalt; WPA, within-plate alkali basalt; WPT, within-plate tholeiitic basalt; BON, boninite; IAT, island-arc tholeiite; WPB, within-plate basalt.

Supplementary Figure S6 (a) Chondrite-normalised REE comparison patterns of the Kyrenia Range felsic rocks and the Helete granites in SE Turkey (data after Nurlu et al., 2016). Chondrite data after Sun and McDonough (1989); (b)-(c) MORB-normalised multi-element spider diagrams for basalts. For comparison, the coloured fields show the composition variations of basalts from the Kyrenia Range (this study), the Misis Complex, S Turkey (Floyd et al., 1991), the Maden Complex, S Turkey (Erturk et al., 2018), the Japan Sea (Chen et al., 2015), the Sarmiento Complex, Chile (Saunders et al., 1979), the Bransfield Strait, Antarctic (Keller et al., 2002), the Guaymas Basin, Caribbean (Saunders et al., 1982) and the Tyrrhenian Sea, Italy (Peccerillo, 2017). MORB-normalised data are from Pearce et al. (1983). N-MORB, E-MORB and OIB data are from Sun and McDonough (1989). Specifically, two representative basalts of different affinities (within-plate vs. volcanic arc) from the Kyrenia Range are indicated.

1480

Listing of Supplementary Tables

Supplementary Table S1. Major element oxides, trace and rare earth elements for the Late Cretaceous Fourkovouno (Selvilitepe) Formation.

Supplementary Table S2. Major element oxides, trace and rare earth element analyses for the latest Cretaceous-Paleogene basaltic volcanics.

Supplementary Table S3. Electron microprobe analyses of feldspar in the latest Cretaceous-Paleogene basaltic volcanics.

Supplementary Table S4. Electron microprobe analyses of pyroxene in the latest Cretaceous-Paleogene basaltic volcanics.

Supplementary Table S5. SIMS zircon U-Pb analyses of the zircon grains separated from the Late Cretaceous Fourkovouno (Selvilitepe) Formation.

Figure 1

Click here to access/download;Figure;Fig. 1.jpg

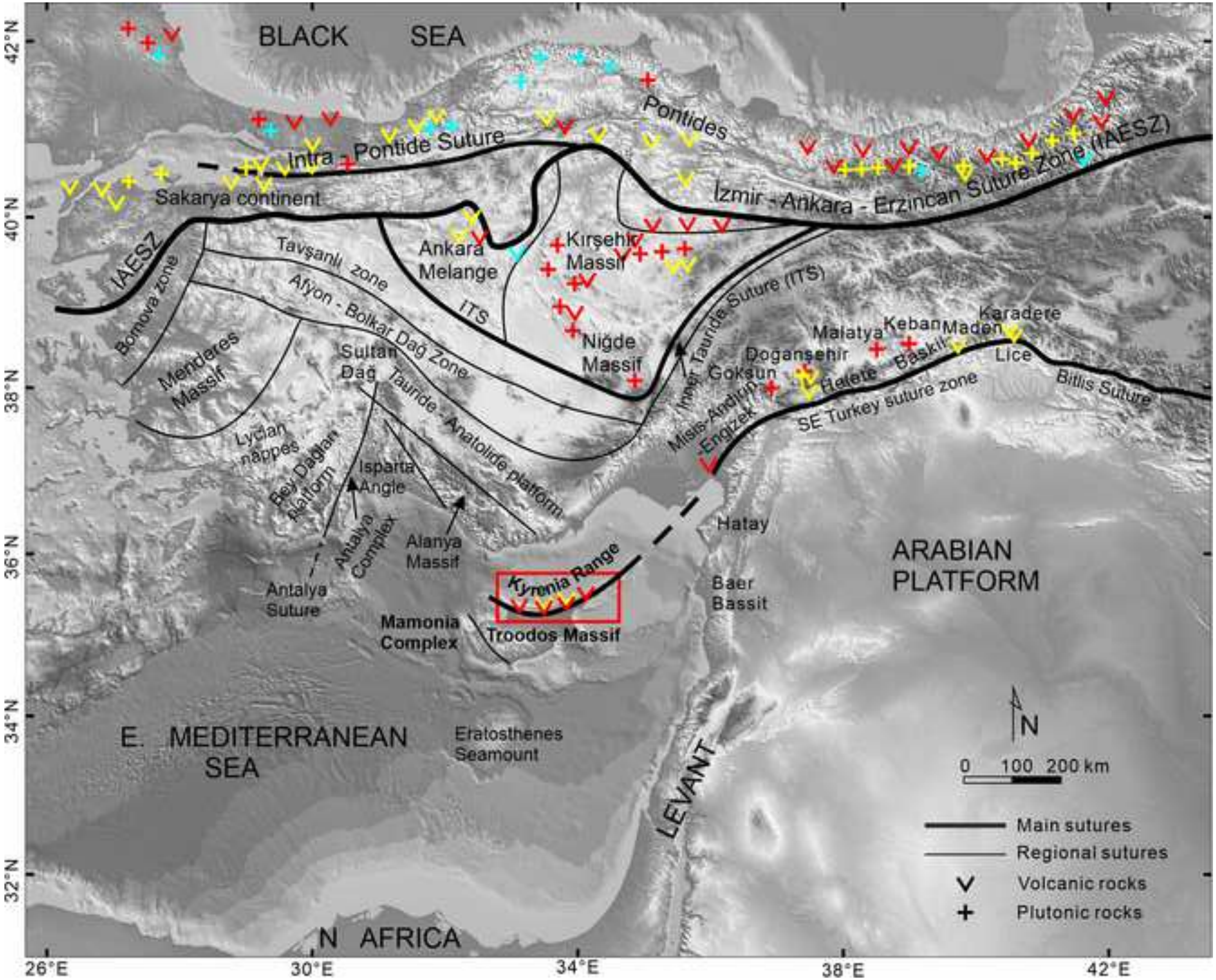

Figure 2 Click here to access/download;Figure;Fig. 2.jpg

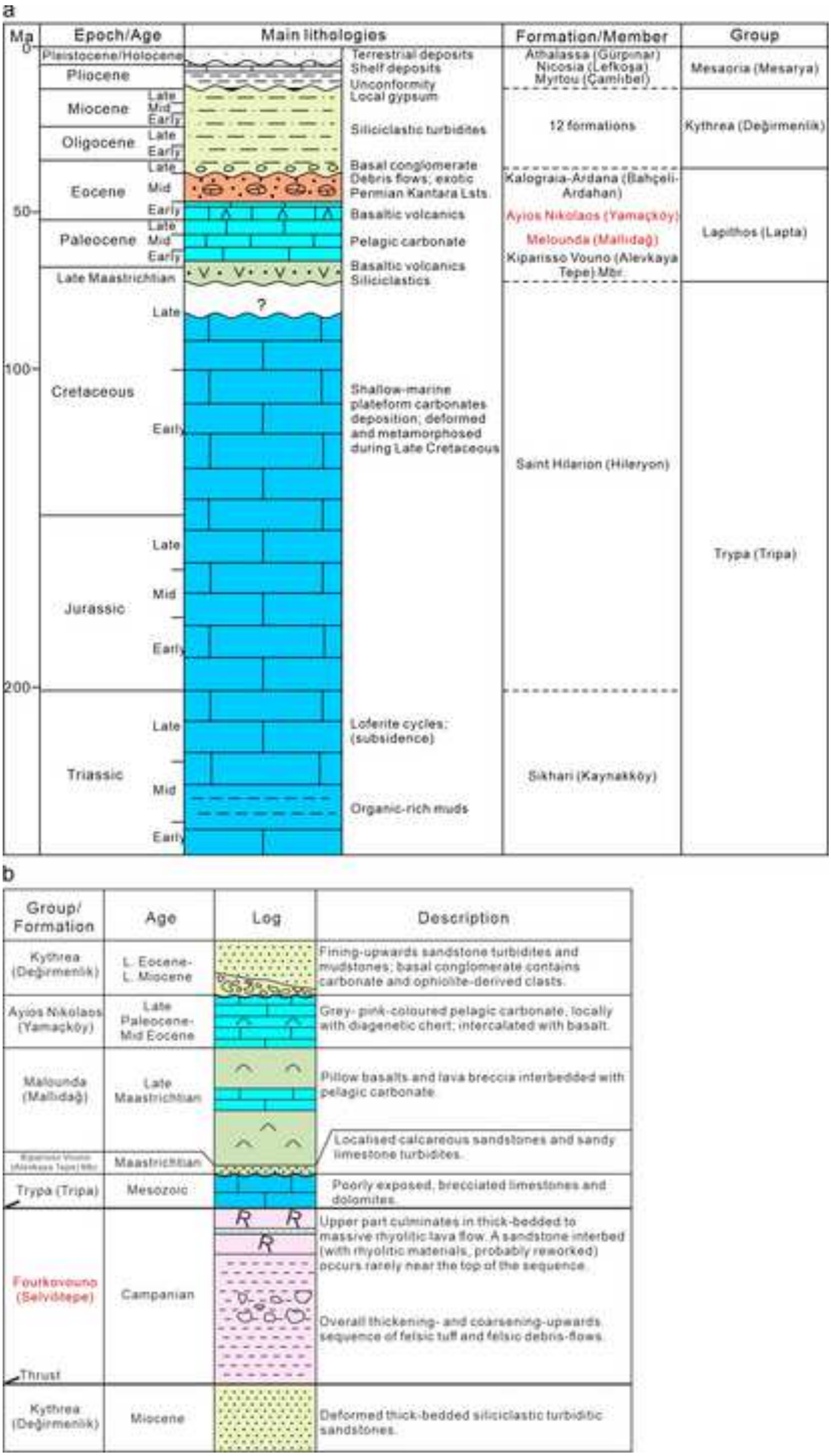

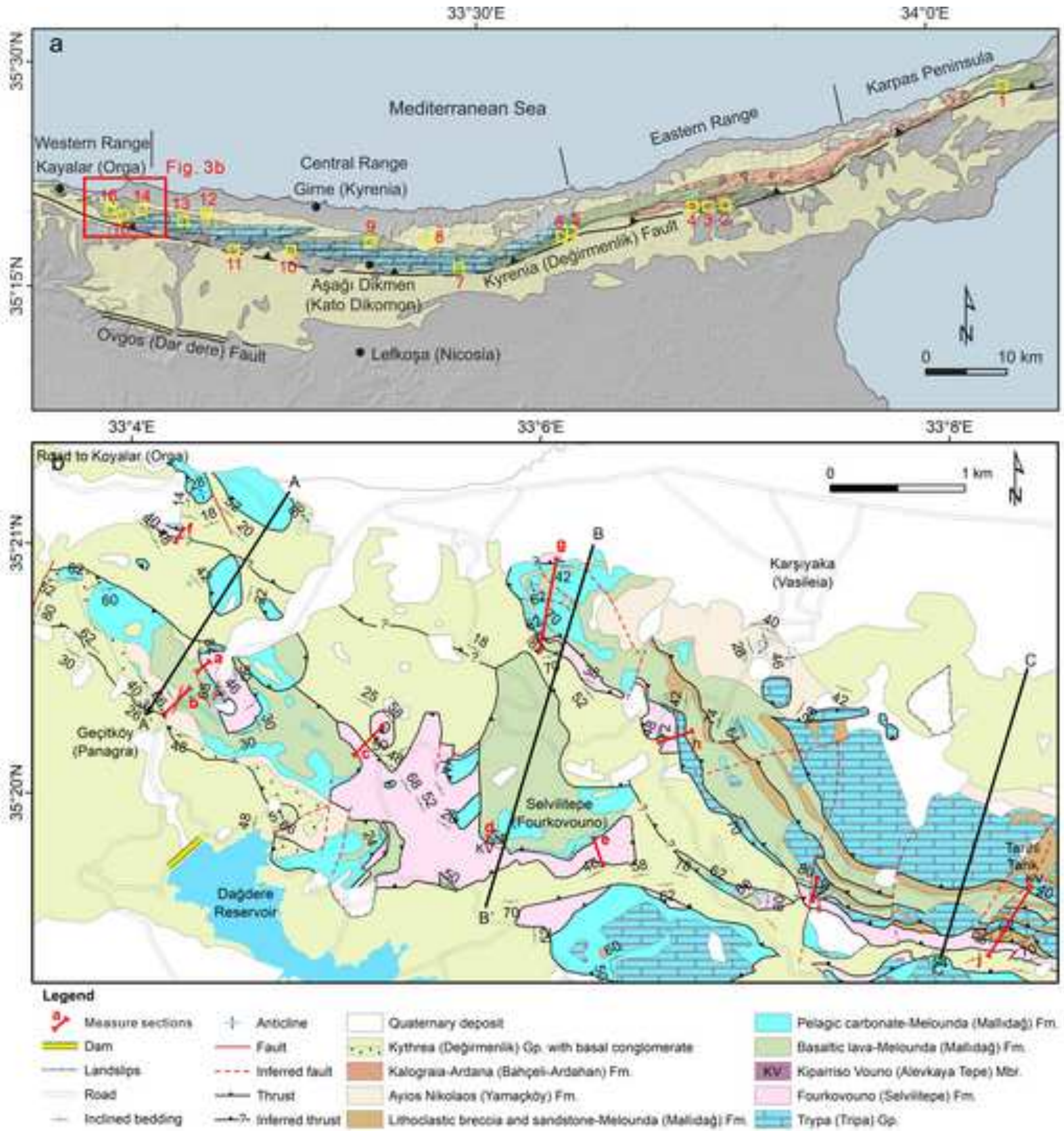
a
Mediterranean Sea
Western Range
Kayalar (Orga)
Fig. 3b
Central Range
Girne (Kyrenia)
Eastern Range
Karpas Peninsula
Kyrenia (Değirmenlik) Fault
Aşağı Dikmen
(Kato Dikomon)
Ovgos (Dar dere) Fault
Lefkoşa (Nicosia)
0 10 km
33°30'E
34°0'E
35°30'N
35°15'N
b
Road to Koyalar (Orga)
0 1 km
33°4'E
33°6'E
33°8'E
35°21'N
35°20'N
Geçitköy
(Panagra)
Karşıyaka
(Vasileia)
Selvilitepe
(Fourkovouno)
Dağdere
Reservoir
Legend
Measure sections
Dam
Landslips
Road
Inclined bedding
Anticline
Fault
Inferred fault
Thrust
Inferred thrust
Quaternary deposit
Kythrea (Değirmenlik) Gp. with basal conglomerate
Kalograia-Ardana (Bahçeli-Ardahan) Fm.
Ayios Nikolaos (Yamaçköy) Fm.
Lithoclastic breccia and sandstone-Melounda (Mallıdağ) Fm.
Pelagic carbonate-Melounda (Mallıdağ) Fm.
Basaltic lava-Melounda (Mallıdağ) Fm.
KV Kiparisso Vouno (Alevkaya Tepe) Mbr.
Fourkovouno (Selvilitepe) Fm.
Trypa (Tripa) Gp.

Figure 4

Click here to access/download;Figure;Fig. 4.jpg

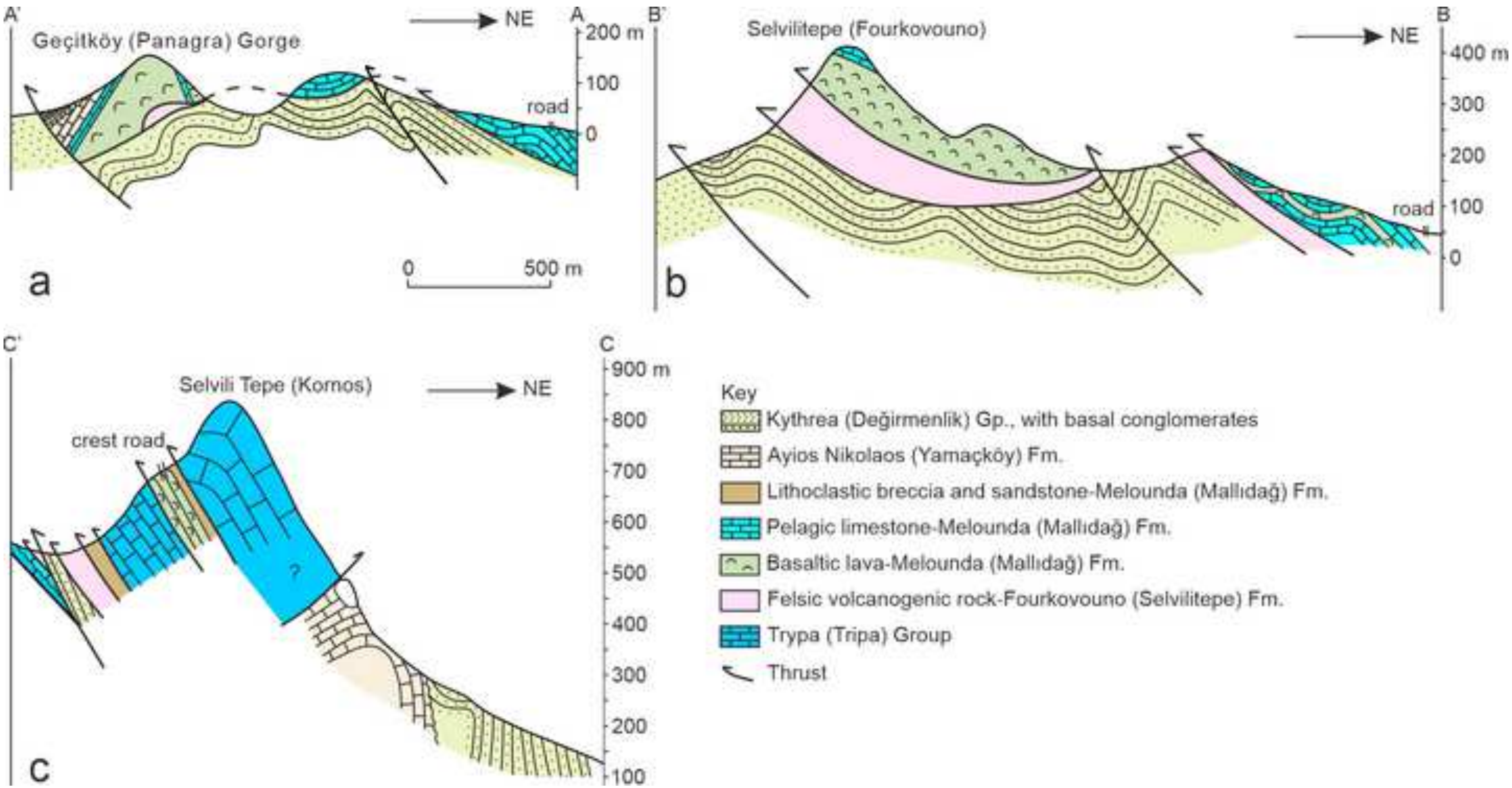

Figure 5

Click here to access/download;Figure;Fig. 5.jpg

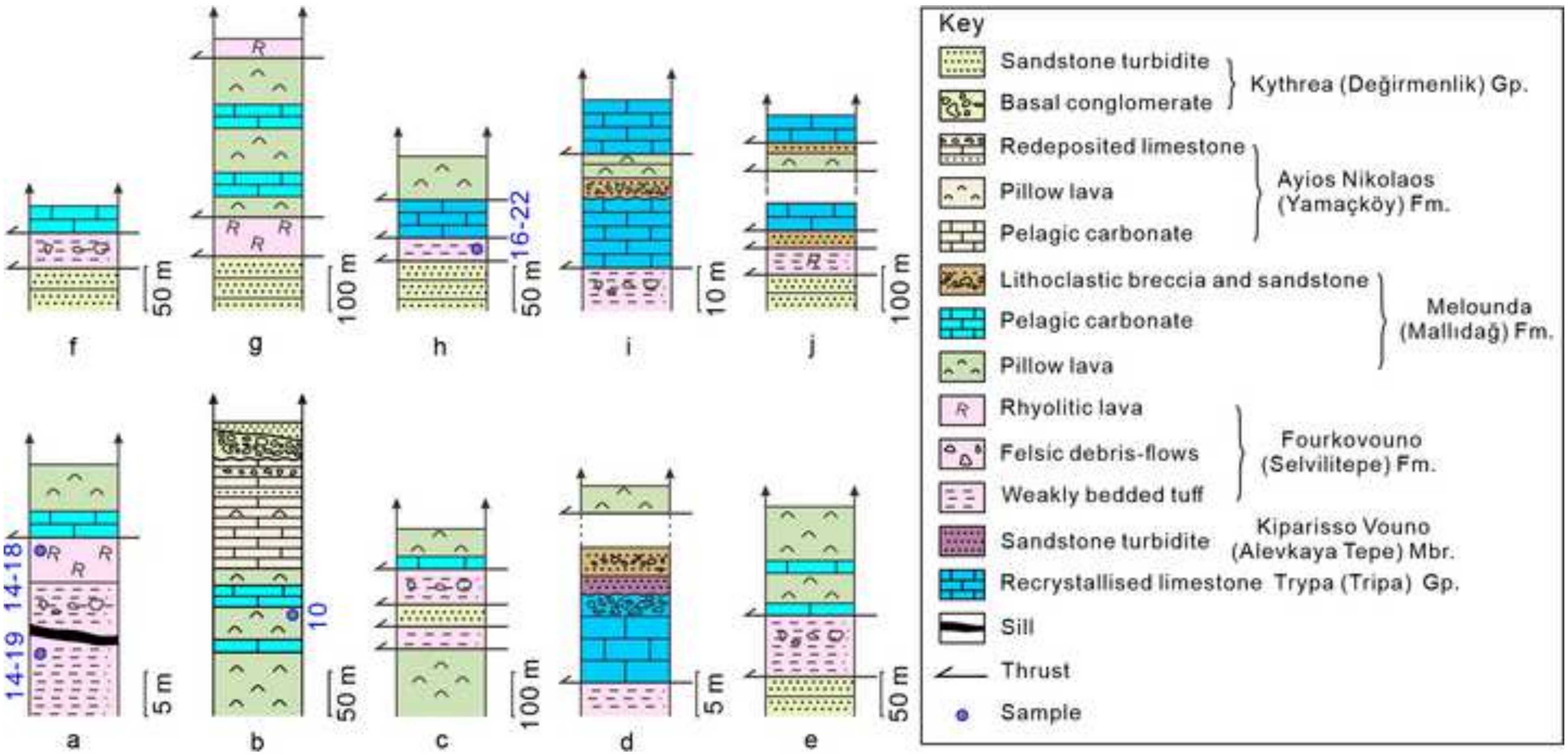

Figure 6

Click here to access/download;Figure;Fig. 6.jpg

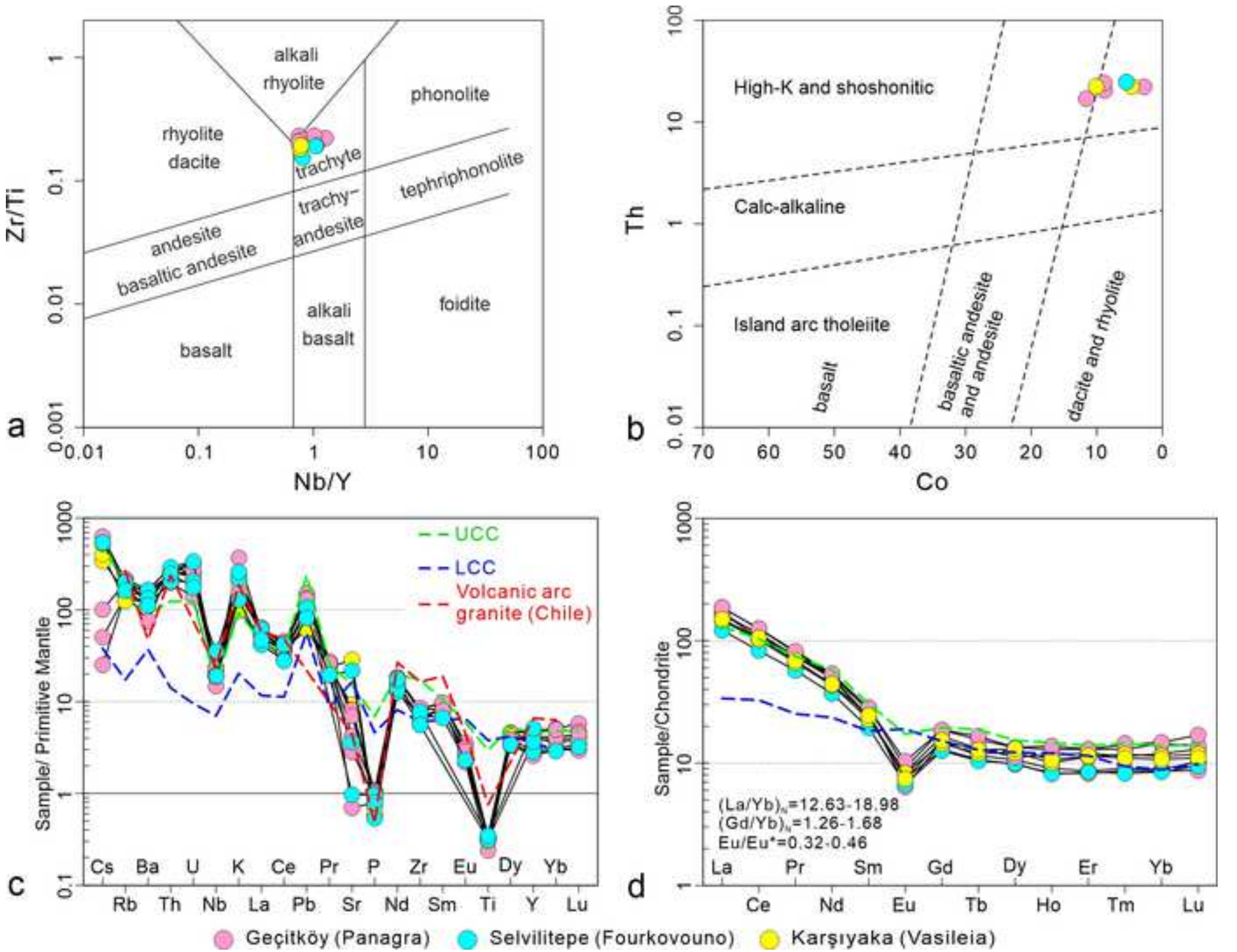

Figure 7 Click here to access/download;Figure;Fig. 7.jpg

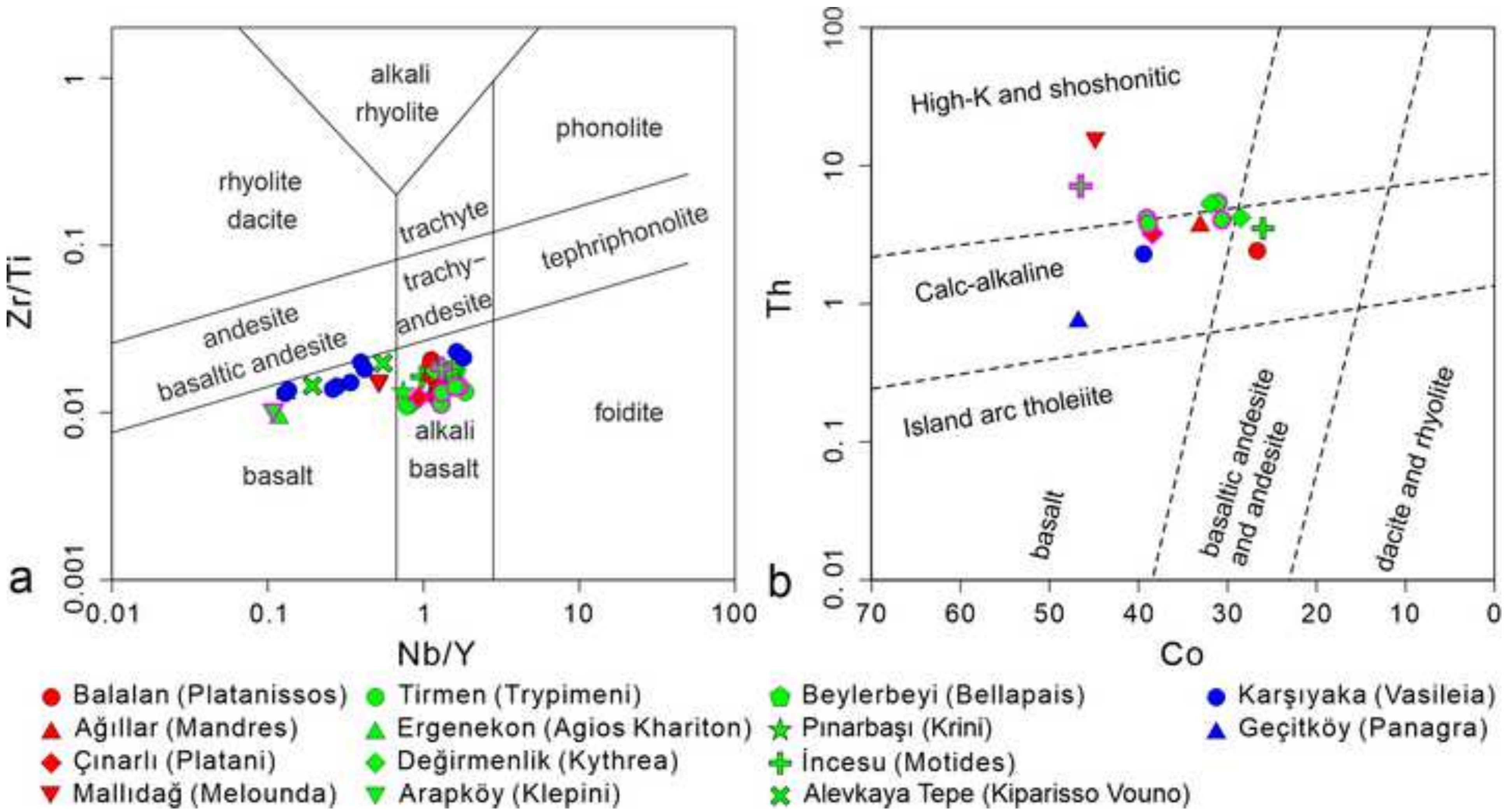

Figure 8

Click here to access/download;Figure;Fig. 8.jpg

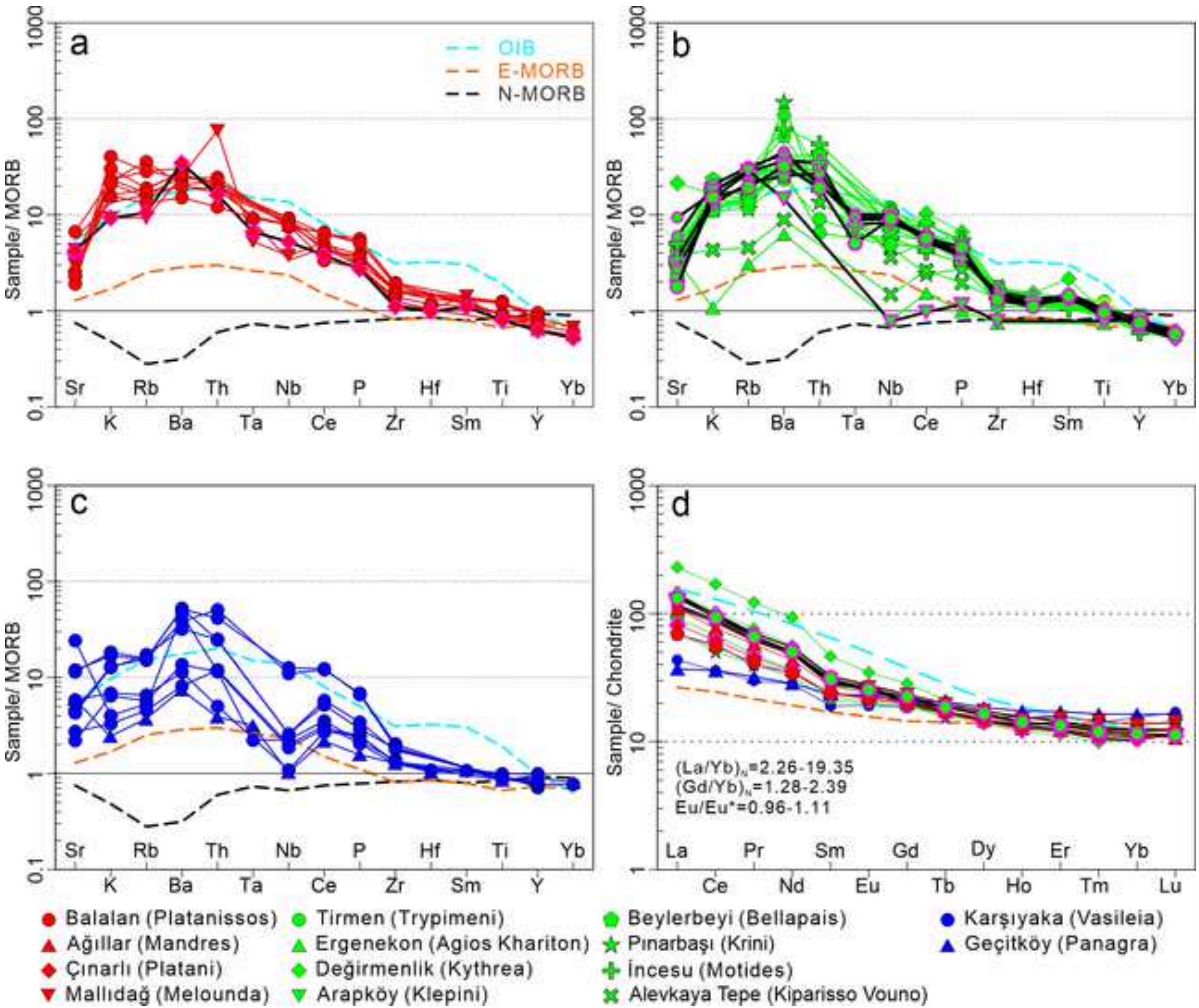

Figure 9

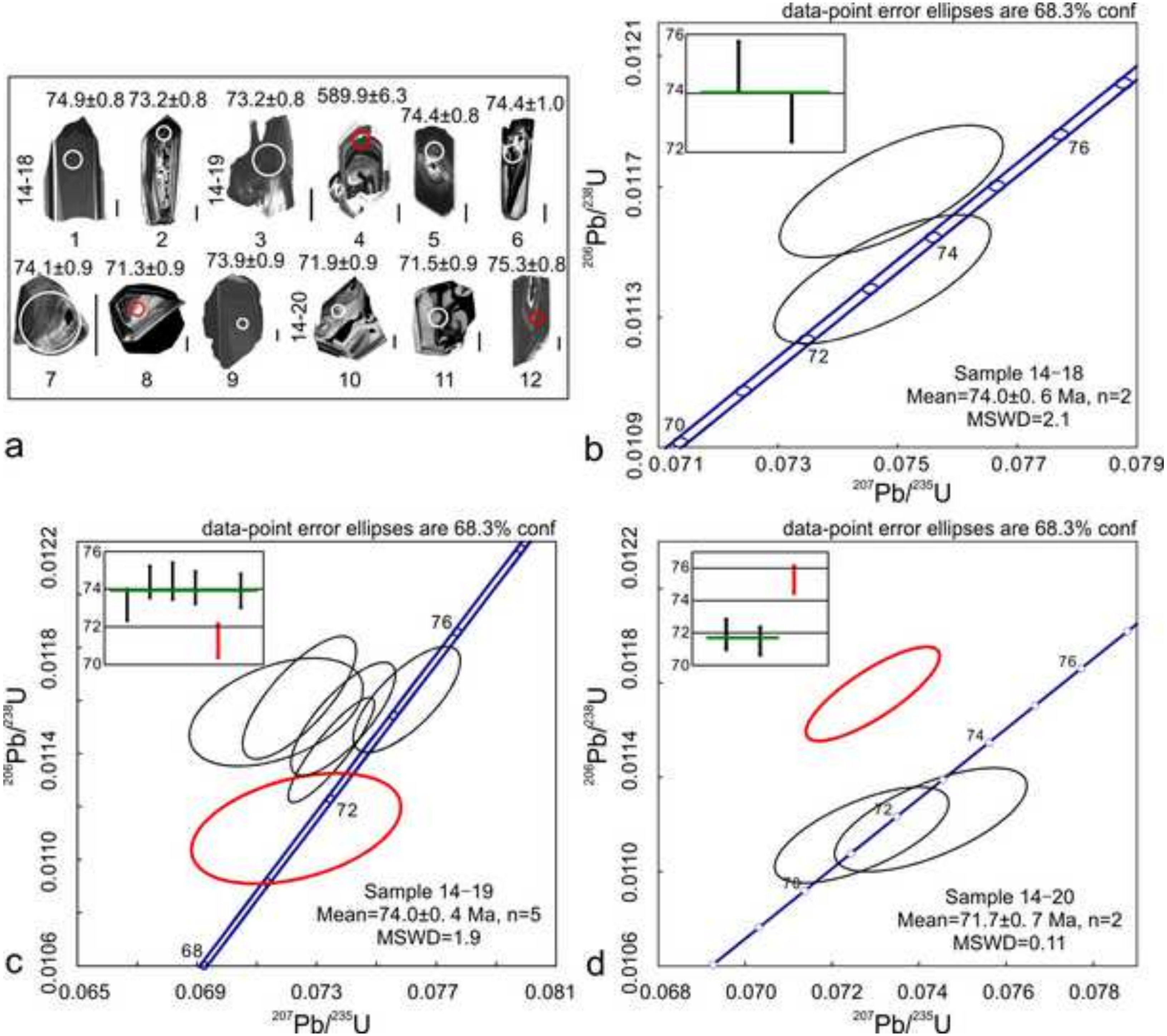

74.9±0.8
73.2±0.8
73.2±0.8
589.9±6.3
74.4±0.8
74.4±1.0
14-18
14-19
1
2
3
4
5
6
74.1±0.9
71.3±0.9
73.9±0.9
71.9±0.9
71.5±0.9
75.3±0.8
14-20
7
8
9
10
11
12
a
data-point error ellipses are 68.3% conf
Sample 14-18
Mean=74.0±0. 6 Ma, n=2
MSWD=2.1
b
^{206}Pb/^{238}U
^{207}Pb/^{235}U
data-point error ellipses are 68.3% conf
Sample 14-19
Mean=74.0±0. 4 Ma, n=5
MSWD=1.9
c
data-point error ellipses are 68.3% conf
Sample 14-20
Mean=71.7±0. 7 Ma, n=2
MSWD=0.11
d

Figure 10

Click here to access/download;Figure;Fig. 10.jpg

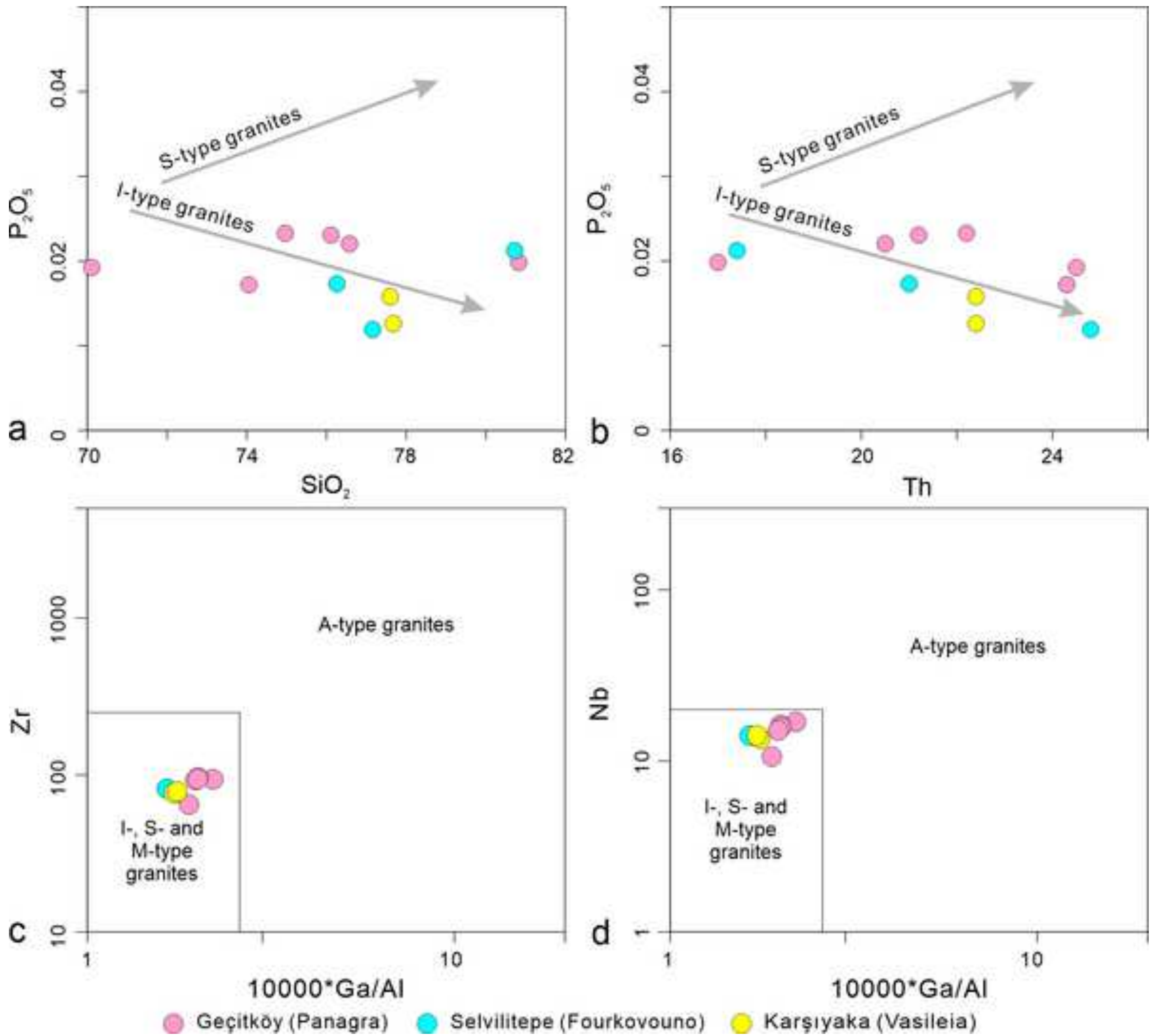

Figure 11

Click here to access/download;Figure;Fig. 11.jpg

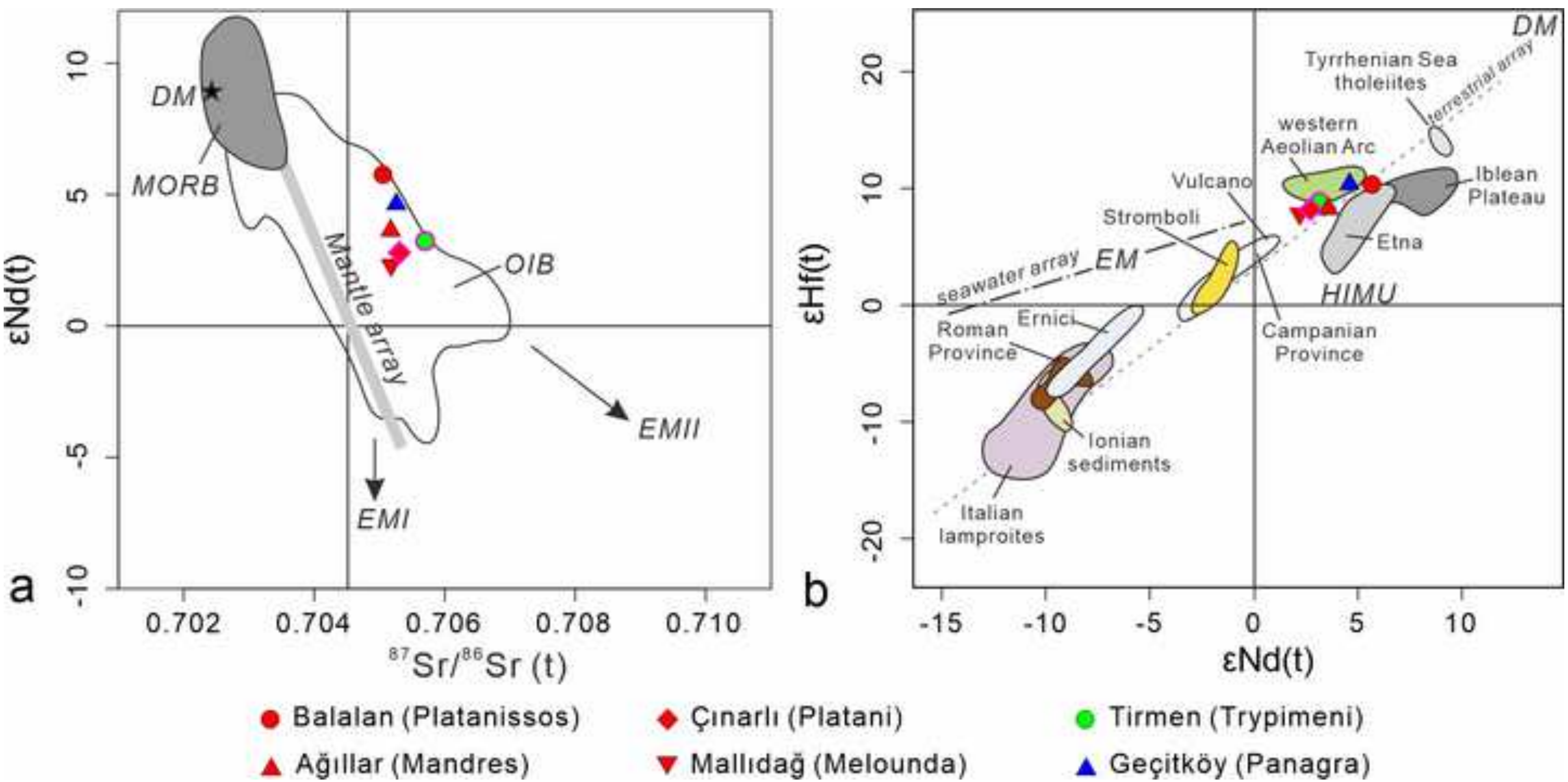

Figure 12

Click here to access/download;Figure;Fig. 12.jpg

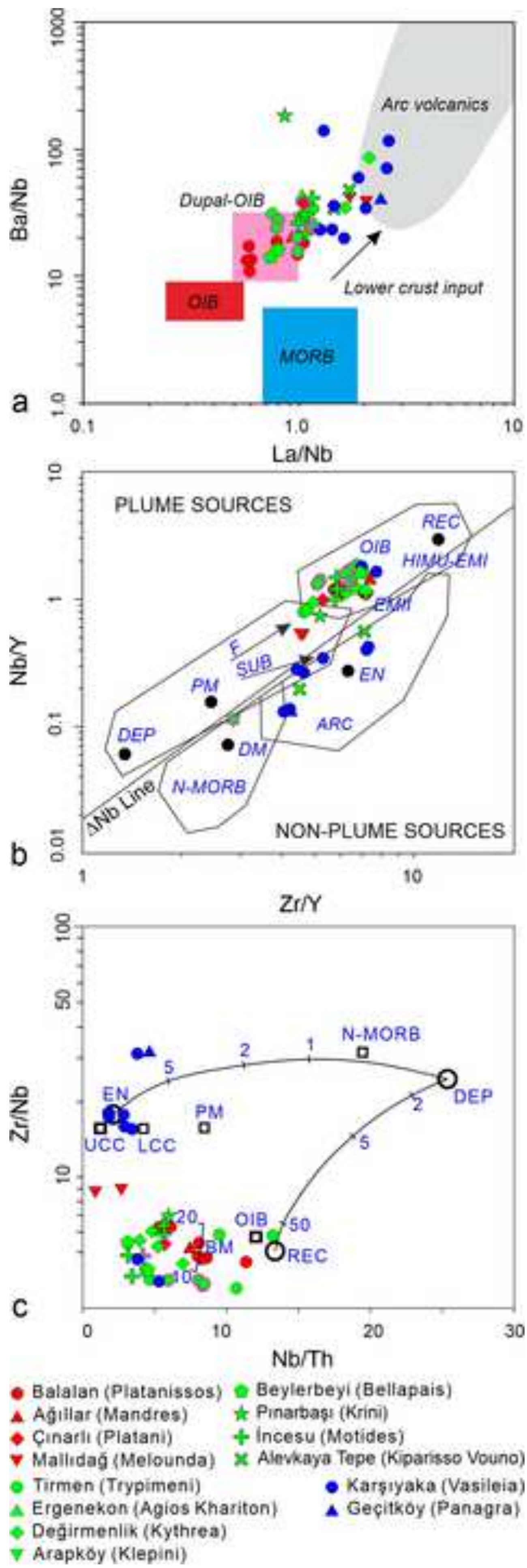

Figure 13 Click here to access/download;Figure;Fig. 13.jpg

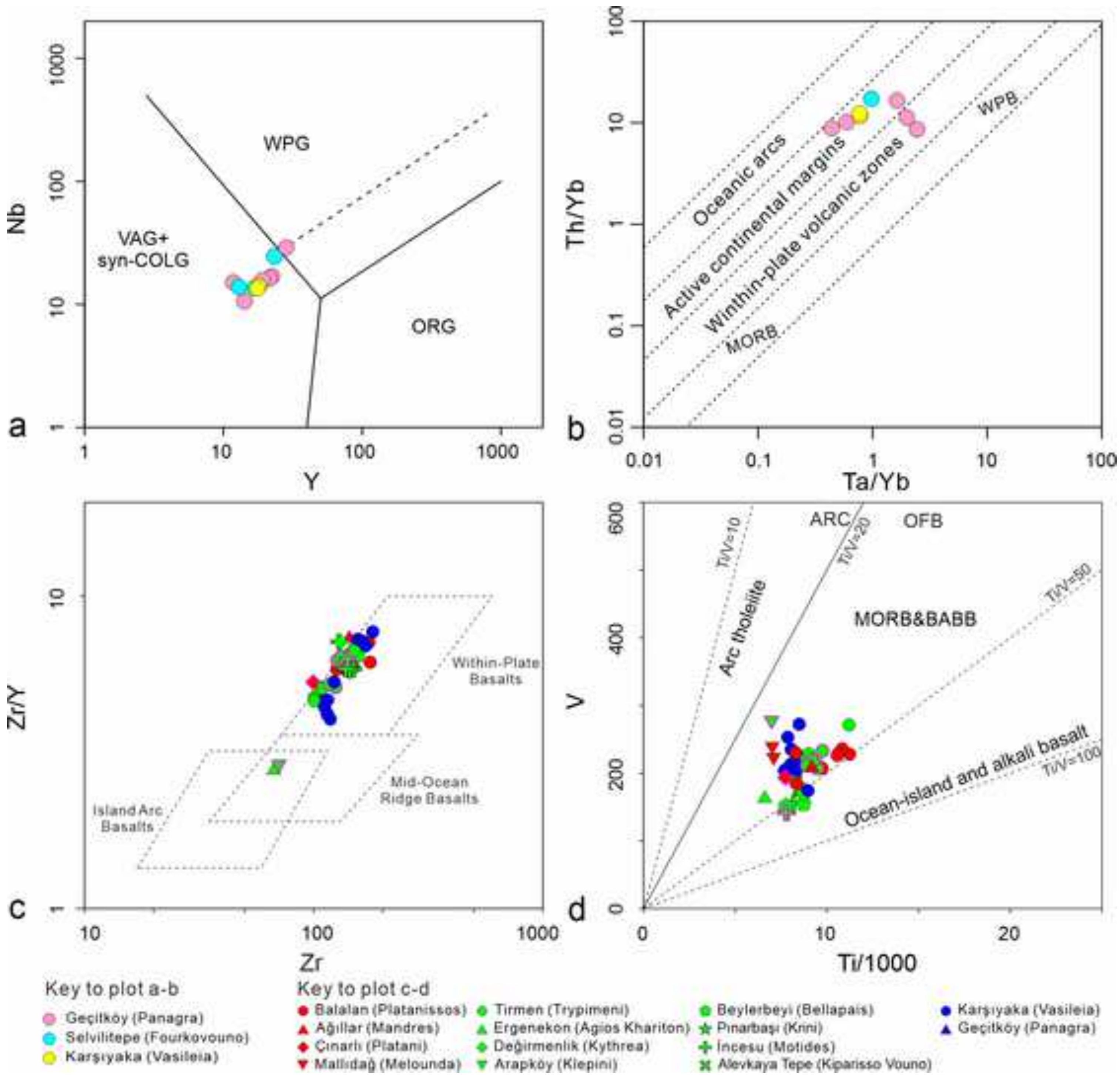

Figure 14

Click here to access/download;Figure;Fig. 14.jpg

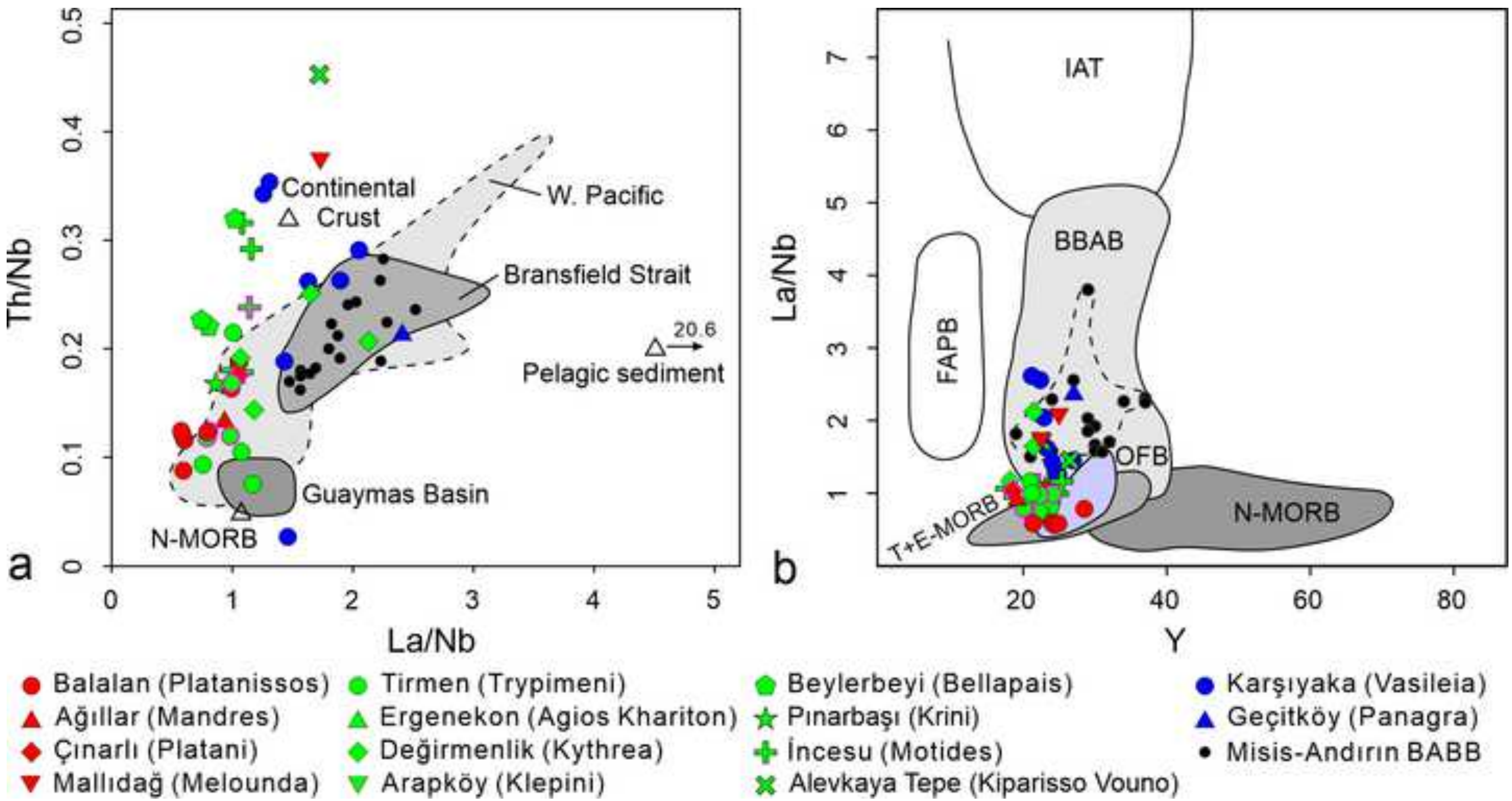

Figure 15

Click here to access/download;Figure;Fig. 15.jpg

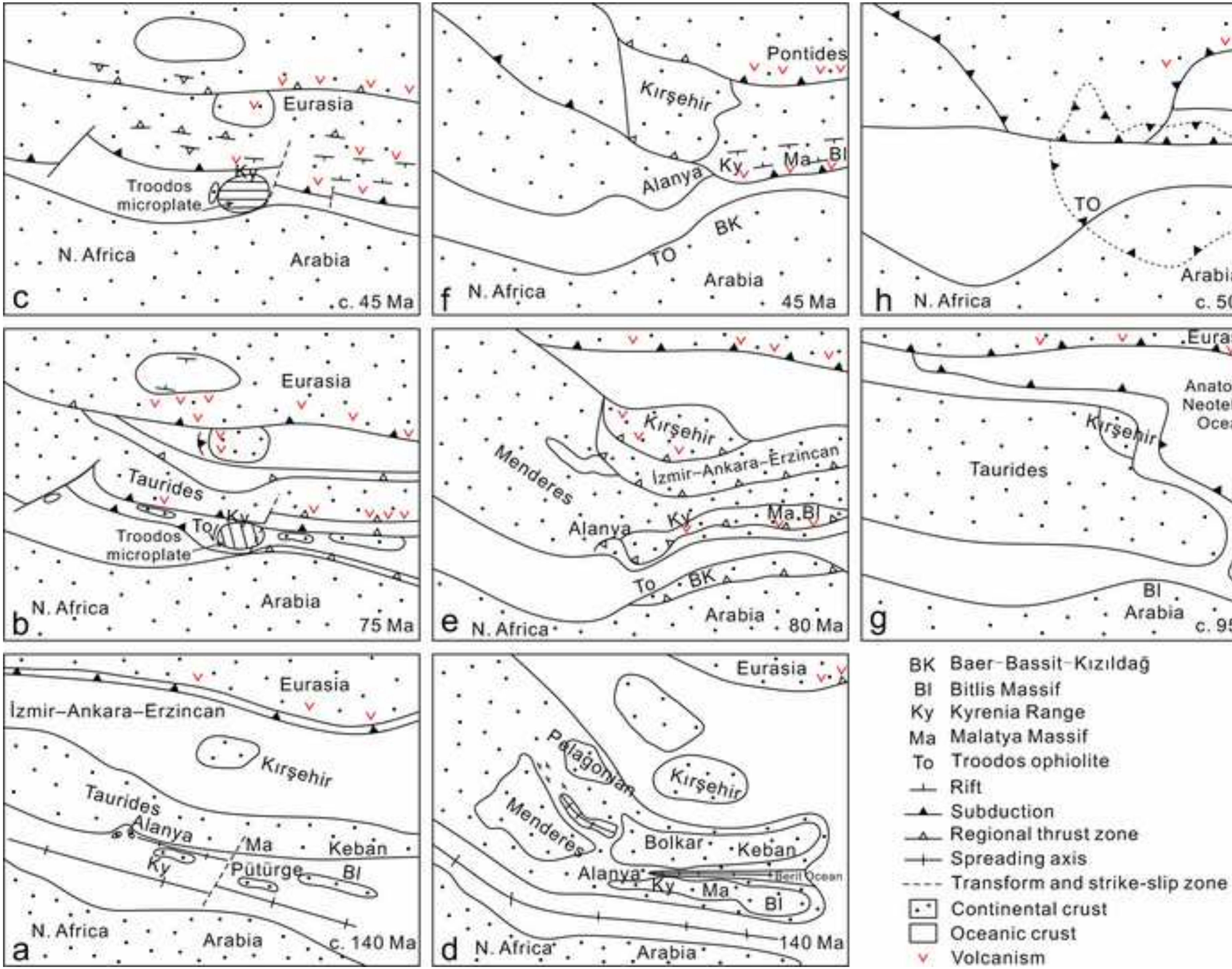

Supplementary Figure S1

Click here to access/download
Supplementary material/Appendix (Files for online publication only)
Supplementary Figure S1.jpg

Supplementary Figure S2

Click here to access/download

Supplementary material/Appendix (Files for online publication only)

Supplementary Figure S2.jpg

Supplementary Figure S3

Click here to access/download
Supplementary material/Appendix (Files for online publication only)
Supplementary Figure S3.jpg

Supplementary Figure S4

Click here to access/download
Supplementary material/Appendix (Files for online publication only)
Supplementary Figure S4.jpg

Supplementary Figure S5

Supplementary Figure S6

Click here to access/download

Supplementary material/Appendix (Files for online publication only)

Supplementary Figure S6.jpg

Click here to access/download

Supplementary material/Appendix (Files for online publication only)

Supplementary Table S3.xlsx

Supplementary Table S4

Click here to access/download
Supplementary material/Appendix (Files for online publication only)
Supplementary Table S4.xlsx

*Declaration of Interest Statement

Declaration of interests

☒ The authors declare that they have no known competing financial interests or personal relationships that could have appeared to influence the work reported in this paper.

☐The authors declare the following financial interests/personal relationships which may be considered as potential competing interests: